Calhoun
Institutional Archive of the Naval Postgraduate School

Calhoun: The NPS Institutional Archive

Theses and Dissertations | Thesis Collection

1986

Numerical models of new HF shipboard communication antenna systems for improved survivability

Lyberopoulos, George L.

Monterey, California: U.S. Naval Postgraduate School

http://hdl.handle.net/10945/22007

DUDLEY KNOX LIBRARY

http://www.nps.edu/library

Calhoun is a project of the Dudley Knox Library at NPS, furthering the precepts and goals of open government and government transparency. All information contained herein has been approved for release by the NPS Public Affairs Officer.

Dudley Knox Library / Naval Postgraduate School
411 Dyer Road / 1 University Circle
Monterey, California USA 93943

NAVAL POSTGRADUATE SCHOOL
MONTEREY, CALIFORNIA 93943-5002

NPS-62-86-006

NAVAL POSTGRADUATE SCHOOL

Monterey, California

...TION
...SCHOOL
...93943

THESIS

NUMERICAL MODELS OF NEW HF SHIPBOARD
COMMUNICATION ANTENNA SYSTEMS
FOR IMPROVED SURVIVABILITY

by

George L. Lyberopoulos

June 1986

Thesis Advisor: Richard W. Adler

Approved for public release; distribution is unlimited.

Prepared for:
Naval Ocean Systems Center
San Diego, CA 92152

T230700

NAVAL POSTGRADUATE SCHOOL
Monterey, CA 93943

Rear Admiral R. H. Shumaker
Superintendent

D. A. Schrady
Provost

This thesis is prepared in conjunction with research sponsored in part by Naval Ocean Systems Center under NPS-62-86-006.

Reproduction of all or part of this report is authorized.

Released by:

JOHN N. DYER
Dean of Science and Engineering

SECURITY CLASSIFICATION OF THIS PAGE

REPORT DOCUMENTATION PAGE

1a REPORT SECURITY CLASSIFICATION UNCLASSIFIED	1b. RESTRICTIVE MARKINGS
2a SECURITY CLASSIFICATION AUTHORITY	3 DISTRIBUTION / AVAILABILITY OF REPORT Approved for public release; distribution is unlimited.
2b DECLASSIFICATION / DOWNGRADING SCHEDULE	
4 PERFORMING ORGANIZATION REPORT NUMBER(S) NPS-62-86-006	5. MONITORING ORGANIZATION REPORT NUMBER(S)
6a. NAME OF PERFORMING ORGANIZATION Naval Postgraduate School 6b OFFICE SYMBOL (If applicable) 62	7a. NAME OF MONITORING ORGANIZATION Monterey, California 93943-5000
6c. ADDRESS (City, State, and ZIP Code) Naval Postgraduate School	7b. ADDRESS (City, State, and ZIP Code) Monterey, California 93943-5000
8a. NAME OF FUNDING / SPONSORING ORGANIZATION 8b. OFFICE SYMBOL (If applicable)	9 PROCUREMENT INSTRUMENT IDENTIFICATION NUMBER
8c. ADDRESS (City, State, and ZIP Code)	10 SOURCE OF FUNDING NUMBERS PROGRAM ELEMENT NO / PROJECT NO / TASK NO / WORK UNIT ACCESSION NO

11 TITLE (Include Security Classification)
NUMERICAL MODELS OF NEW HF SHIPBOARD COMMUNICATION ANTENNA SYSTEMS FOR IMPROVED SURVIVABILITY

12 PERSONAL AUTHOR(S)
George L. Lyberopoulos

13a TYPE OF REPORT	13b TIME COVERED	14 DATE OF REPORT (Year, Month, Day)	15 PAGE COUNT
Master's Thesis	FROM _____ TO _____	1986 June 20	134

16 SUPPLEMENTARY NOTATION

17 COSATI CODES			18 SUBJECT TERMS (Continue on reverse if necessary and identify by block number)
FIELD	GROUP	SUB-GROUP	Combat Survivable Antenna; Computer Modeling of Antennas

19 ABSTRACT (Continue on reverse if necessary and identify by block number)

There are many shipboard communication antenna problems where the number, type, location, or survivability of a given antenna in the system is a parameter which can be varied to determine the overall optimal system.

This thesis investigates computer numerical models for improving the time that an HF shipboard combat survivable antenna system can endure in a given environment. The future generation of ships will have low profile combat survivable antennas; an interim solution for present ships is the elimination of fragile HF antennas by exciting existing masts. The antenna is modeled as a mast with

20 DISTRIBUTION / AVAILABILITY OF ABSTRACT ☒ UNCLASSIFIED/UNLIMITED ☐ SAME AS RPT ☐ DTIC USERS	21 ABSTRACT SECURITY CLASSIFICATION UNCLASSIFIED
22a NAME OF RESPONSIBLE INDIVIDUAL Prof R. W. Adler	22b TELEPHONE (Include Area Code) (408)646-2352 22c. OFFICE SYMBOL 62Ab

DD FORM 1473, 84 MAR 83 APR edition may be used until exhausted
All other editions are obsolete

SECURITY CLASSIFICATION OF THIS PAGE

dimensions 24 x 3 x 3 meters. Several computer models of the driven antenna are modeled using the Numerical Electromagnetic Code (NEC). Input impedances and radiation patterns of the antenna are presented.

Approved for public release; distribution is unlimited.

Numerical Models of New HF Shipboard Communication Antenna Systems for Improved Survivability.

by

George L. Lyberopoulos
Lieutenant, Hellenic Navy
B.S., Hellenic Naval Academy, 1976

Submitted in partial fulfillment of the
requirements for the degree of

MASTER OF SCIENCE IN ENGINEERING SCIENCE

from the

NAVAL POSTGRADUATE SCHOOL
June 1986

ABSTRACT

There are many shipboard communication antenna problems where the number, type, location, or survivability of a given antenna in the system is a parameter which can be varied to determine the overall optimal system.

This thesis investigates computer numerical models for improving the time that an HF shipboard combat survivable antenna system can endure in a given environment. The future generation of ships will have low profile combat survivable antennas; an interim solution for present ships is the elimination of fragile HF antennas by exciting existing masts. The antenna is modeled as a mast with dimensions 24 x 3 x 3 meters. Several computer models of the driven antenna are modeled using the Numerical Electromagnetic Code (NEC). Input impedances and radiation patterns of the antenna are presented.

TABLE OF CONTENTS

I. INTRODUCTION 18

A. AN OVERVIEW OF THE FUNDAMENTALS 18

B. THESIS STATEMENT-SCOPE AND LIMITATIONS 20

II. NUMERICAL ELECTROMAGNETIC CODE 22

A. INTRODUCTION 22

B. MODELING GUIDELINES 23

1. Wire Computer Modeling Guidelines 23

2. Over Ground Computer Modeling Guidelines 25

C. NEC INPUT CARDS 25

III. COMPUTER MODELS 27

A. COMPUTER MODEL DEVELOPMENT 27

IV. COMPUTER MODEL RESULTS 34

A. AVERAGE POWER GAIN 34

B. INPUT IMPEDANCE 36

C. RADIATION PATTERNS 40

D. VOLTAGE STANDING WAVE RATIO (VSWR) 41

V. CONCLUSIONS AND RECOMMENDATIONS 59

A. CONCLUSIONS 59

B. RECOMMENDATIONS 60

APPENDIX A: INTEGRAL EQUATIONS (IE) 62

APPENDIX B: NEC INPUT CARD SUMMARY 66

APPENDIX C: GEOMETRY DATA CARDS FOR FREQUENCY RANGE 2-10 MHZ AND 11-15 MHZ 68

APPENDIX D: AVERAGE POWER GAIN AND IMPEDANCES SAMPLE DATA SET 70

APPENDIX E: VERTICAL AND HORIZONTAL RADIATION PATTERN SAMPLE DATA SET 71

APPENDIX F: INPUT IMPEDANCE CURVES 72

APPENDIX G: RADIATION PATTERNS 81

LIST OF REFERENCES 128

INITIAL DISTRIBUTION LIST 130

LIST OF TABLES

3.1 Mast Model Frequency and Grid Spacings in Wavelengths.....29

3.2 Maximum Time Allowed for Each CLASS.....30

4.1 Average Power Gain of Mast Computer Model in Frequency Range 2-10 MHz vs. Feed Point Positions.....35

4.2 Average Power Gain of Mast Computer Model in Frequency Range 11-15 MHz vs. Feed Point Positions.....36

4.3 Mast Input Impedances for Driving Four Base Segments in Frequency Range 2-6 MHz.....37

4.4 Mast Input Impedances for Driving Four Base Segments in Frequency Range 6-10 MHz.....38

4.5 Mast Input Impedances for Driving All Base Segments in Frequency Range 11-15 MHz.....39

4.6 Frequency Satisfying 3:1 VSWR Criteria.....58

F.1 Mast Input Impedances for Driving Three Base Segments in Frequency Range 2-6 MHz.....73

F.2 Mast Input Impedances for Driving Three Base Segments in Frequency Range 6-10 MHz.....74

F.3 Mast Input Impedances for Driving Two Adjacent Base Segments in Frequency Range 2-6 MHz.....75

F.4 Mast Input Impedances for Driving Two Adjacent Base Segments in Frequency Range 6-10 MHz.....76

F.5 Mast Input Impedances for Driving Two Diagonal Base Segments in Frequency Range 2-6 MHz.....77

F.6 Mast Input Impedances for Driving Two Diagonal Base Segments in Frequency Range 6-10 MHz....78

F.7 Mast Input Impedances for Driving One Base Segment in Frequency Range 2-6 MHz....79

F.8 Mast Input Impedances for Driving One Base Segment in Frequency Range 6-10 MHz....80

LIST OF FIGURES

1.1 Frequency Spectrum....19

2.1 Thin-Wire Modeling....23

2.2 Thin-Wire Approximation Coordinate System....24

3.1 Mast Area of a FFG-45 Frigate....28

3.2 Wire-Grid Mast Model for Frequency Range 2-10 MHz....31

3.3 Wire-Grid Mast Model for Frequency Range 11-15 MHz....32

4.1 Mast Input Impedances for Driving Four Base Segments in Frequency Range 2-6 MHz....37

4.2 Mast Input Impedances for Driving Four Base Segments in Frequency Range 6-10 MHz....38

4.3 Mast Input Impedances for Driving All Base Segments In Frequency Range 11-15 MHz. 39

4.4 E-Field Horizontal Radiation Pattern: F = 2 MHz, vs. Four Feed Point Positions....42

4.5 E-Field Vertical Radiation Pattern: F = 2 MHz, vs. Four Feed Point Positions....43

4.6 E-Field Vertical Radiation Pattern of Whip Antenna Whose Height Is Equal to That of the Antenna of Figures 4.4 and 4.5....44

4.7 E-Field Horizontal Radiation Pattern of Whip Antenna Whose Height Is Equal to That of the Antenna of Figures 4.4 and 4.5....45

4.8 E-Field Vertical Radiation Pattern: F = 6 MHz, vs. Four Feed Point Positions....46

4.9 E-Field Horizontal Radiation Pattern: F = 10 MHz, vs. Two Adjacent Feed Point Positions....47

4.10 E-Field Horizontal Radiation Pattern: F = 10 MHz, vs. One Feed Point Position....48

4.11 E-Field Vertical Radiation Pattern: F = 11 MHz, vs. All Base Feed Point Positions....49

4.12 E-Field Horizontal Radiation Pattern: F = 11 MHz, vs. All Base Feed Point Positions....50

4.13 Smith Chart Showing 3:1 VSWR Matchable Region....51

4.14 Impedance Plot of Four Feed Point Positions in Frequency Range 2-10 MHz....52

4.15 Impedance Plot of Three Feed Point Positions in Frequency Range 2-10 MHz....53

4.16 Impedance Plot of Two Adjacent Feed Point Positions in Frequency Range 2-10 MHz....54

4.17 Impedance Plot of Two Diagonal Feed Point Positions in Frequency Range 2-10 MHz....55

4.18 Impedance Plot of One Feed Point Position in Frequency Range 2-10 MHz....56

4.19 Impedance Plot of All Base Feed Point Positions in Frequency Range 11-15 MHz....57

F.1 Mast Input Impedances for Driving Three Base Segments in Frequency Range 2-6 MHz....73

F.2 Mast Input Impedances for Driving Three Base Segments in Frequency Range 6-10 MHz....74

F.3 Mast Input Impedances for Driving Two Adjacent Base Segments in Frequency Range 2-6 MHz....75

F.4 Mast Input Impedances for Driving Two Adjacent Base Segments in Frequency Range 6-10 MHz....76

F.5 Mast Input Impedances for Driving Two Diagonal Base Segments in Frequency Range 2-6 MHz....77

F.6 Mast Input Impedances for Driving Two Diagonal Base Segments in Frequency Range 6-10 MHz....78

F.7 Mast Input Impedances for Driving One Base Segment in Frequency Range 2-6 MHz....79

F.8 Mast Input Impedances for Driving One Base Segment in Frequency Range 6-10 MHz....80

G.1 E-Field Vertical Radiation Pattern: F = 2 MHz, vs. Four Feed Point Positions....82

G.2 E-Field Horizontal Radiation Pattern: F = 2 MHz, vs. Four Feed Point Positions....83

G.3 E-Field Vertical Radiation Pattern: F = 2 MHz, vs. Three Feed Point Positions....84

G.4 E-Field Horizontal Radiation Pattern: F = 2 MHz, vs. Three Feed Point Positions....85

G.5 E-Field Vertical Radiation Pattern: F = 2 MHz, vs. Two Adjacent Feed Point Positions....86

G.6 E-Field Horizontal Radiation Pattern: F = 2 MHz, vs. Two Adjacent Feed Point Positions....87

G.7 E-Field Vertical Radiation Pattern: F = 2 MHz, vs. Two Diagonal Feed Point Positions....88

G.8 E-Field Horizontal Radiation Pattern: F = 2 MHz, vs. Two Diagonal Feed Point Positions....89

G.9 E-Field Vertical Radiation Pattern: F = 2 MHz, vs. One Feed Point Position....90

G.10 E-Field Horizontal Radiation Pattern: F = 2 MHz, vs. One Feed Point Position....91

G.11 E-Field Vertical Radiation Pattern: F = 4 MHz, vs. Four Feed Point Positions....92

G.12 E-Field Horizontal Radiation Pattern: F = 4 MHz, vs. Four Feed Point Positions....93

G.13 E-Field Vertical Radiation Pattern: F = 6 MHz, vs. Four Feed Point Positions....94

G.14 E-Field Horizontal Radiation Pattern: F = 6 MHz, vs. Four Feed Point Positions....95

G.15 E-Field Vertical Radiation Pattern: F = 6 MHz, vs. Three Feed Point Positions....96

G.16 E-Field Horizontal Radiation Pattern: F = 6 MHz, vs. Three Feed Point Positions....97

G.17 E-Field Vertical Radiation Pattern: F = 6 MHz, vs. Two Adjacent Feed Point Positions....98

G.18 E-Field Horizontal Radiation Pattern: F = 6 MHz, vs. Two Adjacent Feed Point Positions....99

G.19 E-Field Vertical Radiation Pattern: F = 6 MHz, vs. Two Diagonal Feed Point Positions....100

G.20 E-Field Horizontal Radiation Pattern: F = 6 MHz, vs. Two Diagonal Feed Point Positions....101

G.21 E-Field Vertical Radiation Pattern: F = 6 MHz, vs. One Feed Point Position....102

G.22 E-Field Horizontal Radiation Pattern: F = 6 MHz, vs. One Feed Point Position 103

G.23 E-Field Vertical Radiation Pattern: F = 7.74 MHz, vs. Four Feed Point Positions 104

G.24 E-Field Horizontal Radiation Pattern: F = 7.74 MHz, vs. Four Feed Point Positions 105

G.25 E-Field Vertical Radiation Pattern: F = 10 MHz, vs. Four Feed Point Positions 106

G.26 E-Field Horizontal Radiation Pattern: F = 10 MHz, vs. Four Feed Point Positions 107

G.27 E-Field Vertical Radiation Pattern: F = 10 MHz, vs. Three Feed Point Positions 108

G.28 E-Field Horizontal Radiation Pattern: F = 10 MHz, vs. Three Feed Point Positions 109

G.29 E-Field Vertical Radiation Pattern: F = 10 MHz, vs. Two Adjacent Feed Point Positions 110

G.30 E-Field Horizontal Radiation Pattern: F = 10 MHz, vs. Two Adjacent Feed Point Positions 111

G.31 E-Field Vertical Radiation Pattern: F = 10 MHz, vs. Two Diagonal Feed Point Positions 112

G.32 E-Field Horizontal Radiation Pattern: F = 10 MHz, vs. Two Diagonal Feed Point Positions 113

G.33 E-Field Vertical Radiation Pattern: F = 10 MHz, vs. One Feed Point Position 114

G.34 E-Field Horizontal Radiation Pattern: F = 10 MHz, vs. One Feed Point Position 115

G.35 E-Field Vertical Radiation Pattern: F = 11 MHz, vs. All Base Feed Point Positions....116

G.36 E-Field Horizontal Radiation Pattern: F = 11 MHz, vs. All Base Feed Point Positions....117

G.37 E-Field Vertical Radiation Pattern: F = 12.85 MHz, vs. All Base Feed Point Positions....118

G.38 E-Field Horizontal Radiation Pattern: F = 12.85 MHz, vs. All Base Feed Point Positions....119

G.39 E-Field Vertical Radiation Pattern: F = 15 MHz, vs. All Base Feed Point Positions....120

G.40 E-Field Horizontal Radiation Pattern: F = 15 MHz, vs. All Base Feed Point Positions....121

G.41 E-Field Vertical Radiation Pattern of Whip Antenna Whose Height Is Equal to That of the Antenna of Figures G.1-G.40 in Frequency 4 MHz....122

G.42 E-Field Vertical Radiation Pattern of Whip Antenna Whose Height Is Equal to That of the Antenna of Figures G.1-G.40 in Frequency 6 MHz....123

G.43 E-Field Vertical Radiation Pattern of Whip Antenna Whose Height Is Equal to That of the Antenna of Figures G.1-G.40 in Frequency 7.74 MHz....124

G.44 E-Field Vertical Radiation Pattern of Whip Antenna Whose Height Is Equal to That of the Antenna of Figures G.1-G.40 in Frequency 10 MHz....125

G.45 E-Field Vertical Radiation Pattern of Whip Antenna Whose Height Is Equal to That of the Antenna of Figures G.1-G.40 in Frequency 12.85 MHz....126

G.46 E-Field Vertical Radiation Pattern of Whip Antenna Whose Height Is Equal to That of the Antenna of Figures G.1-G.40 in Frequency 15 MHz....127

GLOSSARY

Z	Antenna Impedance = R ± jX where : R = antenna resistance X = antenna reactance
Radiation Pattern	A plot of the electric field strength in polar coordinates.
Polarization	The direction of the electric field vector with respect to a set of coordinate axes.
Linear Polarization	The direction of the resultant electric field vector is constant with time.
Vertical Polarization	Resultant electric vector is perpendicular to the earth surface for the antenna orientation.
Radiation Intensity	The power radiated by an antenna per unit solid angle in a particular direction.
Gain	Ratio of maximum radiation intensity in a given direction to the maximum radiation intensity produced in the same direction by a hypothetical lossless antenna which radiates uniformly in all directions (an isotropic radiator) for the same power input.

Power Budget Equation

$$S_r = P_t G_t G_r \lambda^2 / (4\pi)^2 R^2 L$$

where: S_r = available power in the receiver

P_t = input power

G_r = receiving antenna gain

G_t = transmitting antenna gain

λ = wavelength

R = distance from the transmitter

L = total loss

VSWR

Voltage Standing Wave Ratio = V_{max}/V_{min}

where: $V_{max} = 1 + |\Gamma_L|$

$V_{min} = 1 - |\Gamma_L|$

Γ_L = reflection coefficient.

ACKNOWLEDGEMENTS

I would like to express my gratitude to Dr. Richard W. Adler, for his valuable guidance and assistance.

I would also like to dedicate this thesis to my wife Mary, who relieved me of many family obligations during the final stretch and made it all worth it.

Finally, I wish to thank the 10,000,000 Greek tax-payers for having paid for my course of studies.

I. INTRODUCTION

A. AN OVERVIEW OF THE FUNDAMENTALS

In the recent years, as better equipment was developed, more and more antennas of all type and sizes were installed aboard Navy surface ships.

Naval ships utilize several different bands of frequencies depending on where a ship needs to communicate. Lower frequencies such as HF (high frequency), are used for longer range over the horizon (OTH) communications. Higher frequencies such as VHF (very high frequency), and UHF (ultra high frequency), are used for shorter line-of-sight (LOS) communications. Figure 1.1, Peebles [Ref. 1:p. 3] illustrates the list of frequency bands.

Frequencies are allocated by the International Telecommunications Union (ITU), which allocates the frequency spectrum to the countries of the world. The higher the frequency used the more data can be transmitted per channel as wider bandwidths (BW) are possible at higher frequencies. For instance, the BW between 2 and 3 GHz is much wider than the BW between 2 and 3 MHz. Data rates can be shown by Shannon's law:

$$C = 3.32\,B \log [1 + S/N] \qquad (1.1)$$

where:

C = the maximum number of bits/seconds

B = bandwidth

S/N = signal to noise ratio

Ships carry a variety of communications equipment and antennas in order to use several bands of frequencies at one time. Some UHF and VHF frequencies are utilized within a battle group, so that the ships can communicate with each other with a reduced risk of being detected by the enemy. HF is used for long distance communications of several tens to hundreds of miles.

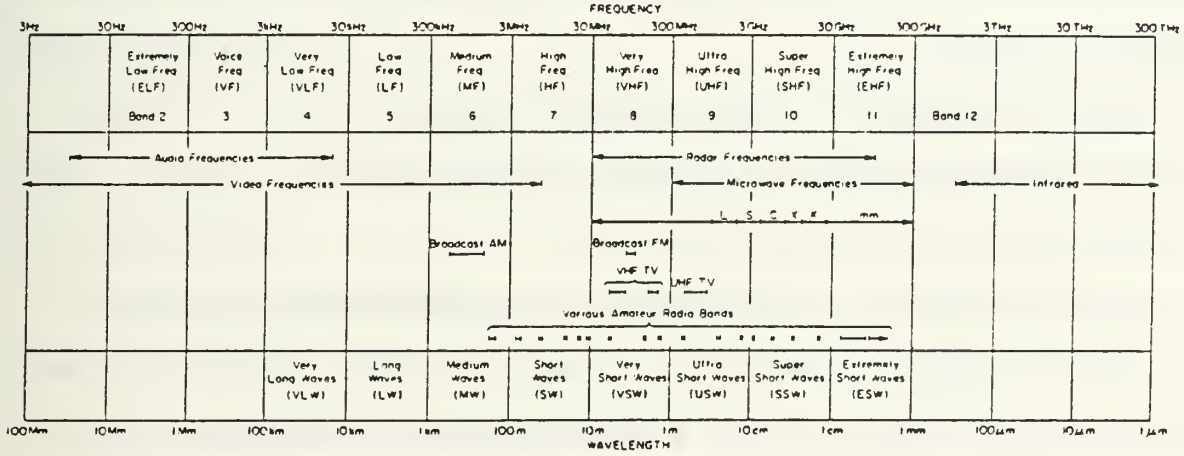

Figure 1.1. Frequency Spectrum

Optimum antenna lengths vary with the frequency in use. The lower the frequency the longer the antenna length. The length of the antenna is calculated by:

$$\lambda = c / f \qquad (1.2)$$

where:

λ = wavelength in meters

c = speed of light ($3 \cdot 10^8$ m/sec)

f = frequency in hertz (sec^{-1})

The ideal antenna for shipboard HF is a quarter-wave vertical antenna. The HF spectrum is from 2-30 MHz, so the 2 MHz frequency requires an antenna of 123 feet or 37.5 meters. This kind of antenna is too large to realistically be installed on a ship.

B. THESIS STATEMENT - SCOPE AND LIMITATIONS

As the number of required antennas increases, location becomes a problem , because:

- The limited amount of space available on a ship.
- The required isolation is needed between the antennas.
- The firing zones of weapons systems.
- The survivability and the vulnerability of the antennas during combat.

Shipboard antenna survivability is defined as the capability of an antenna to avoid and/or withstand a man-made hostile environment.

There are several survivable antenna designs that can be investigated. One design could be to excite sections of the ship's superstructure, such as the ship's masts, or the bulkheads along the superstructure, and another design could be to use a telescopic antenna.

The elimination of tall and large structures make the antennas more survivable during combat.

This thesis investigates the performance of an HF antenna deployed on a simulated mast, created by a wire-grid model, using the Numerical Electromagnetic Code (NEC).

NEC is an advanced method of moments computer code using the Multiple Virtual System (**MVS**) on the main frame of the **IBM 3033** Network.

The frequency range investigated is limited to the HF range of 2-15 MHz due to the computer storage and time limits. As frequency increases, the wavelength λ decreases, and the required number of segments to model an antenna increases.

The thesis begins with a discussion of the NEC in Chapter II and continues in Chapter III with several computer models of the driven antenna. An attempt to develop the best way of feeding the mast is another goal of this thesis.

Chapter IV shows, with more emphasis, results in average power gain, input impedance, radiation patterns and a 3:1 VSWR standard of the survivable antenna.

The final chapter, Chapter V, summarizes the results of this investigation and presents discussion, conclusions and recommendations that might be considered for future study.

II. NUMERICAL ELECTROMAGNETIC CODE

A. INTRODUCTION

Numerical Electromagnetic Code (NEC), [Ref. 2], is the most advanced method of moments computer code which analyzes the electromagnetic response of thin-wire antennas and other metallic arbitrary structures consisting of wires and surfaces in free space or over a ground plane. The NEC was developed by Lawrence Livermore Laboratories, under the joint sponsorship of the Naval Ocean Systems Center and the Air Force Weapons Laboratory.

NEC is a powerful tool for many engineering applications and it is ideal for modeling co-site antenna environments in which the interaction between antenna and environment cannot be ignored. The NEC requires the support of and access to a large main frame computer system and these computer systems are expensive and not always readily available.

The program is based on the numerical solution of integral equations (I.E) for the currents induced on the structure by an exciting field; in Appendix A, there is a brief description of I.E. The solution includes a Numerical Green's Function (NGF) for partitioned matrix solution and a treatment for lossy grounds, accurate for antennas very close to the ground surface.

A NEC model may include nonradiating networks and transmission lines, perfect and non-perfect conductors, lumped element loading, and ground planes. Excitation may be either voltage sources on the structure, an

incident plane wave of linear or elliptic polarization, or the field due to a Hertzian dipole. Output may include induced currents and charges, near or far zone electric or magnetic fields, impedance or admittance, and radiation patterns. Also many other commonly used parameters such as gain and directivity, power budget, and antenna to antenna coupling are also available.

B. MODELING GUIDELINES

The basic modeling structures using the NEC code are short, straight segments for wires and flat patches of surfaces. The most critical step to obtain results with high accuracy is to select the proper choice of the segments and patches for the model. The number of segments and patches should be the minimum required for accuracy because the running time of the program increases with a geometrical progression as this number increases. Guidelines for choosing segments and patches are given below.

1. Wires Computer Modeling Guidelines

A wire segment is defined from two parameters: the coordinates of its two end points and its radius. Figure 2.1 illustrates the wire segments parameters.

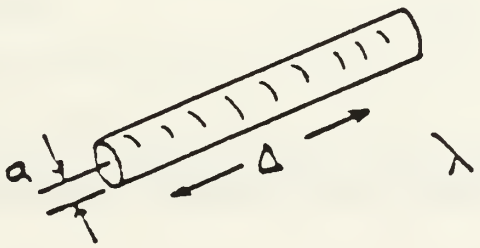

Figure 2.1. Thin-Wire Modeling

The segment length, Δ, should be less than about 0.1 wavelength, λ, at the desired frequency, F. Longer segments can be acceptable on long wires and shorter segments, 0.05 λ or less, are needed in modeling critical regions of an antenna. Segments smaller than 10^{-3} λ should be avoided since the similarity of constant and cosine components lead to numerical inaccuracy.

The radius of the wire, a, relative to λ depends on the kernel used in the IE, and there are available two approximations in NEC: the thin-wire kernel and the extended thin-wire kernel. Both of these approximations require $2\pi a/\lambda \ll 1$. The accuracy of the numerical solution is also dependent on Δ/a. For the thin-wire kernel, Δ/a must be greater than 8 and for the extended thin-wire may be as small as 2 for errors of less than 1%.

Figure 2.2 illustrates the coordinate system used, Tertocha [Ref.3:p. 16] with the thin-wire approximation.

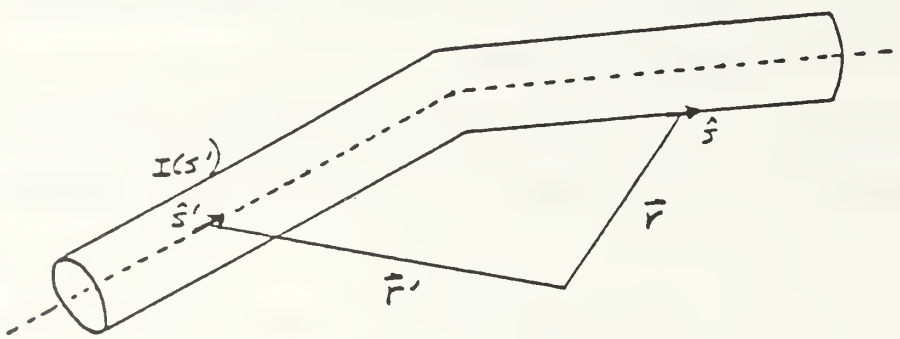

Figure 2.2. Thin-Wire Approximation Coordinate System

Some rules for the segment models follow:

- segments (or patches) may not overlap;

- a large radius change between connected segments may decrease accuracy, particularly with small Δ/a;
- a segment is required at each point where a network connection or voltage source will be located;
- the two segments on each side of a charge density discontinuity voltage source should be parallel and have the same length and radius;
- when wires are parallel and very close together, the segments should be aligned to avoid incorrect current perturbations from offset match points and segments junctions;
- it is safe to specify that wires should be several radii apart.

2. Over Ground Computer Modeling Guidelines

When a perfectly conducting ground is present, the code generates a reflected image. Structures may be close to the ground. For a horizontal wire with radius a and height h to the wire axis we have:

$$\sqrt{h^2 + a^2} > 10^{-6}\lambda$$

The height should be at least several times the radius for the thin-wire approximation to be valid. This method doubles the time to fill the interaction matrix.

C. NEC INPUT CARDS

Finishing with this overview of NEC, we next present the data that describe the input cards of the code. The data-card set consists of three types of cards: comment cards, structure geometry cards, and program control cards.

Every data card has a two-letter alphabetic code in columns one and two to identify the card to the program. All cards having numeric data are

punched in a similar format, with integer numbers first followed by real numbers. In Appendix B, there is a NEC input cards summary.

III. COMPUTER MODELS

This chapter presents the computer models used in this thesis. The models are masts with dimensions 24 x 3 x 3 meters, and were run over a perfect ground.

A. COMPUTER MODEL DEVELOPMENT

Using NEC geometry cards, the first step of this thesis was to build, with wires, the mast of a FFG-45 frigate.

Figure 3.1, from [Ref. 4:p. 11], illustrates the mast area of a FFG-45 frigate.

A 24 x 3 x 3 meter mast above a perfect ground was modeled with 0.05 meter radii wires over the frequency range 2-15 MHz.

Two different grid densities were chosen for two frequency ranges, 2-10 MHz and 11-15MHz. This was done to minimize computer time and storage. The important design considerations required to develop these computer models were the segmentation size, the radius of the segments and the proper geometrical model. For wire modeling, the main electrical consideration is segment length, Δ, relative to the wavelength, λ. For accurate results, as shown in Chapter II, Δ should be less than approximately 0.1 λ at the desired frequency. The wire radius, a, relative to the wavelength, is limited to the approximation, that the relationship of, $[(2\pi a)/\lambda] \ll 1$ must hold for the configuration.

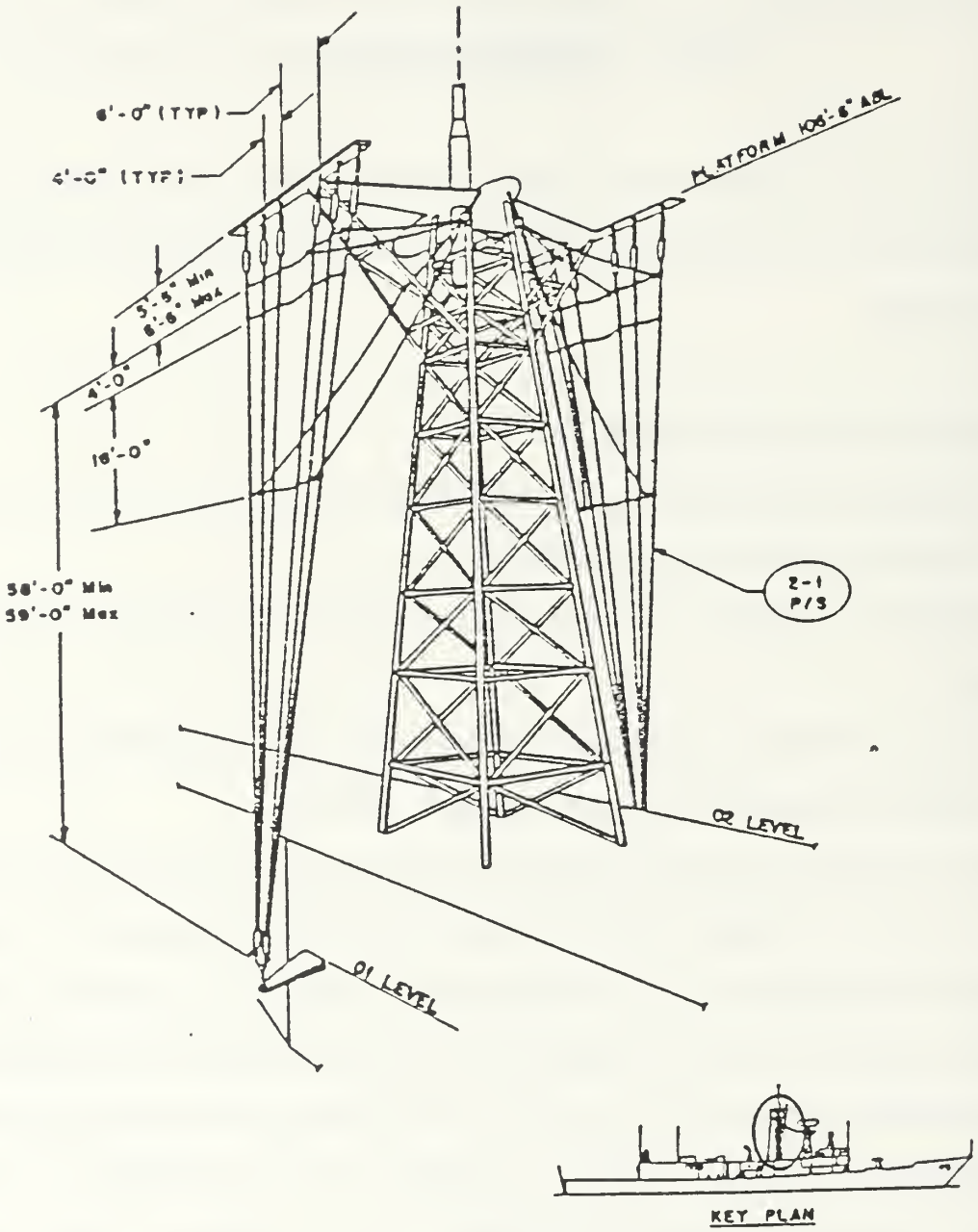

Figure 3.1 Mast Area of a FFG-45 Frigate.

Table 3.1 lists the frequency, and corresponding grid spacings. For choosing the frequency, we used the formula: $\Delta f = (f_{LO} \cdot f_{HI})^{1/(N-1)}$, so for f_{LO} = 2 MHz, and f_{HI} = 6 MHz, we will have f = 3.46 MHz = $f_{LO} \cdot \Delta f$, if N=3

TABLE 3.1

MAST MODEL FREQUENCY AND GRID SPACINGS IN WAVELENGTHS

Frequency in MHz	No. of Segments	Grid Spacing in Meters	Wavelength in Meters	Low Frequen. Grid Spacing in Wavelengths	High Frequen. Grid Spacing in Wavelengths
2.00	96	3	149.99	0.02001	0.01010
2.63	96	3	114.00	0.02632	0.01316
3.00	96	3	99.93	0.03002	0.01501
3.46	96	3	86.65	0.03462	0.01731
4.00	96	3	74.95	0.04003	0.02001
4.56	96	3	65.75	0.04563	0.02282
5.23	96	3	57.32	0.05233	0.02617
6.00	96	3	49.97	0.06004	0.03002
6.80	96	3	44.09	0.06805	0.03402
7.74	96	3	38.73	0.07745	0.03873
8.80	96	3	34.07	0.08806	0.04403
10.00	96	3	29.98	0.05003	0.10007
11.00	688	1	27.25	0.03669	0.01835
11.90	688	1	25.19	0.03969	0.01985
12.85	688	1	23.33	0.04286	0.02143
13.90	688	1	21.57	0.04636	0.02318
15.00	688	1	19.99	0.05003	0.02502

Figures 3.2 and 3.3 show the wire-grid mast model used.

The wire-grid mast models were run at seventeen different frequencies to produce the Numerical Green's Function (NGF). Appendix C shows the geometry data cards for the frequency range 2-10 MHz, and the frequency range 11-15 MHz.

MVS was used on the main frame of the IBM 3033 Network because the programs were CLASS C and J.

Table 3.2, from [Ref. 5:p. 29], lists the CPU time per job, and corresponding CLASS of batch jobs.

TABLE 3.2

MAXIMUM TIME ALLOWED FOR EACH CLASS

CLASS	TAPE DRIVERS	CPU TIME (per job)
A	No	5 sec.
B (default)	No	30 sec.
C	No	3 min.
E	Yes-2	30 sec.
F	Yes-3	3 min.
G	Yes/No	15 min.
J	No	60 min.
K	Yes-up to 6	60 min.

- J-class and K-class jobs are overnight jobs. Present default REGION size is 512K.
- The numbers in column two represent the MAXIMUM number of tape drivers to be used by the job at one time for the designated class

Front-View

THETA = 60.00 PHI = 60.00 ETA = 90.00

Side-View

THETA = 90.00 PHI = 90.00 ETA = 90.00

Top-View

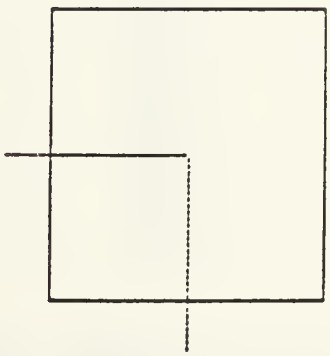

THETA = 0.00 PHI = 90.00 ETA = 90.00

Figure 3.2 Wire-Grid Mast Model for Frequency Range 2-10 MHz.

Front-View

THETA = 60.00 PHI = 60.00 ETA = 90.00

Top-View

Side-View

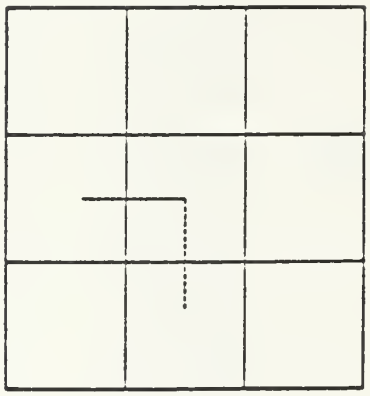

THETA = 90.00 PHI = 90.00 ETA = 90.00

THETA = 0.00 PHI = 90.00 ETA = 90.00

Figure 3.3 Wire-Grid Mast Model for Frequency Range 11-15 MHz.

The NEC was designed for a 64 bit computer, and the IBM 3033 Network has 32 bits, so double precision is often needed. This was verified in the calculation of the average power gain ($\overline{G}$) and by smooth impedance variation.

The next step was to energize the mast at its base to study the change of the mast input impedance with frequency variation, and to evaluate the average power gain ($\overline{G}$), and the vertical and horizontal radiation patterns. Five different methods of feeding the bottom of the mast, by four corners , three corners, two adjacent corners, two diagonal corners, and one corner, were modeled to evaluate the characteristics of the driven antenna.

Appendix D shows a typical data set used to calculate the average power gain, and the impedance. Appendix E shows two data sets used to evaluate the vertical and horizontal radiation pattern, respectively.

IV. COMPUTER MODEL RESULTS

This chapter presents the results of the computer models described in Chapter III.

A. AVERAGE POWER GAIN

A common criterion applied to antenna computer models is to calculate the accuracy of the model with average power gain ($\overline{G}$). An average power gain of 2.0 is used to represent a theoretical antenna radiating in a half space over a perfect ground. Average gain is obtained by integrating the radiated power density to find the total radiated power, then compare that to the total input power at the feed points. These should be equal for a valid solution.

Five data sets in seventeen different frequencies were run to evaluate the average power gain, as a function of the method of driving the mast computer models. The results are shown in the next tables.

Tables 4.1 lists the calculated ($\overline{G}$), for five different methods of driving the mast computer model at its base, in the frequency range 2-10 MHz.

Tables 4.2 lists the calculated ($\overline{G}$), for driving all base segments of the mast computer model , in the frequency range 11-15 MHz.

The average gain was not acceptable in the cases of feeding three base segments and two adjacent base segments. The computer model used is apparently not adequate for the case of unsymmetrical feeds.

The data presented in Tables 4.1 and 4.2 is over a limited range and more investigation needs to be done before any firm conclusions may be drawn.

TABLE 4.1

AVERAGE POWER GAIN OF MAST COMPUTER MODEL
IN FREQUENCY RANGE 2-10 MHz vs. FEED POINT POSITIONS

Frequency in MHz	4 Base Segm.	3 Base Segm.	2 Adjac. Base Segm.	2 Diag. Base Segm.	1 Base Segm.
2.00	1.99	2.04	2.07	2.00	1.99
2.63	1.99	2.08	2.12	1.99	1.99
3.00	1.99	2.10	2.15	1.99	2.00
3.46	1.99	2.13	2.19	1.99	2.00
4.00	1.99	2.17	2.24	1.98	2.00
4.56	1.99	2.21	2.29	1.97	2.00
5.23	1.99	2.25	2.35	1.96	2.00
6.00	1.99	2.28	2.38	1.95	1.99
6.80	1.99	2.24	2.33	1.95	1.99
7.74	1.99	2.13	2.19	1.98	1.99
8.80	1.99	2.21	2.30	1.95	1.99
10.00	1.99	2.35	2.46	1.91	2.01

TABLE 4.2

AVERAGE POWER GAIN OF MAST COMPUTER MODEL
IN FREQUENCY RANGE 11-15 MHz vs. FEED POINT POSITIONS

Frequency in MHz	For Driving 12 Base Segments
11.00	1.99
11.90	1.99
12.85	1.99
13.90	1.99
15.00	1.99

B. INPUT IMPEDANCE

The data set shown in Appendix D was run to evaluate the variation of input impedances of the mast computer models as a function of the way the mast is driven. The results are illustrated on two different curves, one for the resistances (R), and the other for the reactances (jX).

Figures 4.1-4.3 are curves for driving four and twelve segments of the mast in the frequency ranges 2-10 MHz, and 11-15 MHz respectively. Tables 4.3-4.5 list the plotted values of the input impedances. There is a set of curves, in Appendix F, for four different methods of feeding the bottom of the mast computer model, in the frequency range 2-10 MHz. From these curves it is seen that, the impedances for the four and twelve feed points

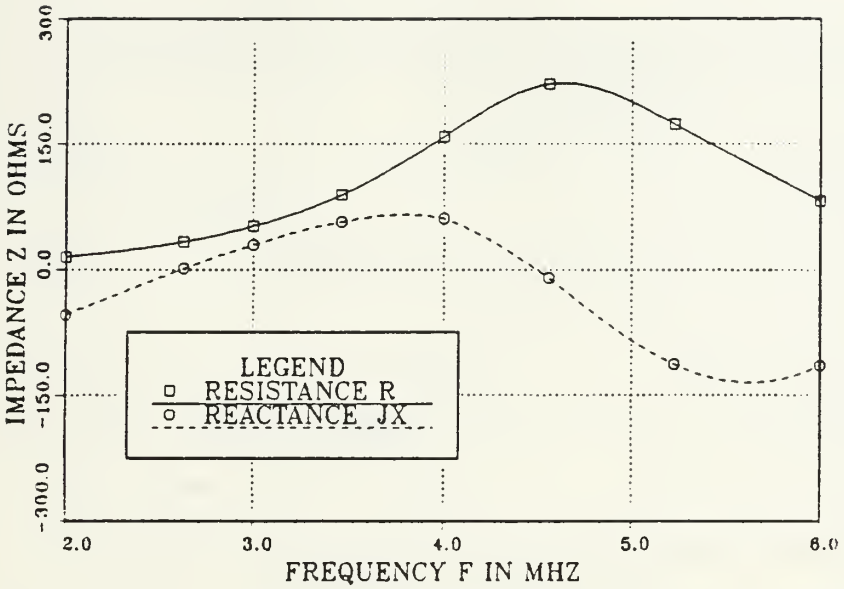

Figure 4.1 Mast Input Impedances for Driving Four Base Segments in Frequency Range 2-6 MHz.

TABLE 4.3

MAST INPUT IMPEDANCES FOR DRIVING FOUR BASE SEGMENTS IN FREQUENCY RANGE 2-6 MHZ.

Frequency (in MHz)	Resistance (R in Ω)	Reactance (jX in Ω)
2.00	15.00	-53.60
2.63	33.20	+1.40
3.00	51.90	+29.00
3.46	89.20	+56.80
4.00	158.80	+60.70
4.56	221.80	-10.00
5.23	173.40	-112.90
6.00	82.00	-114.00

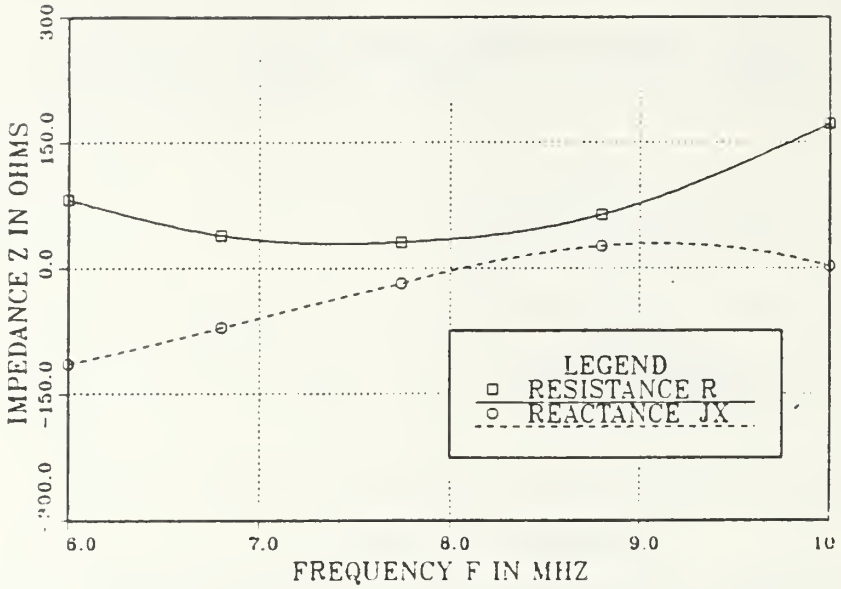

Figure 4.2 Mast Input Impedances for Driving Four Base Segments in Frequency Range 6-10 MHz.

TABLE 4.4

MAST INPUT IMPEDANCES FOR DRIVING FOUR BASE SEGMENTS IN FREQUENCY RANGE 6-10 MHZ.

Frequency (in MHz)	Resistance (R in Ω)	Reactance(jX in Ω)
6.00	82.00	-114.00
6.80	38.90	-71.00
7.74	30.70	-18.30
8.80	64.00	+26.50
10.00	172.00	+2.00

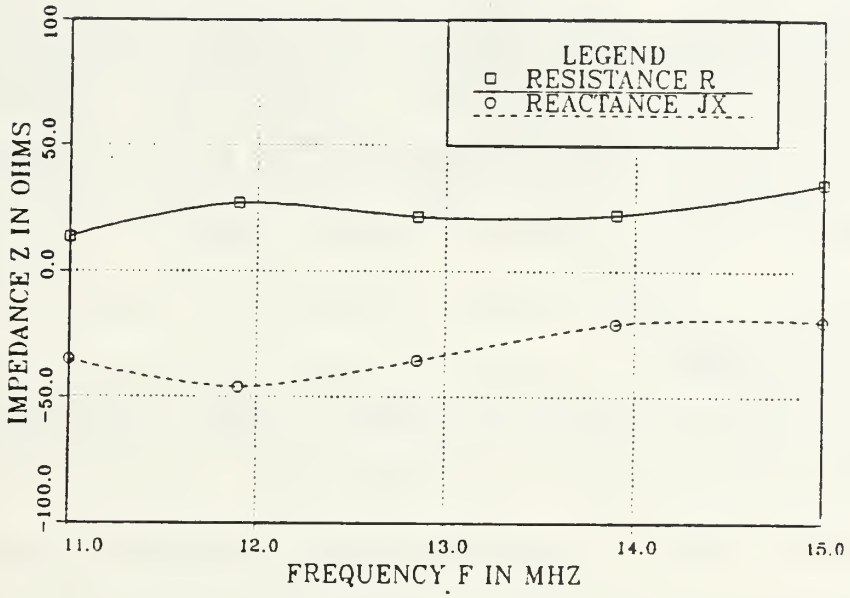

Figure 4.3 Mast Input Impedances for Driving All Base Segments in Frequency Range 11-15 MHz.

TABLE 4.5

MAST INPUT IMPEDANCES FOR DRIVING ALL BASE SEGMENTS IN FREQUENCY RANGE 11-15 MHZ.

Frequency (in MHz)	Resistance (R in Ω)	Reactance (jX in Ω)
11.00	13.60	-35.00
11.90	27.00	-45.70
12.85	21.50	-35.60
13.90	22.30	-21.10
15.00	34.65	-20.10

tend to be more stable than from the other methods of driving the model. The resistances of those models, four and twelve feed points, are typically more than those of the other feed models. In addition their reactances are typically more capacitive than the reactances of the other feed models. Low resistance is hard to match, and high resistance is easier to match.

C. RADIATION PATTERNS

Radiation patterns for the mast computer models driven with E-gap voltage source were obtained in the frequency range 2-15 MHz. The data sets shown in Appendix E were run in eight different frequencies 2, 4, 6, 7.74, 10, 11, 12.85, and 15 MHz with five different methods of driving the base of the mast computer models.

For frequencies less than 6 MHz, the radiation patterns looked like patterns of equal height whip antenna. The horizontal patterns became omnidirectional and the vertical patterns looked similar to those of an equal size whip antenna. Figure 4.4 is a typical of the horizontal pattern of the mast computer model at 2 MHz showing the omnidirectional shape. Figure 4.5 is a typical vertical pattern at 2 MHz, and Figure 4.6 and 4.7 is the vertical and horizontal pattern of a whip antenna of equal height provided for comparison.

At frequencies over the 6 MHz, the vertical patterns looked similar to those of an equal height whip antenna but with less lobing near vertical incident ± 30 deg. Figure 4.8 is a typical vertical pattern at 6 MHz. The horizontal patterns became omnidiarectional and at the freuqency of 10 MHz we have an azimuth variation. Figure 4.9 and 4.10 are typical horizontal

pattern at 10 MHz showing the azimuth variation . For the frequency range 11-15 MHz the horizontal patterns became omnidirectional and the vertical patterns looked similar to those of an equal size whip antenna. Figure 4.11 and 4.12 are typical vertical and horizontal patterns at 11 MHz, respectively. In Appendix G there is a complete set for vertical and horizontal patterns vs the method of driving the base of the mast computer models for the frequency range 2-15 MHz. Also, in Appendix G, provided for comparison is a set of vertical patterns of the whip antenna of equal height.

D. VOLTAGE STANDING WAVE RATIO (VSWR)

A 3:1 VSWR is considered a reasonable criterion for broadband antenna operation [Ref. 3:pp. 68-72]. Not too many antennas satisfy this criterion over an operating band of interest but many may be brought into this region by use of series inductance or capacitance. Figure 4.13 shows the 3:1 VSWR circle. The shaded region represents the impedance region of the Smith Chart which may be moved into the 3:1 VSWR circle by use of series reactances. This thesis will consider impedances that fall in this region and the 3:1 VSWR circle as acceptable impedances for operational requirements.

Figures 4.14 through 4.19 are Smith Chart plots of the impedance characteristics for the mast computer models. Table 4.6 lists the frequencies which fall in the 3:1 VSWR circle or are matchable by series reactances to the 3:1 VSWR. This table reveals that the four feed point position survivable antenna design has a superior bandwidth. Based on the frequency ranges over which the antenna's impedance is series matchable to

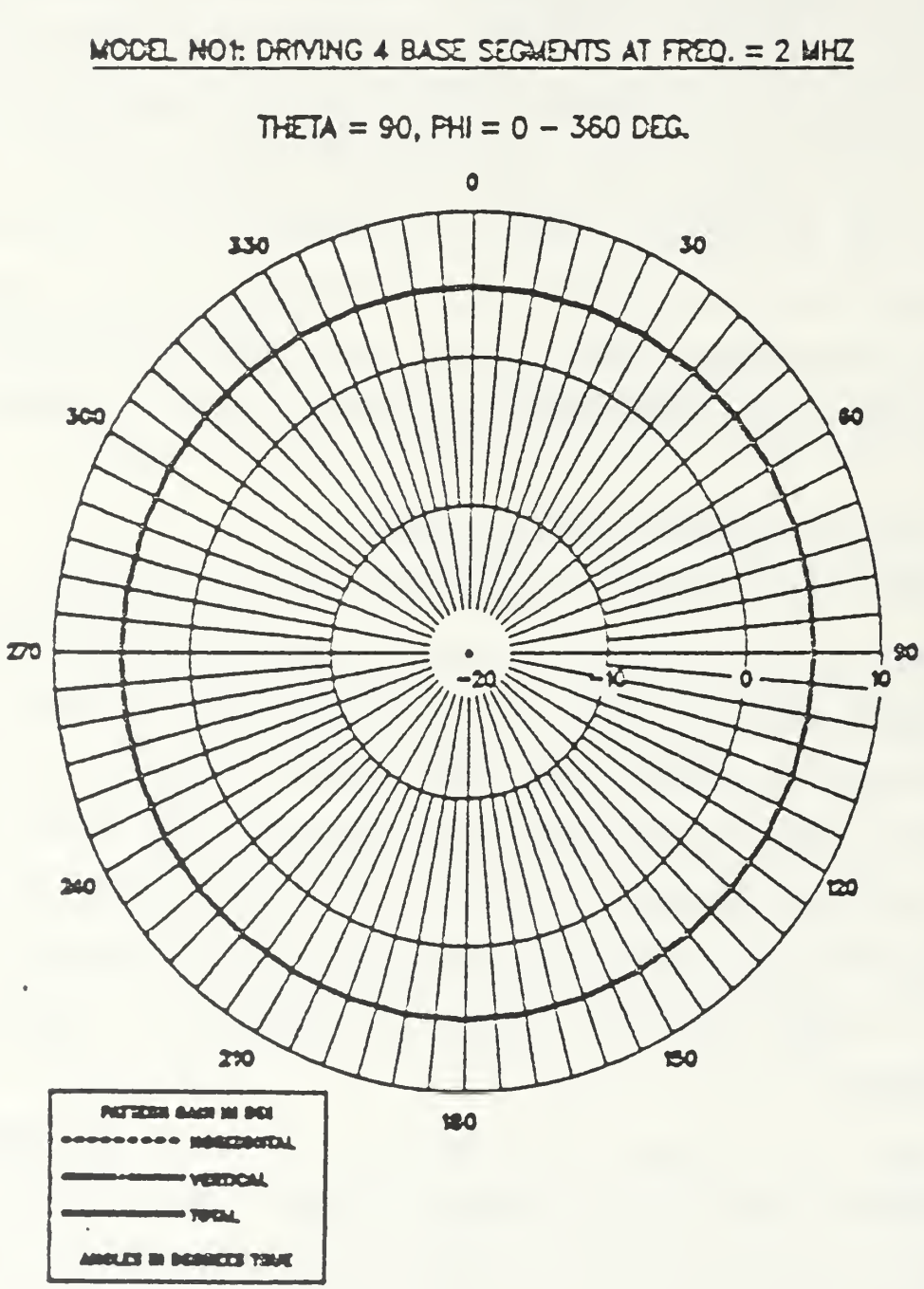

Figure 4.4 E-Field Horizontal Radiation Pattern: F = 2 MHz, vs. Four Feed Point Positions.

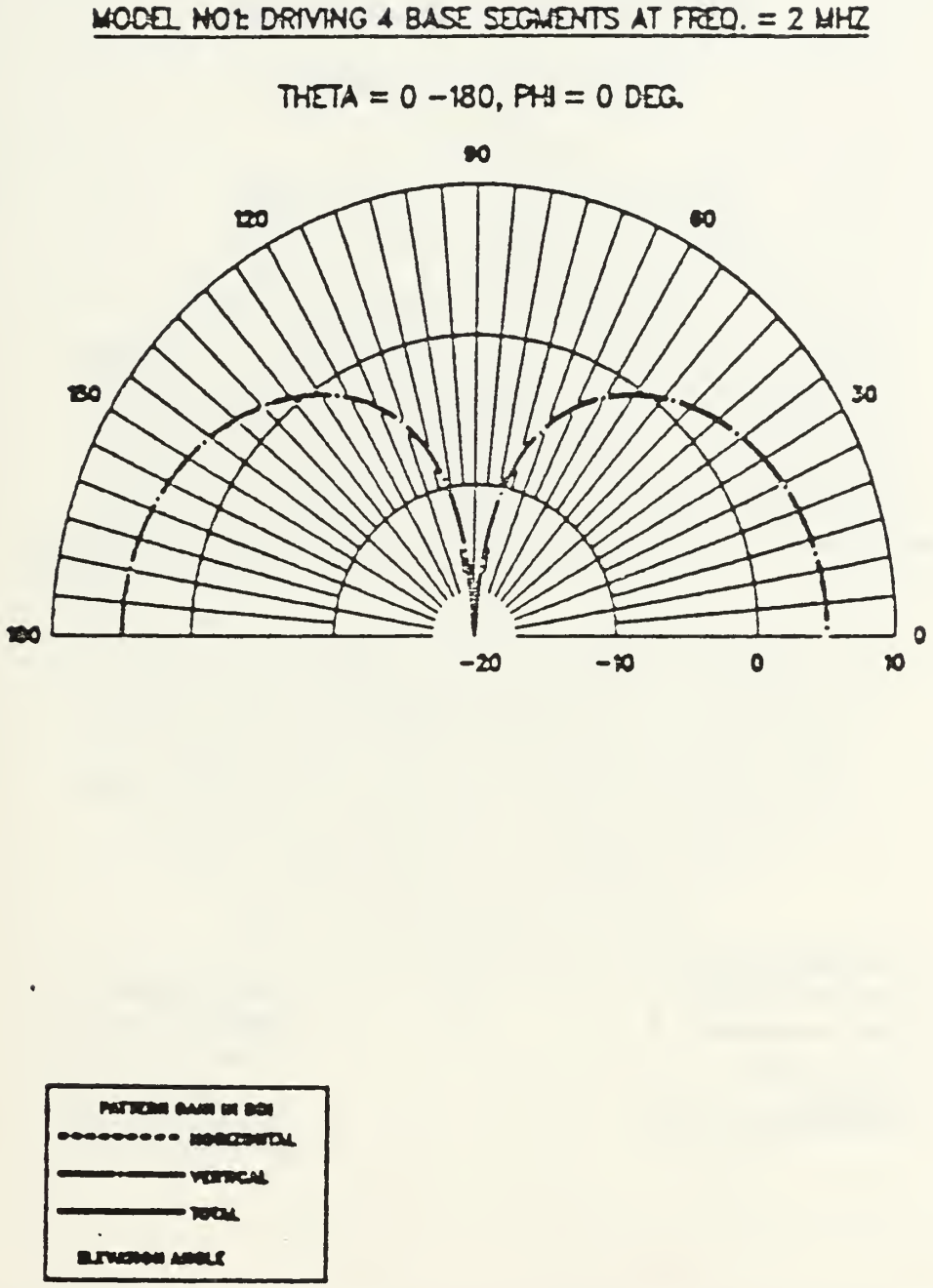

Figure 4.5 E-Field Vertical Radiation Pattern: F = 2 MHz, vs. Four Feed Point Positions.

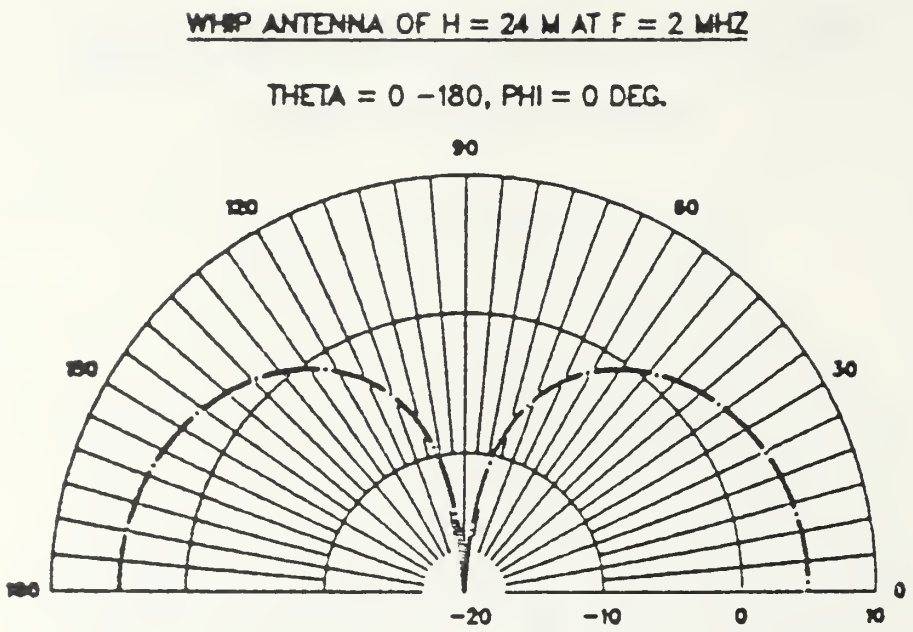

Figure 4.6 E-Field Vertical Radiation Pattern of Whip Antenna Whose Height Is Equal to That of the Antenna of Figures 4.4 and 4.5.

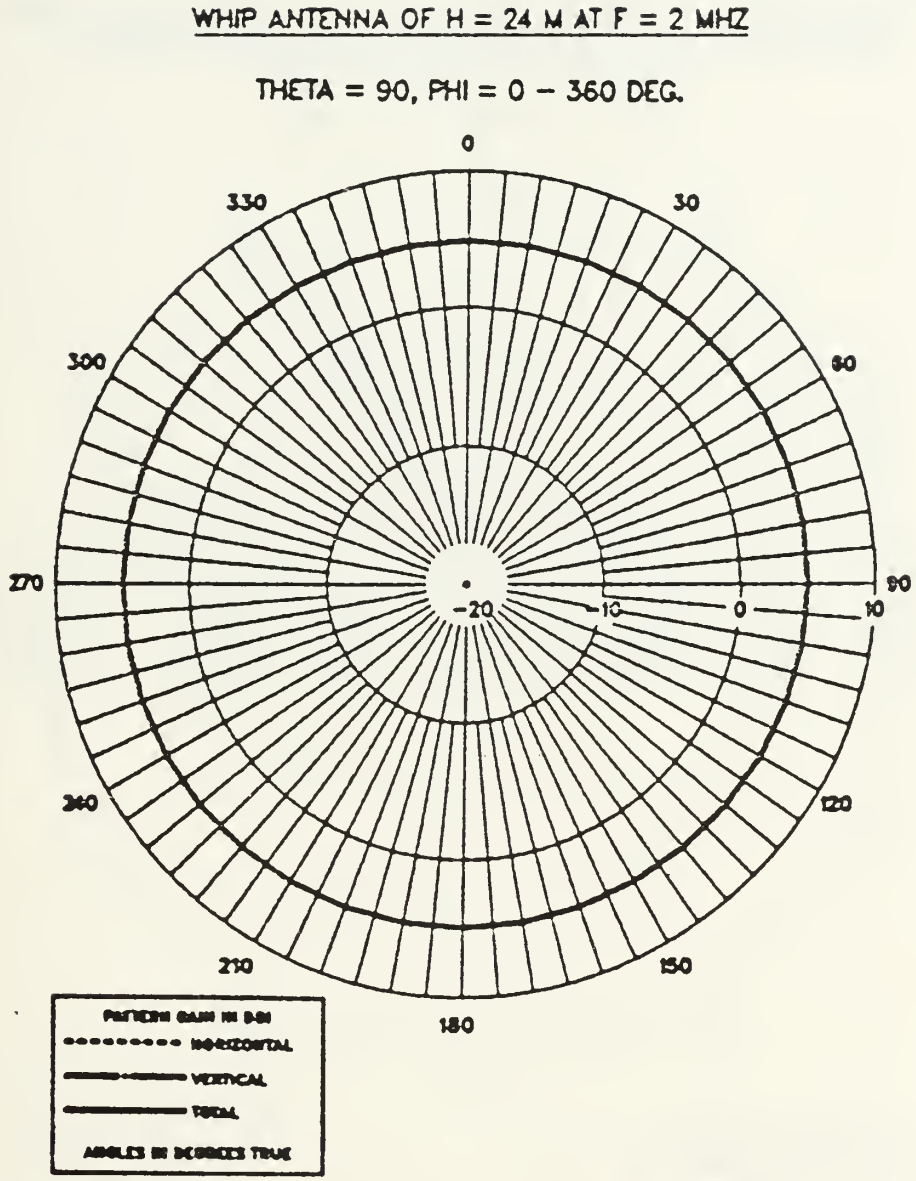

Figure 4.7 E-Field Horizontal Radiation Pattern of Whip Antenna Whose Height Is Equal to That of the Antenna of Figures 4.4 and 4.5.

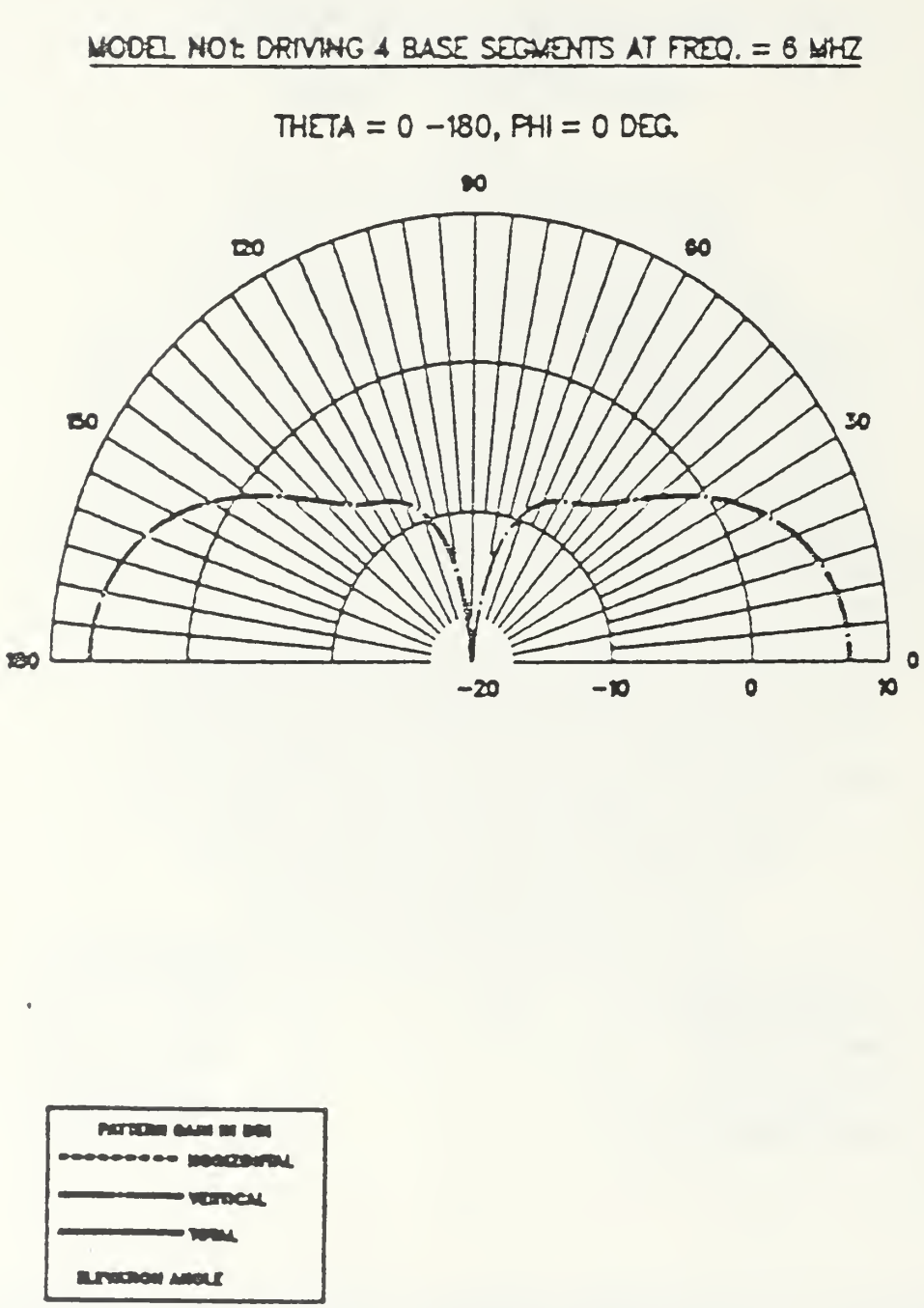

Figure 4.8 E-Field Vertical Radiation Pattern: F = 6 MHz, vs. Four Feed Point Positions.

MODEL NO1: DRIVING 2 ADJACENT BASE SEGMENTS AT FREQ = 10 MHZ

THETA = 90, PHI = 0 - 360 DEG.

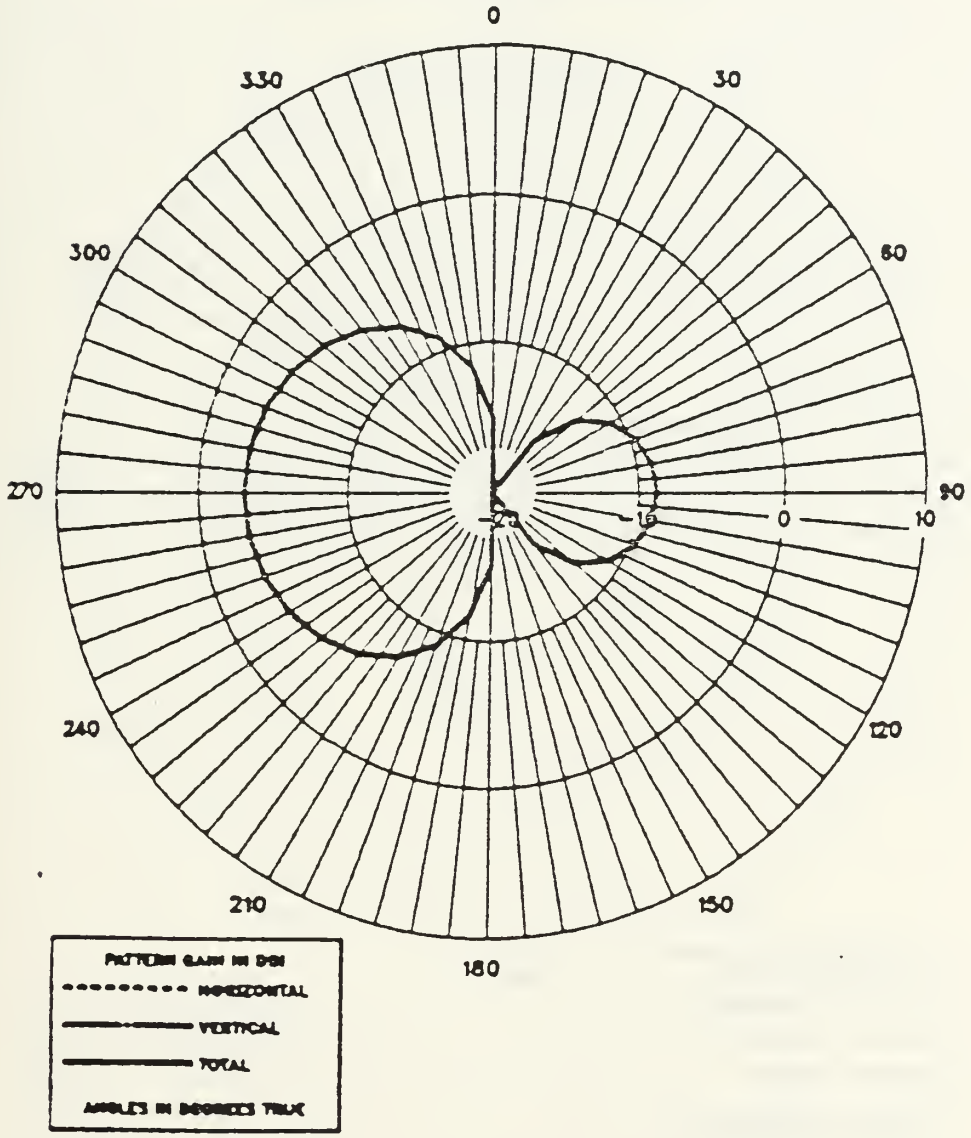

Figure 4.9 E-Field Horizontal Radiation Pattern: F = 10 MHz, vs. Two Adjacent Feed Point Positions.

MODEL NO1: DRIVING 1 BASE SEGMENT AT FREQ. = 10 MHZ

THETA = 90, PHI = 0 – 360 DEG.

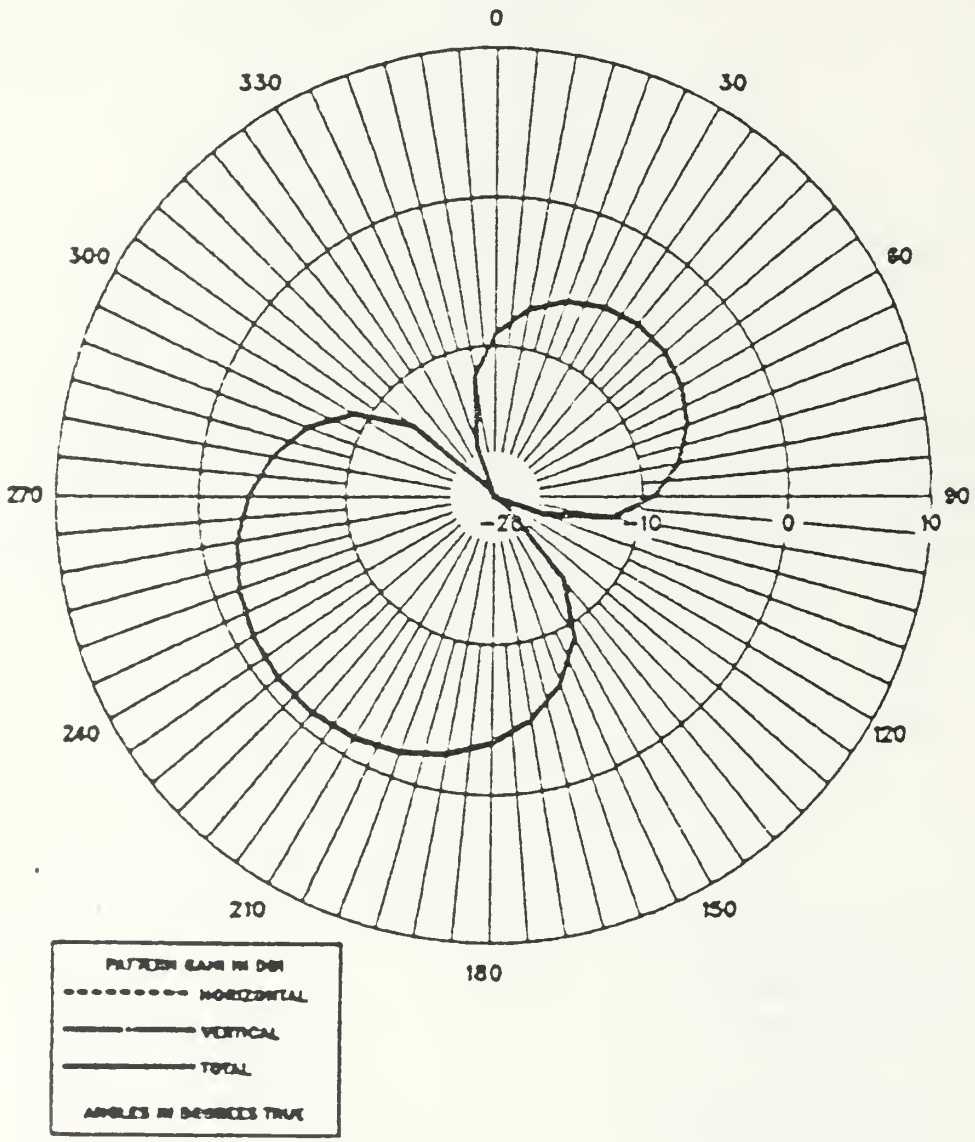

Figure 4.10 E-Field Horizontal Radiation Pattern: F = 10 MHz, vs. One Feed Point Position.

MODEL NO 2: DRIVING 12 BASE SEGMENTS AT FREQ. = 11 MHZ

THETA = 0 -180, PHI = 0 DEG.

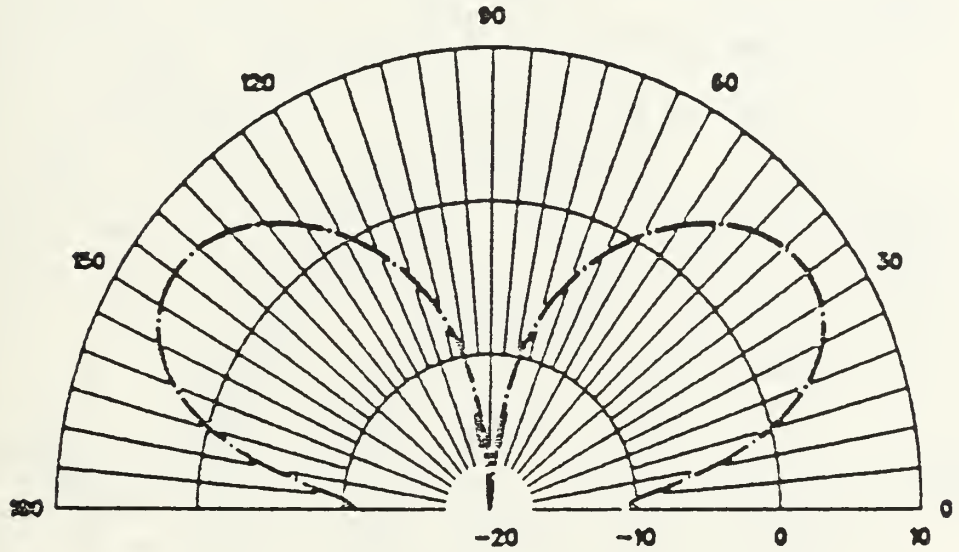

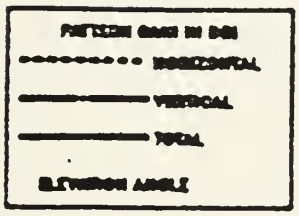

Figure 4.11 E-Field Vertical Radiation Pattern: F = 11 MHz, vs. All Base Feed Point Positions.

MODEL NO 2: DRIVING 12 BASE SEGMENTS AT FREQ. = 11 MHZ

THETA = 90, PHI = 0 – 360 DEG.

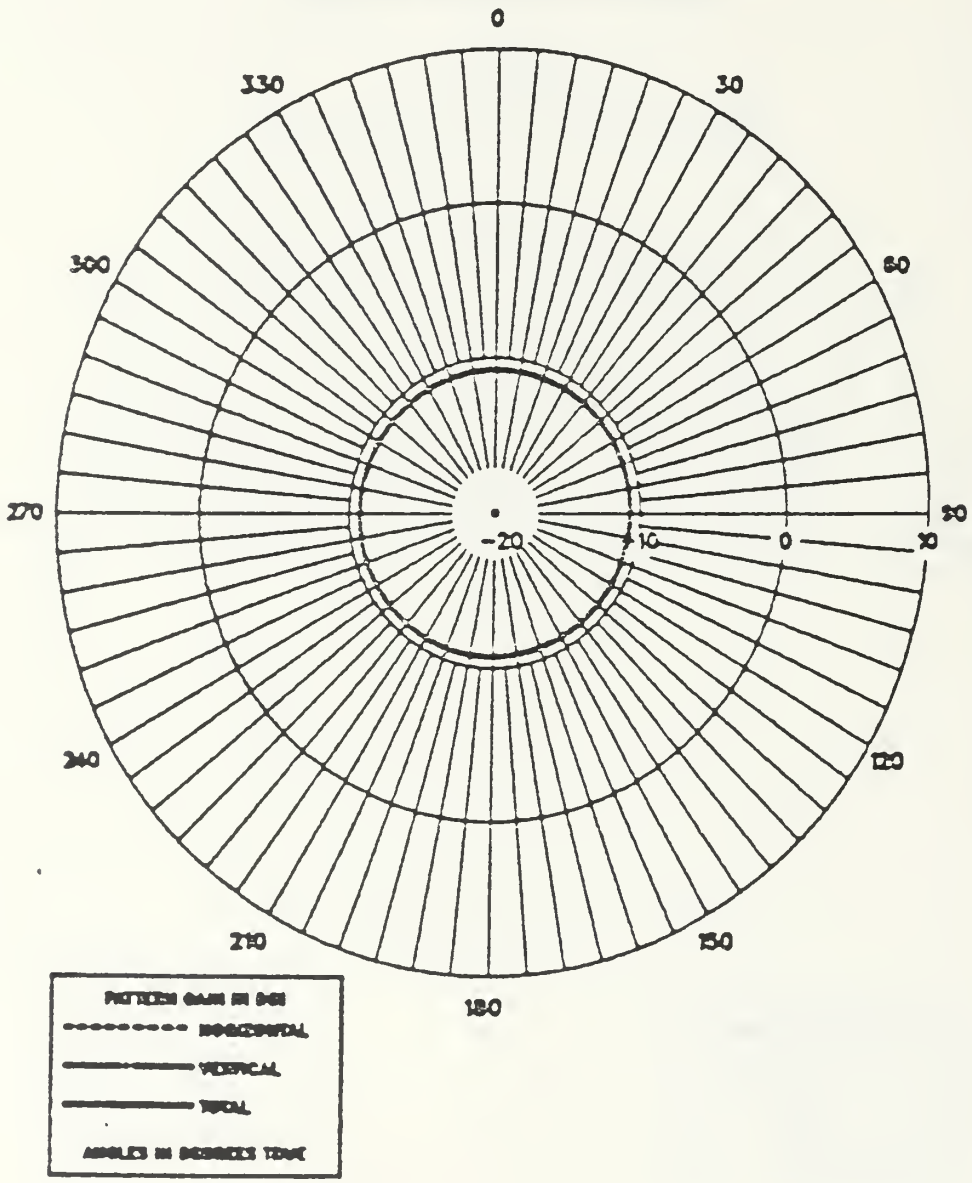

Figure 4.12 E-Field Horizontal Radiation Pattern: F = 11 MHz, vs. All Base Feed Point Positions.

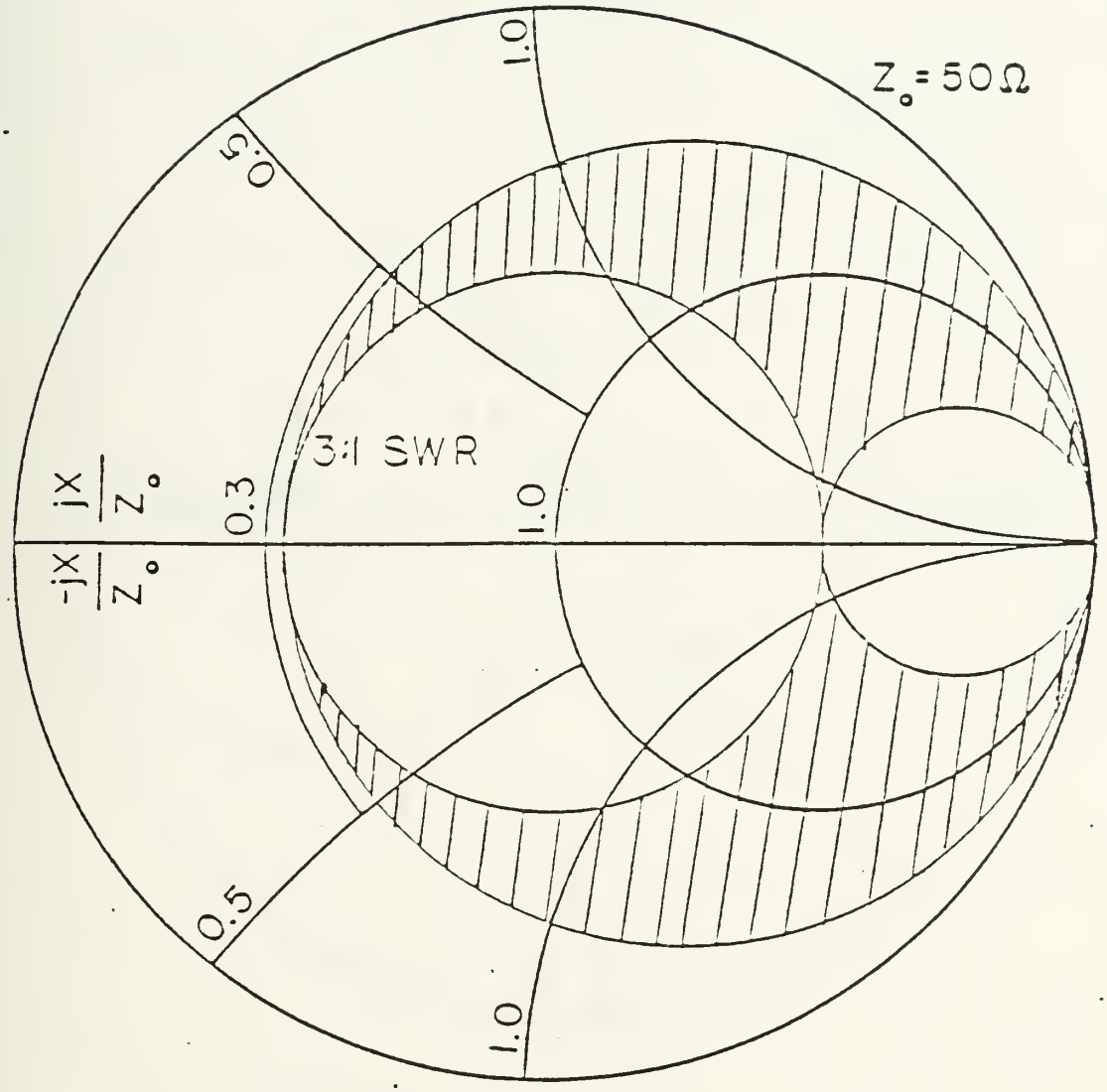

Figure 4.13 Smith Chart Showing 3:1 VSWR Matchable Region.

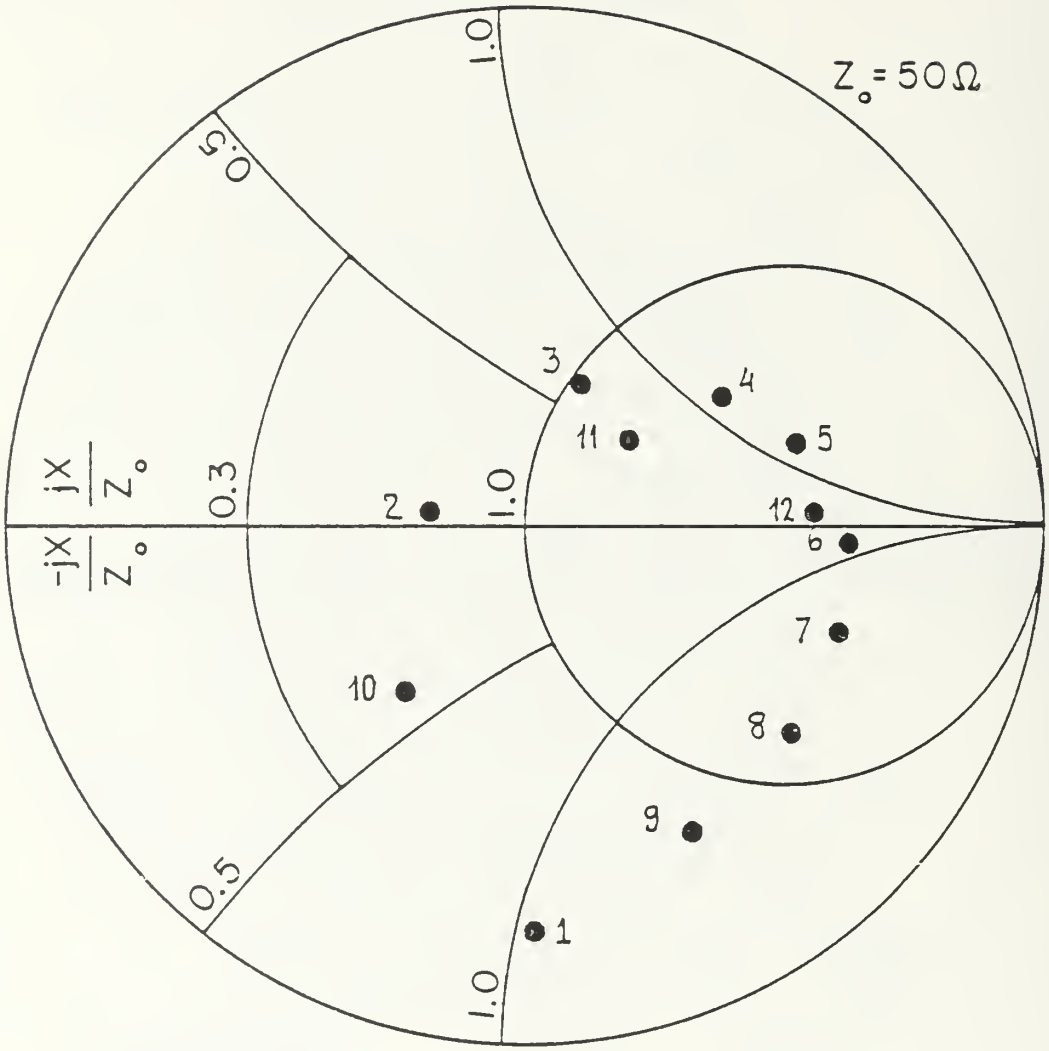

Figure 4.14 Impedance Plot of Four Feed Point Positions in Frequency Range 2-10 MHz.

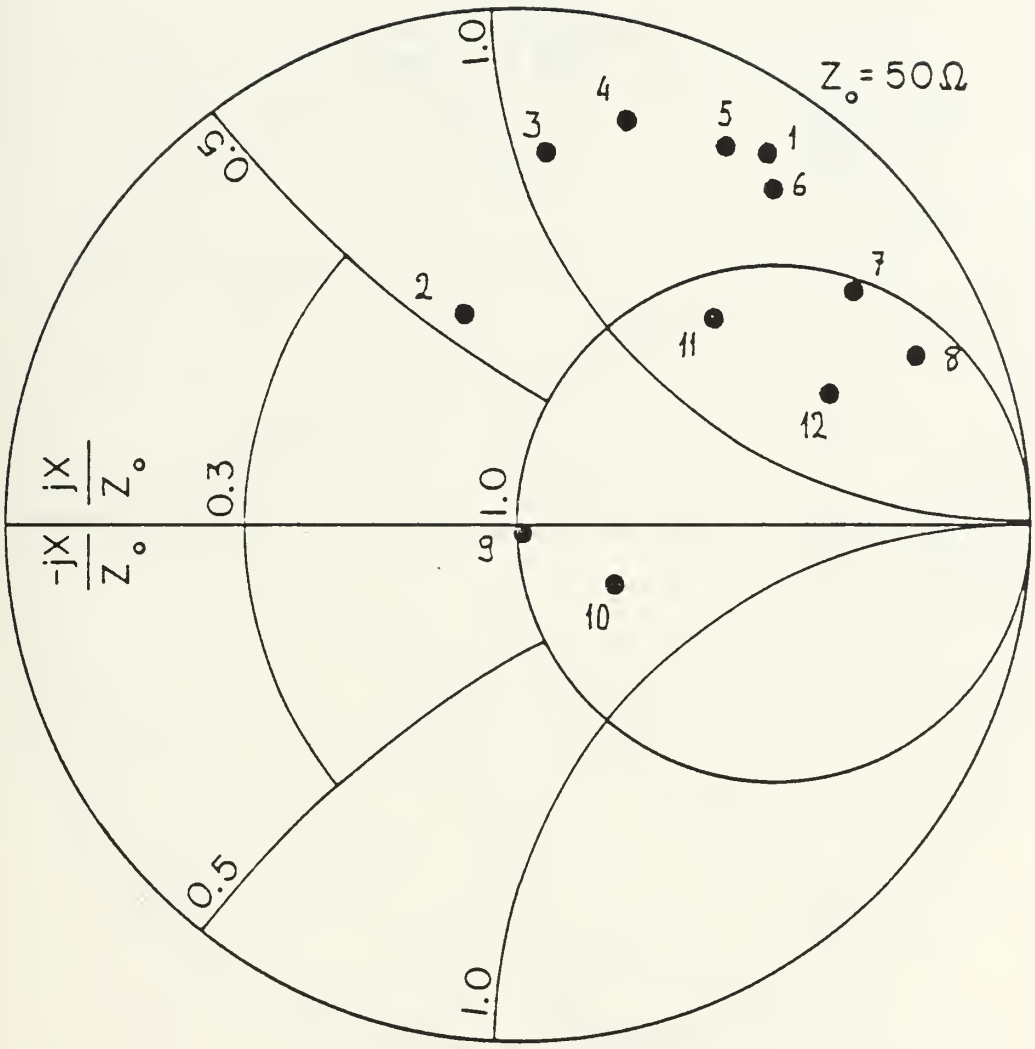

Figure 4.15 Impedance Plot of Three Feed Point Positions in Frequency Range 2-10 MHz.

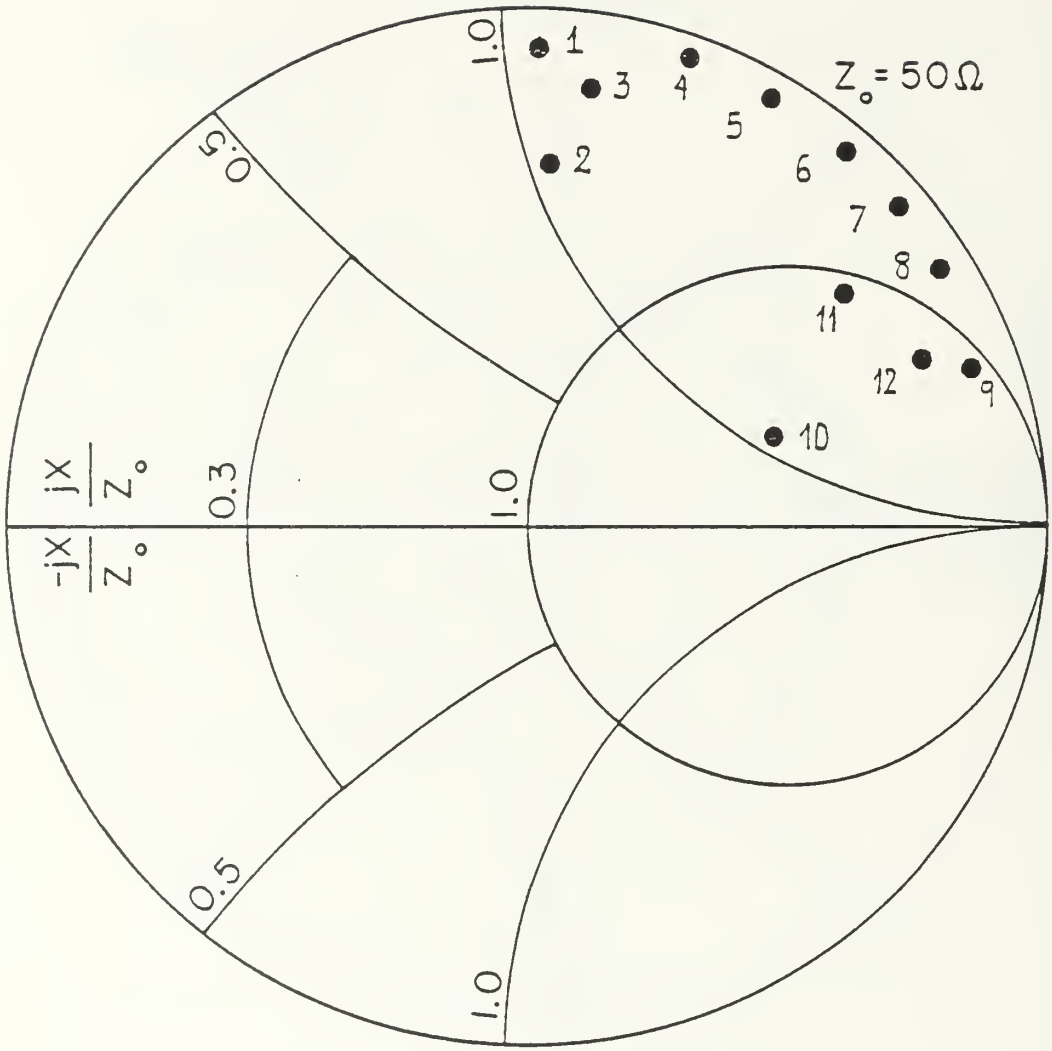

Figure 4.16 Impedance Plot of Two Adjacent Feed Point Positions in Frequency Range 2-10 MHz.

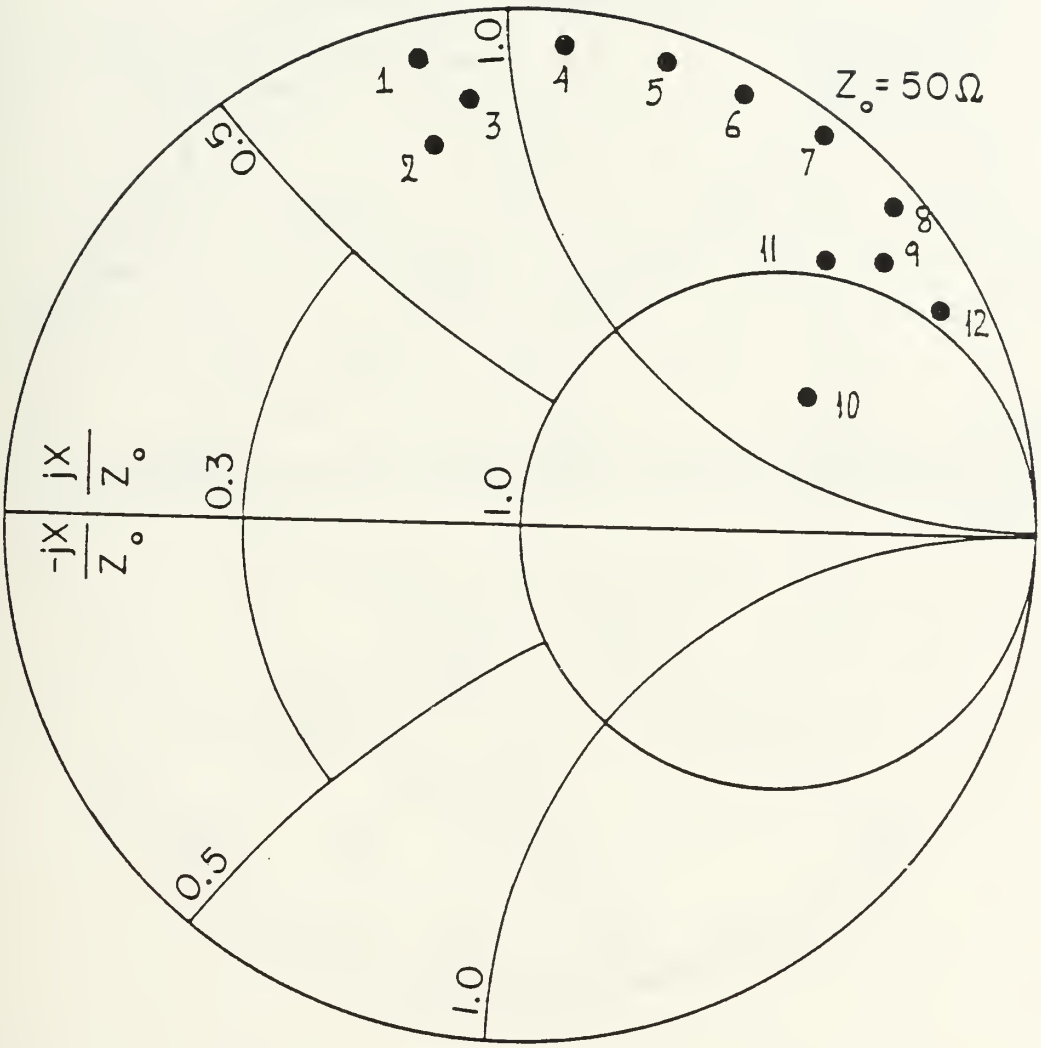

Figure 4.17 Impedance Plot of Two Diagonal Feed Point Positions in Frequency Range 2-10 MHz.

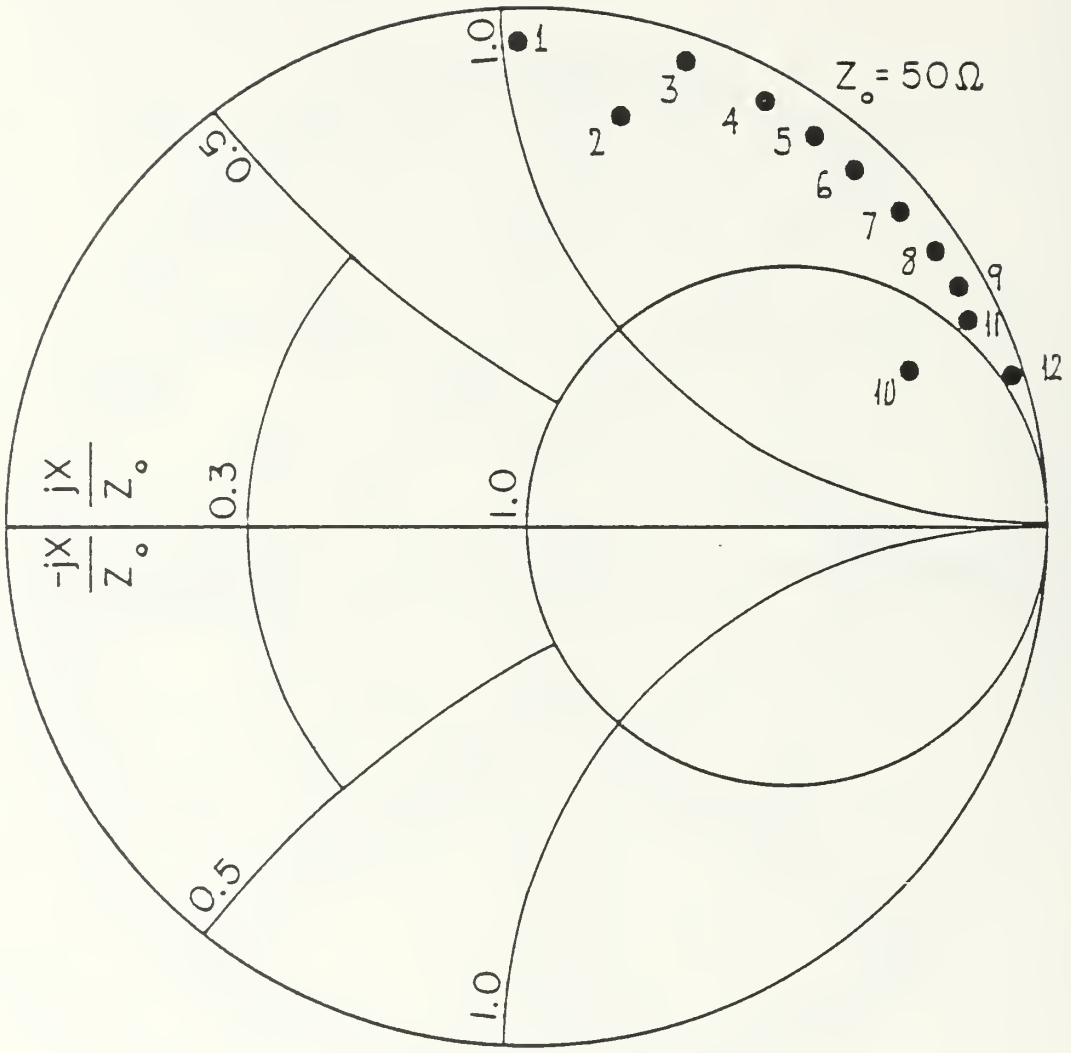

Figure 4.18 Impedance Plot of One Feed Point Position in Frequency Range 2-10 MHz.

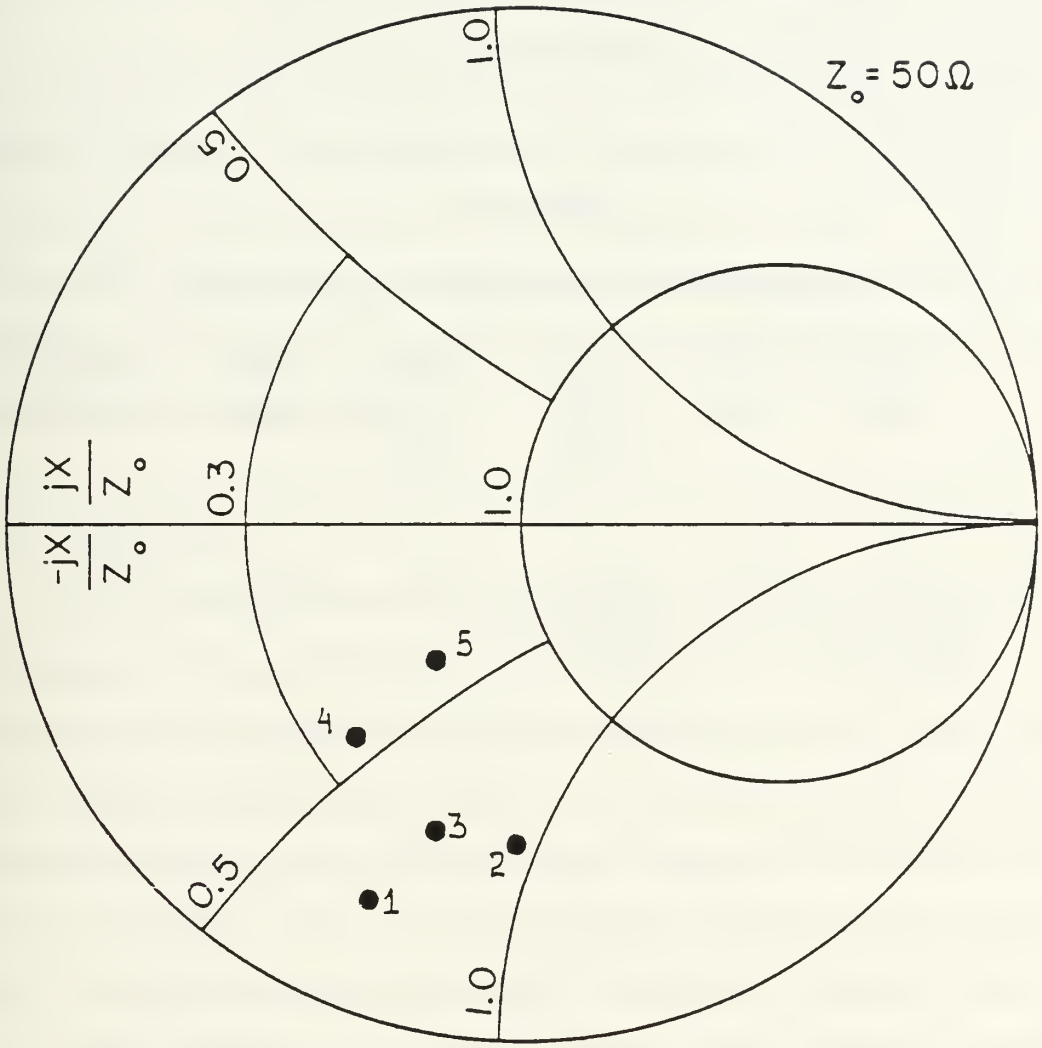

Figure 4.19 Impedance Plot of All Base Feed Point Positions in Frequency Range 11-15 MHz.

a 3:1 VSWR, this antenna design has an acceptable frequency range from 2-4 and 5.23-10 MHz. Also the twelve feed point position survivable antenna design has an acceptable frequency range from 11-15 MHz.

TABLE 4.6

FREQUENCIES SATISFYING 3:1 VSWR CRITERIA

	4 Feed Segm.	3 Feed Segm.	2 Adjac. Feed Segm.	2 Diag. Feed Segm	1 Feed Segm.	12 Feed Segm.
Frequ. in MHz.	2-4	2-8.8	2-6.8	2-10	2-10	11-15
	5.23-10		8.8-10			

V. CONCLUSIONS AND RECOMMENDATIONS

This thesis has taken a mast of a FFG-45 frigate and developed computer models for the antenna which was deployed on a simulated mast, created by a wire-grid model, in two frequencies ranges 2-10 MHz, and 11-15 MHz, using the NEC. The simulated mast used to determine the input impedance and radiation patterns of the survivable antenna over the HF frequency range of 2-15 MHz.

A. CONCLUSIONS

For the simulated mast survivable antenna, the input impedance is the impedance seen by the voltage source used to drive the antenna. A grid spacing of 0.1 wavelength is usually adequate, however, the grid density does affect the impedance of a computer model. Grid density is not the only parameter affecting the computer model's impedance. The type of voltage source, the number and size of feed segments, and the radius of the wires also affect the impedance. The manner in which the impedance varies with the modeling parameters cannot be predicted without a parameter variation study. The radiation patterns define the gain. This thesis checked the spatial distribution of the phi (ϕ) and theta (θ) polarized electric field componets radiated in the far-field zone of the antenna.

The results of this investigation indicate that a simulated mast driven at its base in five different methods of feeding does possess radiation patterns and impedance characteristics which make it a feasible design.

Of the two structures investigated the four feed position survivable antenna design has the superior impedance characteristics. This antenna is matchable to 3:1 VSWR over the frequency ranges of 2-4 MHz and 5.23-10 MHz and possesses a 3:1 VSWR without the need of matching network (series reactances) over the frequency ranges of 2.63-4 MHz and 7.74-10 MHz.

For frequencies less than 6 MHz, the radiation patterns of the five different methods of driving the base of the mast computer models are similar to those of an equal height whip antenna. Antennas which are electrically short produce similar radiation patterns almost independent of the antenna's geometry. This indicates that the mast itself has the dominant effect. At frequencies over the 6 MHz, the vertical pattern looked similar to those of an equal height whip antenna but with less lobing near vertical incidence, $\theta = \pm 30$ deg. As frequency increases, we have an azimuth variation at 10 MHz. For the frequency range 11-15 MHz the horizontal pattern becomes omnidirectional and the vertical pattern looks like that of an equal height whip antenna.

B. RECOMMENDATIONS

There are many aspects of this study which warrant further investigation.

- Determine the antenna's response at higher frequencies.
- Use an elevated feed for the mast computer model, similar to a sleeve antenna.

- Reduce the height of the simulated mast to increase the survivability of the antenna during combat.

- Increase the number of segments in the vicinity of the feed points in the case of unsymmetrical feed which suffered from poor average gain.

- Finally,physical models of the survivable antenna should be built for comparison to the computer model.

APPENDIX A

INTEGRAL EQUATIONS (IE)

A widely used technique for solving the **IE** is the application of the method of moments. The method of moments, Moore and Pizer [Ref. 6:pp. 8-10], is the technique for solving **IE** by taking moments, multiplying by appropriate weighting functions, and then integrating.

The method applies to an inhomogeneous equation

$$L_{\omega}\Phi = \Gamma \tag{A.1}$$

where:

L_{ω} = a linear operator

Γ = a known function for a given excitation

Φ = a distribution of electric current

The distribution Φ is expressed in terms of known functions using undetermined parameters, for example, as a linear combination of a finite number of basis or expansion function φ_j in the domain of L_{ω};

$$\Phi = \sum_j a_j \varphi_j \tag{A.2}$$

So now, the constants a_j, finite in number, are the quantities to be determined. Substituting Equation (A.2) in Equation (A.1) and since L_{ω} is linear, we have:

$$\sum_j a_j L_{\omega}(\varphi_j) = \Gamma \tag{A.3}$$

Let a suitable inner product $\langle a, b \rangle$ be defined for the problem in terms of an integral over a space S for which the distribution Φ is defined:

$$\langle a, b \rangle = \int_S ab \, d\tau$$

Define also a set of weighting functions W_j, in the range of the L_ω, and take the inner product of Equation (A.3) with each W_j to get:

$$\sum_j a_j \langle W_i, L_\omega \varphi_j \rangle = \langle W_i, \Gamma \rangle \qquad (A.4)$$

which can written in matrix notation as:

$$[L]\,[a] = [\breve{o}] \qquad (A.5)$$

where:

$[L] = \langle W_i, L_\omega \varphi_j \rangle$

$[a] = a_n \qquad n=1,2,\ldots$

$[\breve{o}] = \langle W_i, \Gamma \rangle$

Equation (A.5) can be solved by standard methods such as factorisation of the matrix L. The efficiency of computations and accuracy of solution is largely dependent on the choice of the basis function W_j. Factors, Thomson [Ref. 7:pp 43-45], which should guide this choice are:

- Accuracy of desired solution.
- Ease of evaluation of matrix elements.
- Matrix sizes that can be inverted.
- Realization of a "well-conditioned" matrix.

There are two types of basis functions, entire domain and sub-domain. The sub-domain has fewer elements, and its execution time is usually less.

1. Integral Equation Formulation

The **NEC** code uses both [Ref. 8], an electric-field integral equation (**EFIE**) and a magnetic-field integral equation (**MFIE**) to model the electromagnetic response of general structures. The **EFIE** is well suited for thin-wire structures of small or vanishing conductor volume while the **MFIE**,is more attractive for large smooth closed surfaces. For a structure containing both wires and surfaces the **EFIE** and **MFIE** are coupled.

2. Electric-Field Integral Equation

The **EFIE** for thin-wires used in **NEC** is given by:

$$-\hat{s}\,\bar{E}^i(\bar{r}) = \frac{-j}{4\pi\omega\epsilon}\int_{c(\bar{r})} I(s')\left(\hat{s}.\hat{s}'\,k^2 - \frac{\partial^2}{\partial s\,\partial s'}\right) g(\bar{r},\bar{r}')\,ds' \qquad (A.6)$$

where:

$\hat{s}$ = distance along the wire axis r

s' = unit vector along the wire axis

$E^i(\bar{r})$ = incident electric field at $\bar{r}$

ω = $2\pi f$ = radian frequency

ϵ = permittivity

$I(s')$ = axial current

k = $\omega\sqrt{\mu\epsilon}$

μ = permeability

$\bar{r}$ = source point

$\bar{r}'$ = observation point

$g(\bar{r},\bar{r}')$ = $\exp(-jkR)/R$ = free space Green's function

R = $[\bar{r}-\bar{r}']$

3. Magnetic-Field Integral Equation

The **MFIE** for closed conducting surfaces other than wires used in **NEC** is given by:

$$\overline{J}_S(\overline{r}) = 2\hat{n} \times \overline{H}^{inc}(\overline{r}) + \frac{1}{2\pi} \hat{n} \times \int_S \overline{J}_S(\overline{r}') \times \nabla' g \, ds' \qquad \overline{r} \in S \qquad (A.7)$$

where:

$\overline{J}_S(\overline{r})$ = surface current density

$H^{inc}(\overline{r})$ = incident magnetic field at the observation point

$\hat{n}$ = unit normal vector

APPENDIX B

NEC INPUT CARD SUMMARY

COMMENT CARDS

- CM: description of run
- CE: description of run

STRUCTURE GEOMETRY CARDS

- GA: wire arc
- GE: end geometry data
- GF: use numerical Green's functions
- GM: shift and duplicate structure
- GP: suppress geometry print
- GR: generate cylindrical structure
- GS: scale structure dimensions
- GW: specify wire
- GX: reflect structure
- SP: specify surface patch
- SM: generate multiple surfaces patches

PROGRAM CONTROL CARDS

I. Alter Matrix

- EK: extended thin-wire kernel flag
- FR: frequency specification
- GN: ground parameter specification
- KH: interaction approximation range

- LD: structure impedance loading

II. Alter Current

- EX: structure excitation card
- NT: two-port network specification
- TL: transmission line specification

III. Performance Selection

- CP: compute maximum coupling
- EN: end of data flag
- GD: additional ground parameter specifications
- NE: near electric field
- NH: near magnetic field
- NX: next structure flag
- PQ: wire charge dencity print control
- PT: wire-current print control
- RP: radiation pattern
- WG: write numerical Green's function file
- XQ: execute card.

The required cards used in every NEC model are: CE, GE, EX, and EN.

APPENDIX C

GEOMETRY DATA CARDS FOR FREQUENCY RANGE 2-10 MHZ

```
CM
CM
CM                METAL MAST COMPUTER MODEL
CM
CM             DIMENSIONS:        L =  3.00  M
CM                                W =  3.00  M
CM                                H = 24.00  M
CM
CM             WIRE RADIUS        A =  0.05  M
CM
CM             FREQUENCY RANGE:   2 - 10  MHZ
CM
CE
GW 1,1,1.5,0,24,1.5,1.5,24,.05
GW 2,1,1.5,1.5,24,1.5,1.5,21,.05
GM 2,7,0,0,0,0,0,-3
GW 17,1,1.5,1.5,24,0,1.5,24,.05
GM 1,7,0,0,0,0,0,-3,17,17
GX 24,100
GX 48,010
GE 1
GN 1
FR 0,0,0,0,2
WG
EN
```

GEOMETRY DATA CARDS FOR FREQUENCY RANGE 11-15 MHZ

```
CM
CM
CM                  METAL MAST COMPUTER MODEL
CM
CM              DIMENSIONS:         L =  3.00  M
CM                                  W =  3.00  M
CM                                  H = 24.00  M
CM
CM              WIRE RADIUS:        A =  0.05  M
CM
CM              FREQUENCY RANGE:    11 - 15  MHZ
CM
CE
GW 1,1,1.5,0,24,1.5,,5,24,,05
GW 2,1,1.5,,5,24,1.5,,5,23,,05
GW 3,1,1.5,,5,24,1.5,1.5,24,,05
GW 4,1,1.5,1.5,24,1.5,1.5,23,,05
GM 4,23,0,0,0,0,0,-1
GW 97,1,1.5,,5,24,,5,,5,24,,05
GW 98,1,,5,,5,24,,5,0,24,,05
GW 99,1,,5,,5,24,0,,5,24,,05
GW 100,1,1.5,1.5,24,,5,1.5,24,,05
GW 101,1,,5,1.5,24,,5,,5,24,,05
GW 102,1,,5,1.5,24,0,1.5,24,,05
GW 103,1,1.5,1.5,23,,5,1.5,23,,05
GW 104,1,,5,1.5,23,,5,1.5,24,,05
GW 105,1,,5,1.5,23,0,1.5,23,,05
GM 3,22,0,0,0,0,0,-1,103,105
GW 172,1,,5,1.5,1,,5,1.5,0,,05
GX 172,100
GX 344,010
GE 1
GN 1
FR 0,0,0,0,11
WG
EN
```

APPENDIX D

AVERAGE POWER GAIN AND IMPEDANCE DATA SET

```
CM
CM                    AVERAGE POWER GAIN OF S.S.M.A
CM
CE                         FREQUENCY = 2 TO 10 MHZ
GF
GE 1
EX 0.16.1.00.1
EX 0.40.1.00.1
EX 0.64.1.00.1
EX 0.88.1.00.1
RP 0.91.3.1501.0.0.1.45
EN
```

APPENDIX E

VERTICAL RADIATION PATTERN DATA SET

```
CM
CM                          VERTICAL PATTERN OF S.S.H.A
CM
CM                    ANGLES: THETA = 0 - 180, PHI = 0 DEG.
CM
CE                          FREQUENCY = 2 TO 10 MHZ
GF
GE 1
EX 0.40.1.00.1
PL 3.1.0.4
RP 0.181.1.1000.-90.0.1.0
EN
```

HORIZONTAL RADIATION PATTERN DATA SET

```
CM
CM                          HORIZONTAL PATTERN OF S.S.H.A
CM
CM                    ANGLES: THETA = 90, PHI = 0 - 360 DEG.
CM
CE                          FREQUENCY = 2 TO 10 MHZ
GF
GE 1
EX 0.40.1.00.1
PL 3.2.0.4
RP 0.1.361.1000.90.0.0.10
EN
```

APPENDIX F

Contained in this appendix are curves of input impedances for driving three, two, and one segment of the base of the mast computer model in the frequency range 2-10 MHz. The tables list the plotted values of the input impedances.

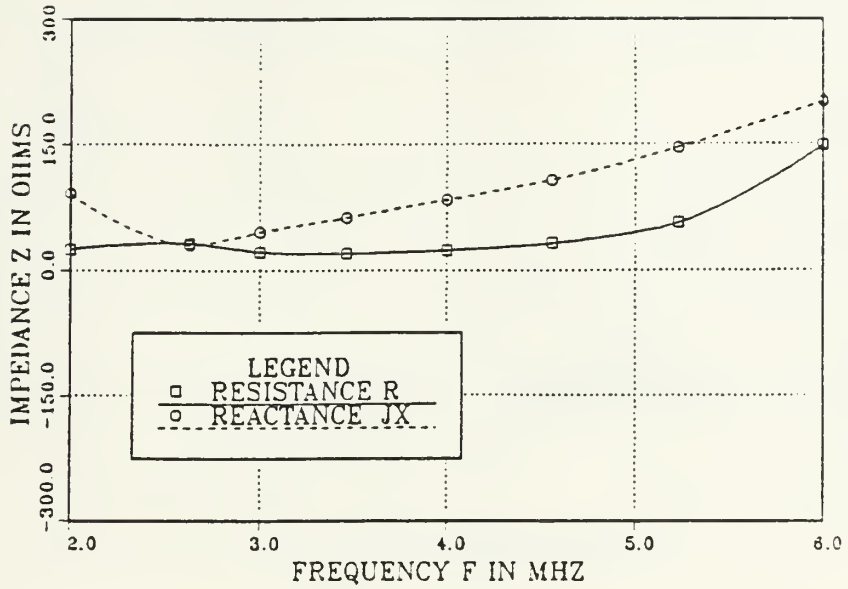

Figure F.1 Mast Input Impedances for Driving Three Base Segments in Frequency Range 2-6 MHz.

TABLE F.1

MAST INPUT IMPEDANCES FOR DRIVING THREE BASE SEGMENTS IN FREQUENCY RANGE 2-6 MHZ.

Frequency (in MHz)	Resistance (R in Ω)	Reactance (jX in Ω)
2.00	24.72	+92.08
2.63	31.57	+29.51
3.00	21.55	+46.30
3.46	19.69	+63.31
4.00	23.77	+84.19
4.56	31.58	+106.94
5.23	56.37	+145.70
6.00	148.71	+201.24

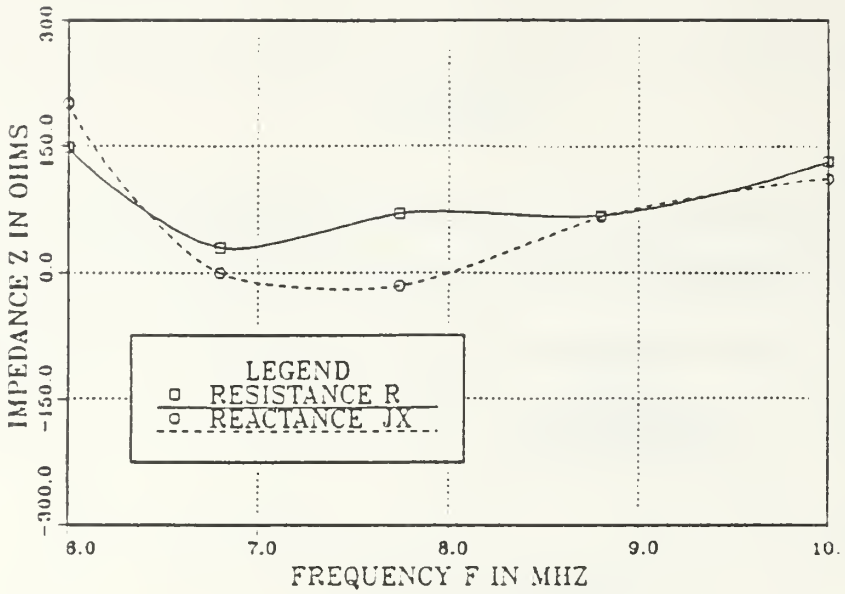

Figure F.2 Mast Input Impedances for Driving Three Base Segments in Frequency Range 6-10 MHz.

TABLE F.2

MAST INPUT IMPEDANCES FOR DRIVING THREE BASE SEGMENTS IN FREQUENCY RANGE 6-10 MHZ.

Frequency (in MHz)	Resistance (R in Ω)	Reactance (jX in Ω)
6.00	148.71	+201.24
6.80	29.84	-0.40
7.74	70.00	-16.20
8.80	68.00	+66.00
10.00	131.70	+110.50

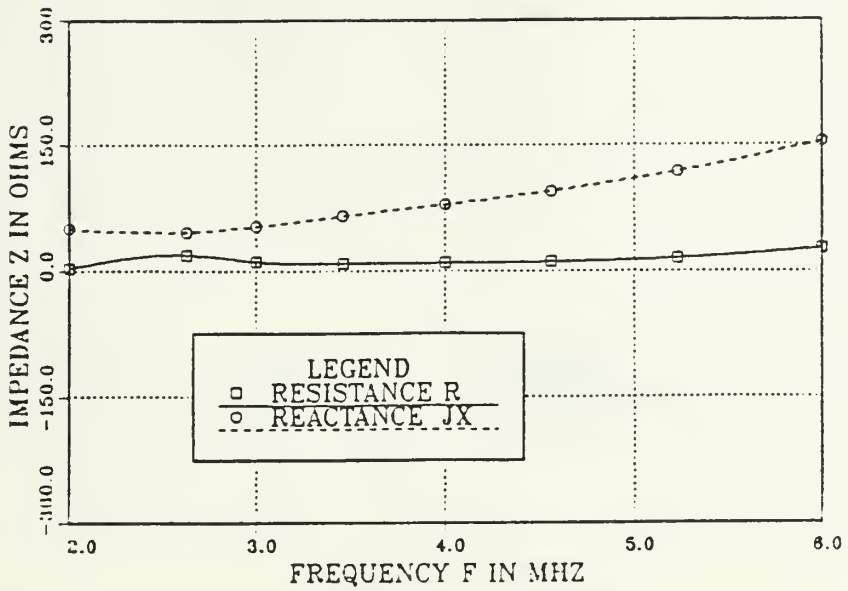

Figure F.3 Mast Input Impedances for Driving Two Adjacent Base Segments in Frequency Range 2-6 MHz.

TABLE F.3

MAST INPUT IMPEDANCES FOR DRIVING TWO ADJACENT BASE SEGMENTS IN FREQUENCY RANGE 2-6 MHZ.

Frequency (in MHz)	Resistance (R in Ω)	Reactance (jX in Ω)
2.00	3.09	+50.23
2.63	18.70	+46.20
3.00	10.87	+53.17
3.46	8.90	+65.10
4.00	9.00	+79.50
4.56	10.80	+95.60
5.23	15.17	+118.26
6.00	27.15	+153.90

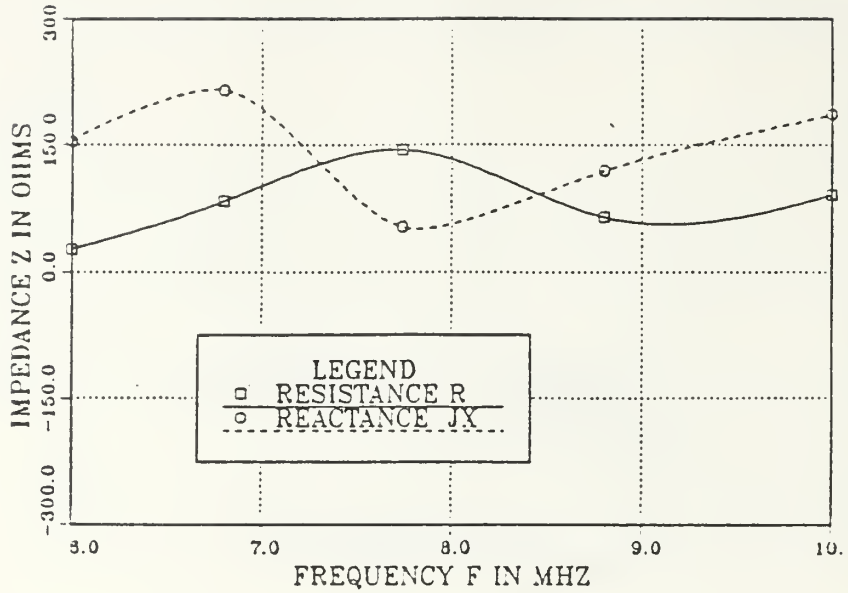

Figure F.4 Mast Input Impedances for Driving Two Adjacent Base Segments in Frequency Range 6-10 MHz.

TABLE F.4

MAST INPUT IMPEDANCES FOR DRIVING TWO ADJACENT BASE SEGMENTS IN FREQUENCY RANGE 6-10 MHZ.

Frequency (in MHz)	Resistance (R in Ω)	Reactance (jX in Ω)
6.00	27.15	+153.90
6.80	83.60	+214.76
7.74	143.73	+52.85
8.80	65.48	+120.43
10.00	91.24	+185.75

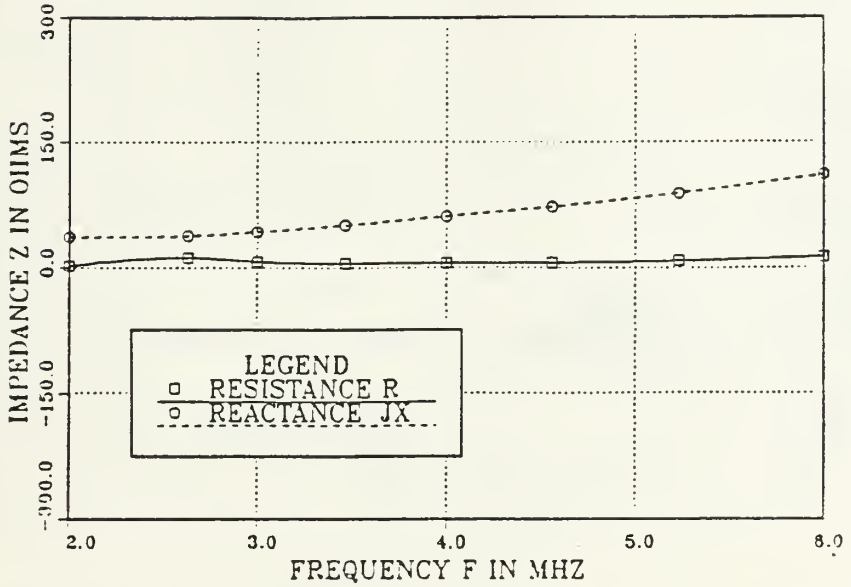

Figure F.5 Mast Input Impedances for Driving Two Diagonal Base Segments in Frequency Range 2-6 MHz.

TABLE F.5

MAST INPUT IMPEDANCES FOR DRIVING TWO DIAGONAL BASE SEGMENTS IN FREQUENCY RANGE 2-6 MHZ.

Frequency (in MHz)	Resistance (R in Ω)	Reactance (jX in Ω)
2.00	1.75	+37.18
2.63	11.90	+37.96
3.00	6.88	+42.74
3.46	5.33	+51.40
4.00	5.29	+61.81
4.56	6.80	+73.25
5.23	8.02	+88.67
6.00	13.08	+111.35

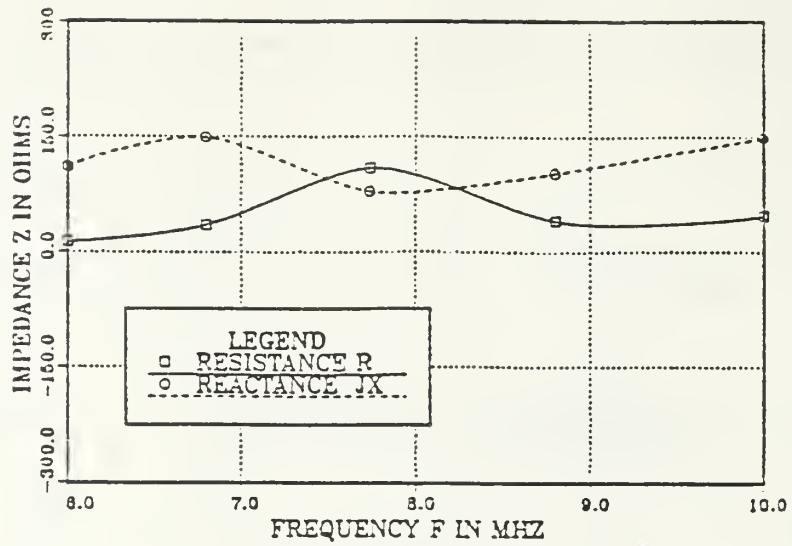

Figure F.6 Mast Input Impedances for Driving Two Diagonal Base Segments in Frequency Range 6-10 MHz.

TABLE F.6

MAST INPUT IMPEDANCES FOR DRIVING TWO DIAGONAL BASE SEGMENTS IN FREQUENCY RANGE 6-10 MHZ.

Frequency (in MHz)	Resistance (R in Ω)	Reactance (jX in Ω)
6.00	13.08	+111.35
6.80	35.00	+149.00
7.74	109.50	+79.00
8.80	41.50	+103.50
10.00	47.50	+148.93

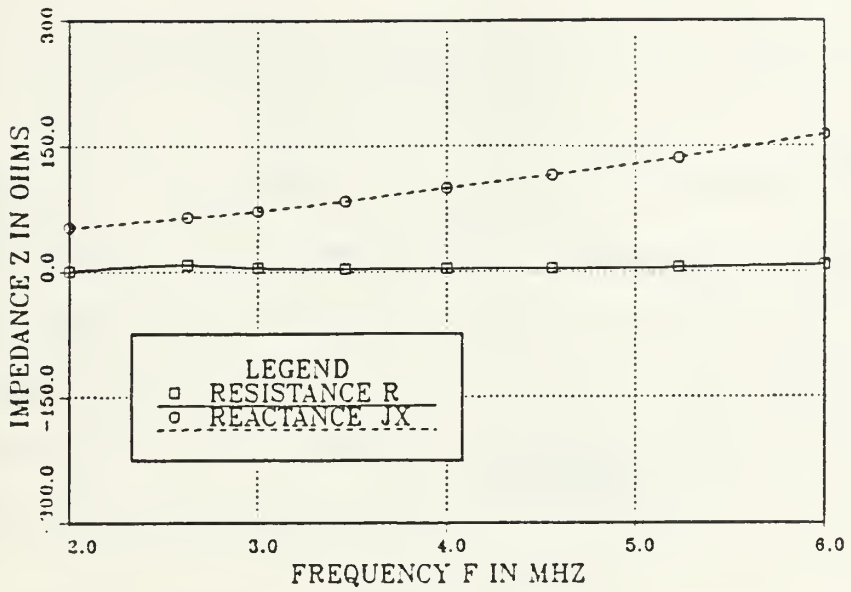

Figure F.7 Mast Input Impedances for Driving One Base Segment in Frequency Range 2-6 MHz.

TABLE F.7

MAST INPUT IMPEDANCES FOR DRIVING ONE BASE SEGMENT IN FREQUENCY RANGE 2-6 MHZ.

Frequency (in MHz)	Resistance (R in Ω)	Reactance (jX in Ω)
2.00	0.87	+53.23
2.63	8.10	+65.03
3.00	4.91	+72.66
3.46	3.70	+85.14
4.00	3.62	+100.23
4.56	4.10	+116.42
5.23	5.28	+137.05
6.00	7.97	+163.89

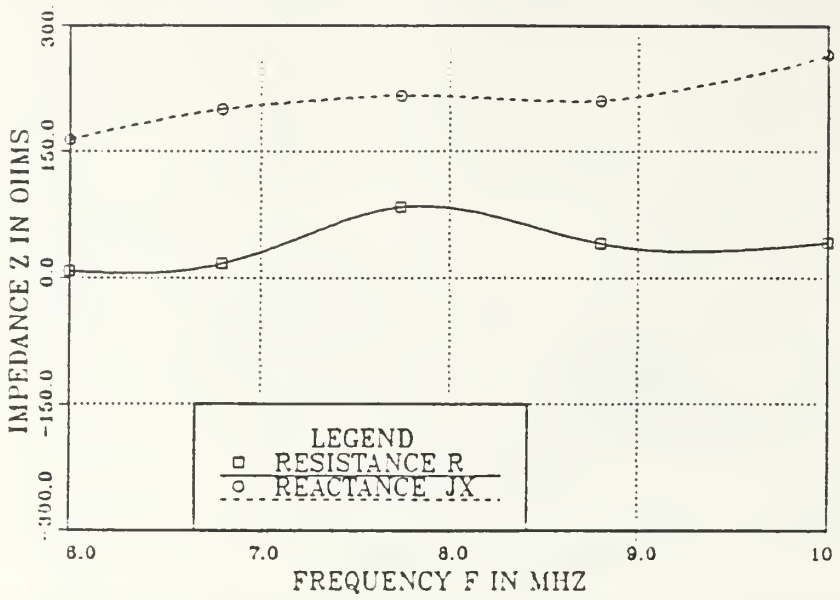

Figure F.8 Mast Input Impedances for Driving One Base Segment in Frequency Range 6-10 MHz.

TABLE F.8

MAST INPUT IMPEDANCES FOR DRIVING ONE BASE SEGMENT IN FREQUENCY RANGE 6-10 MHZ.

Frequency (in MHz)	Resistance (R in Ω)	Reactance (jX in Ω)
6.00	7.97	+163.89
6.80	16.80	+200.00
7.74	84.50	+216.70
8.80	41.45	+210.00
10.00	42.00	+265.27

APPENDIX G

Contained in this appendix are radiation patterns generated by the NEC computer analysis for the mast computer models in the frequency range 2-15 MHz versus feed point positions, and for the whip antenna of equal height, provided for comparison. The heading for each radiation pattern contains the information necessary for the interpretation of the pattern. The first line of the heading contains the following:

- type antenna / feed point position / frequency

The second line contains the following:

- type pattern (phi [φ] = horizontal - theta [θ] = vertical)

The first forty (40) patterns are for the mast computer models, while the remaining six (6) are for the whip antenna of equal height.

MODEL NO1: DRIVING 4 BASE SEGMENTS AT FREQ. = 2 MHZ

THETA = 0 -180, PHI = 0 DEG.

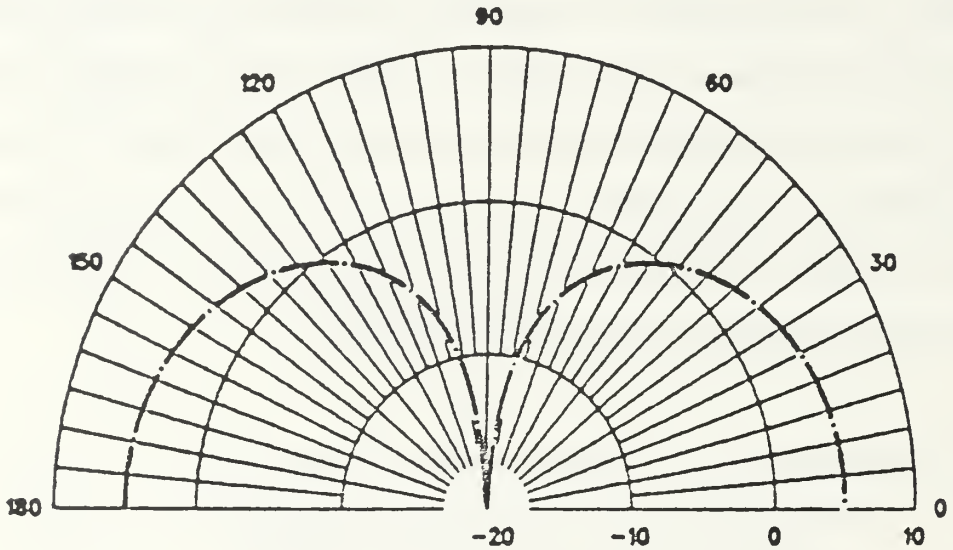

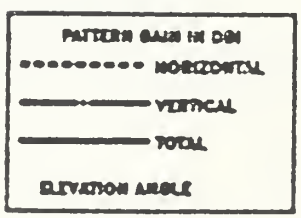

Figure G.1 E-Field Vertical Radiation Pattern: F = 2 MHz, vs. Four Feed Point Positions.

MODEL NO1: DRIVING 4 BASE SEGMENTS AT FREQ. = 2 MHZ

THETA = 90, PHI = 0 – 360 DEG.

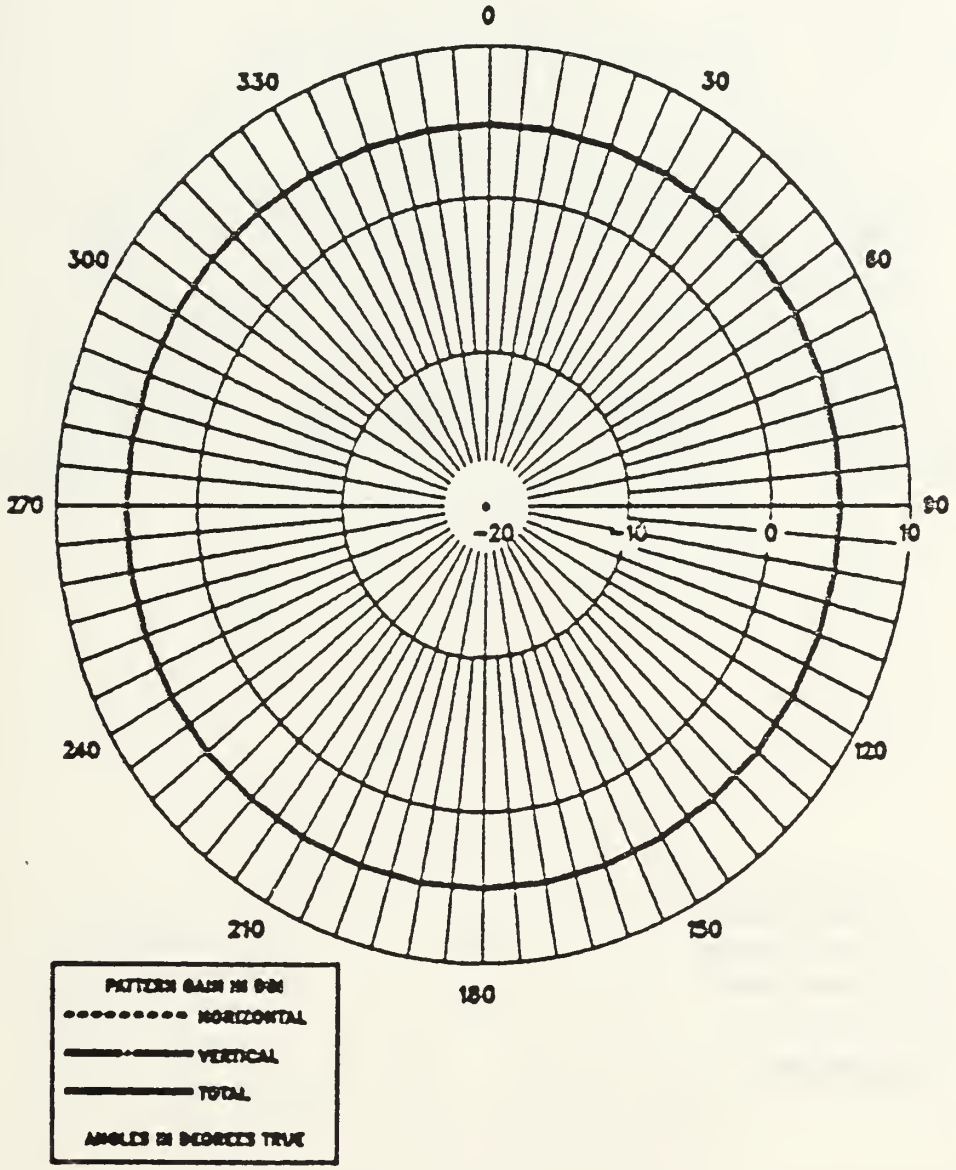

Figure G.2 E-Field Horizontal Radiation Pattern: F = 2 MHz, vs. Four Feed Point Positions.

MODEL NO1: DRIVING 3 BASE SEGMENTS AT FREQ. = 2 MHZ

THETA = 0 −180, PHI = 0 DEG.

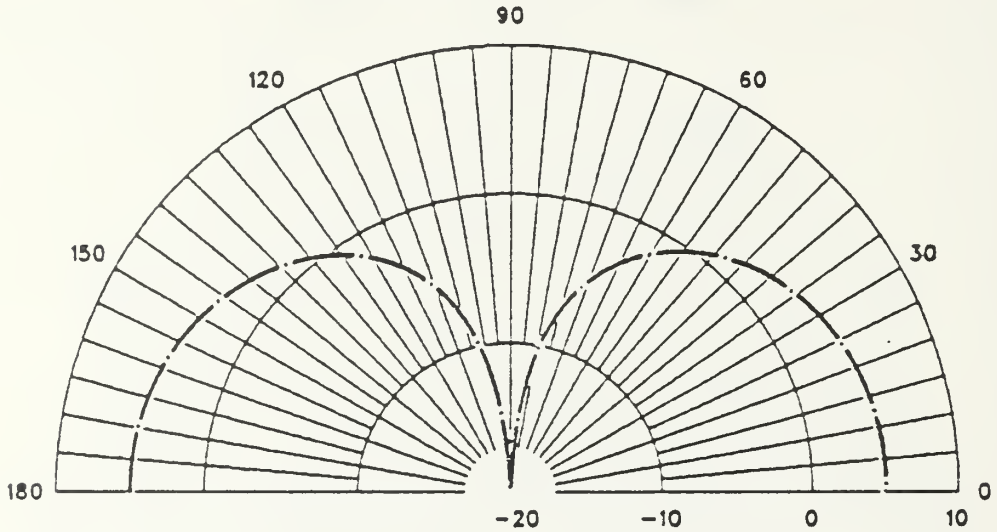

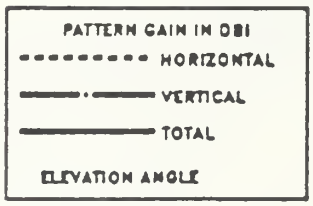

Figure G.3 E-Field Vertical Radiation Pattern: F = 2 MHz, vs. Three Feed Point Positions.

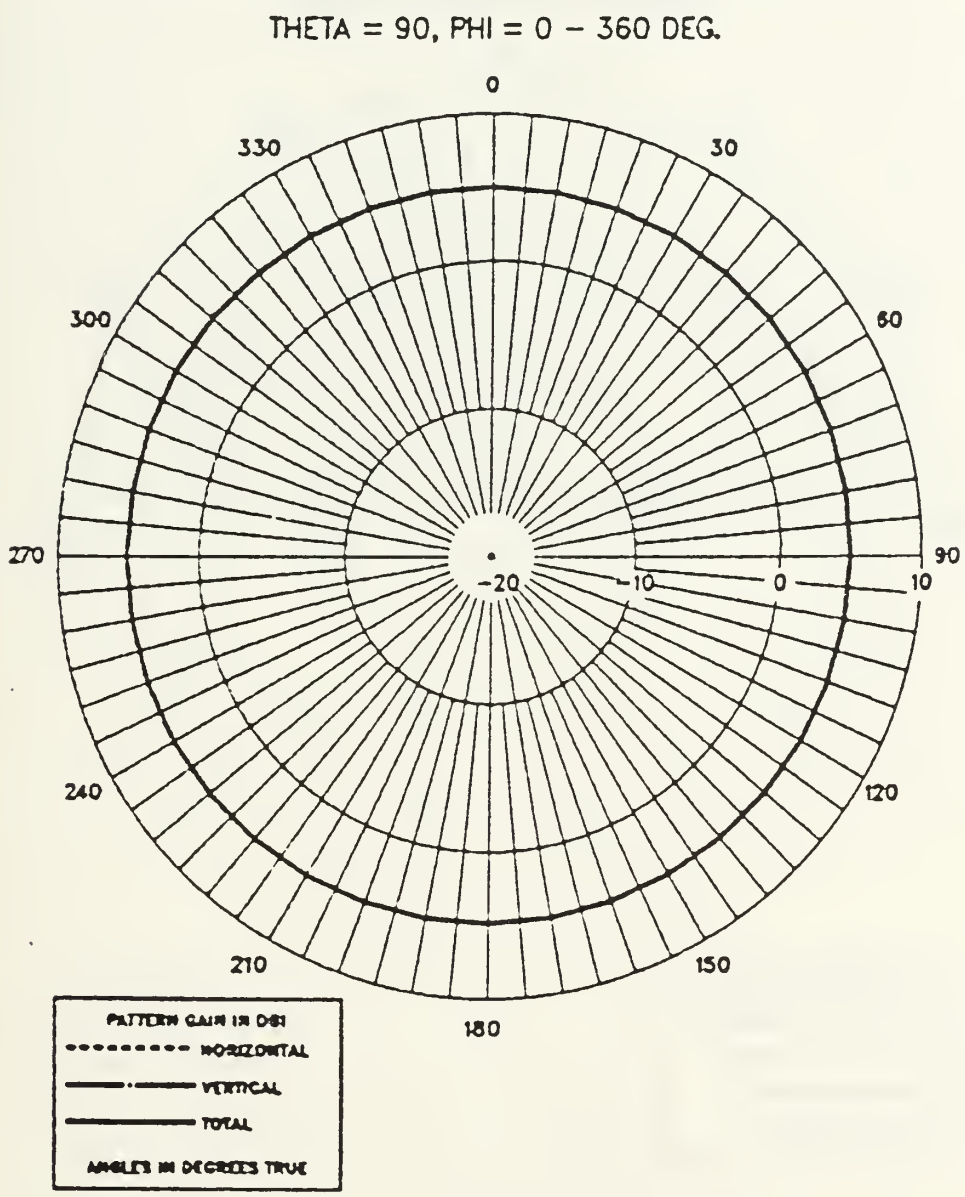

Figure G.4 E-Field Horizontal Radiation Pattern: F = 2 MHz, vs. Three Feed Point Positions.

MODEL NO1: DRIVING 2 ADJACENT BASE SEGMENTS AT FREQ. = 2 MHZ

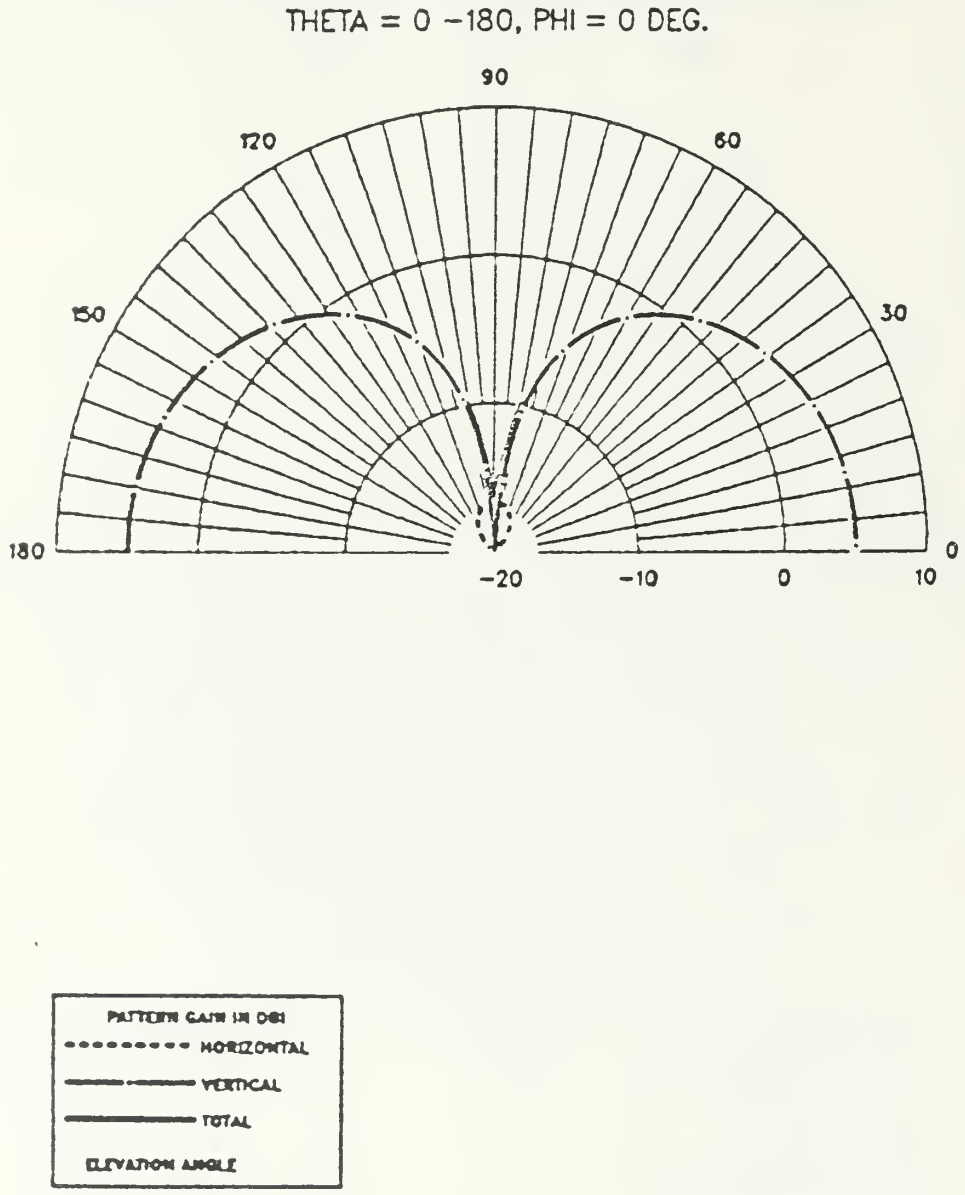

Figure G.5 E-Field Vertical Radiation Pattern: F = 2 MHz, vs. Two Adjacent Feed Point Positions.

MODEL NO1: DRIVING 2 ADJACENT BASE SEGMENTS AT FREQ. = 2 MHZ

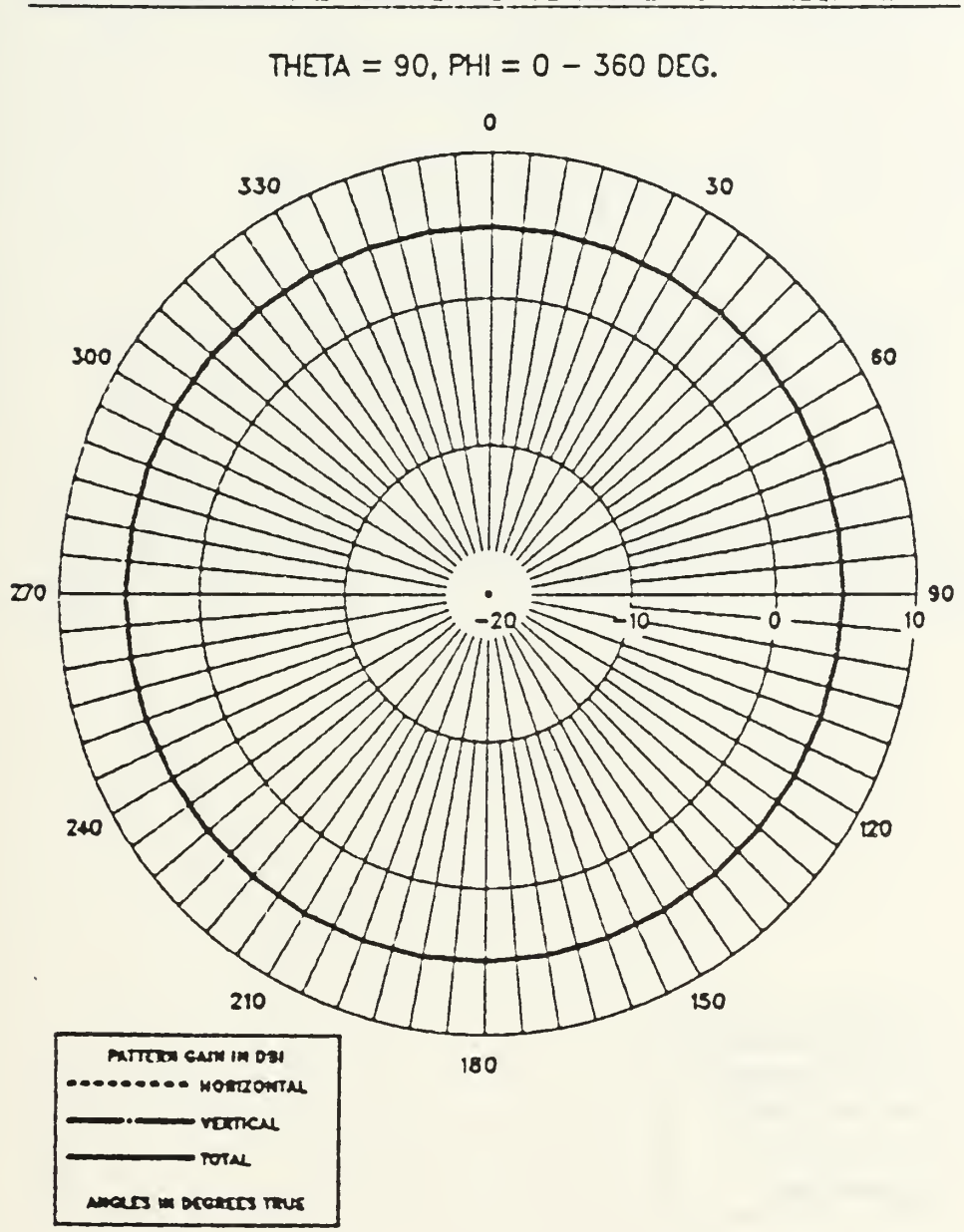

Figure G.6 E-Field Horizontal Radiation Pattern: F = 2 MHz, vs. Two Adjacent Feed Point Positions.

MODEL NO1: DRIVING 2 DIAGONAL BASE SEGMENTS AT FREQ. = 2 MHZ

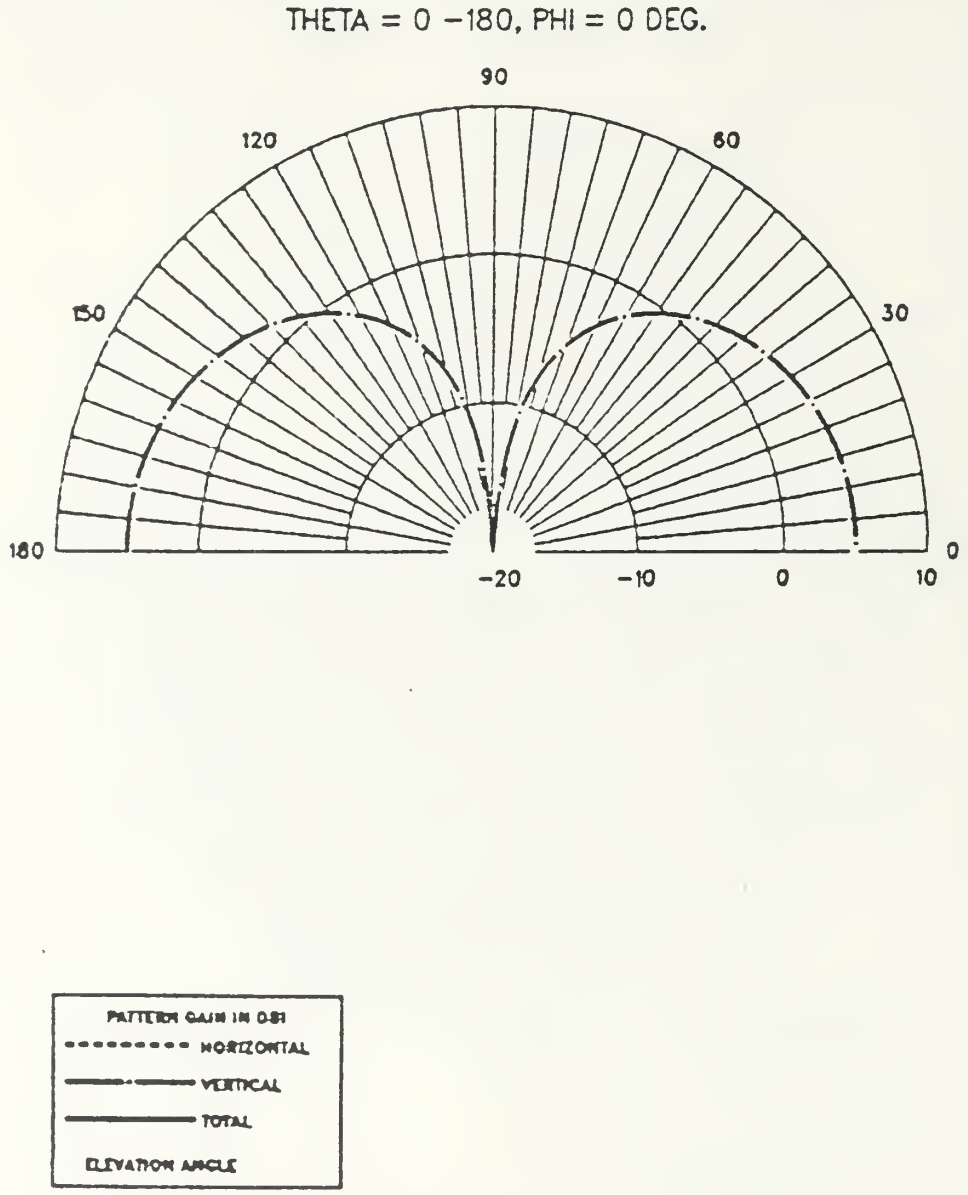

Figure G.7 E-Field Vertical Radiation Pattern: F = 2 MHz, vs. Two Diagonal Feed Point Positions.

MODEL NO1: DRIVING 2 DIAGONAL BASE SEGMENTS AT FREQ = 2 MHZ

THETA = 90, PHI = 0 – 360 DEG.

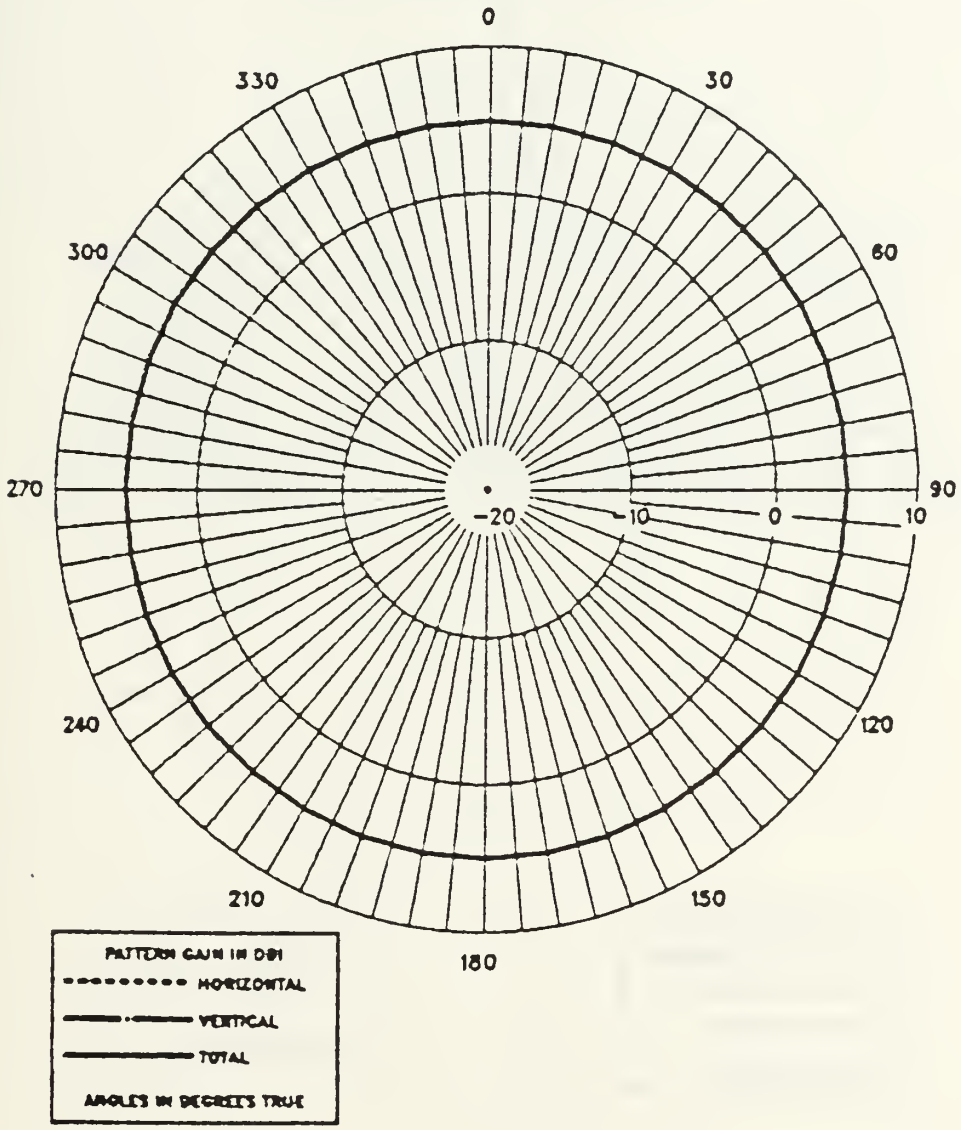

Figure G.8 E-Field Horizontal Radiation Pattern: F = 2 MHz, vs. Two Diagonal Feed Point Positions.

MODEL NO1: DRIVING 1 BASE SEGMENT AT FREQ. = 2 MHZ

THETA = 0 -180, PHI = 0 DEG.

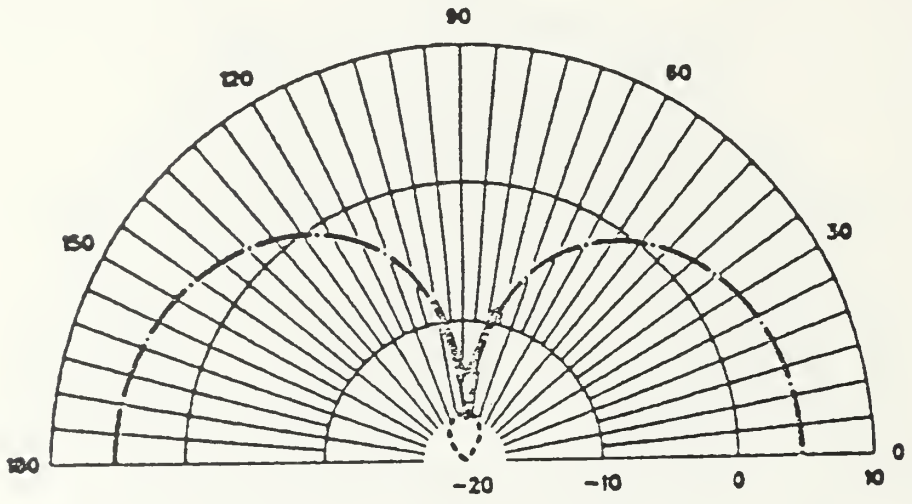

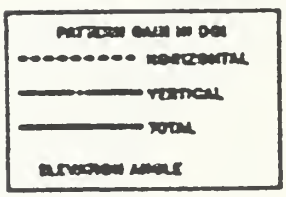

Figure G.9 E-Field Vertical Radiation Pattern: F = 2 MHz, vs. One Feed Point Position.

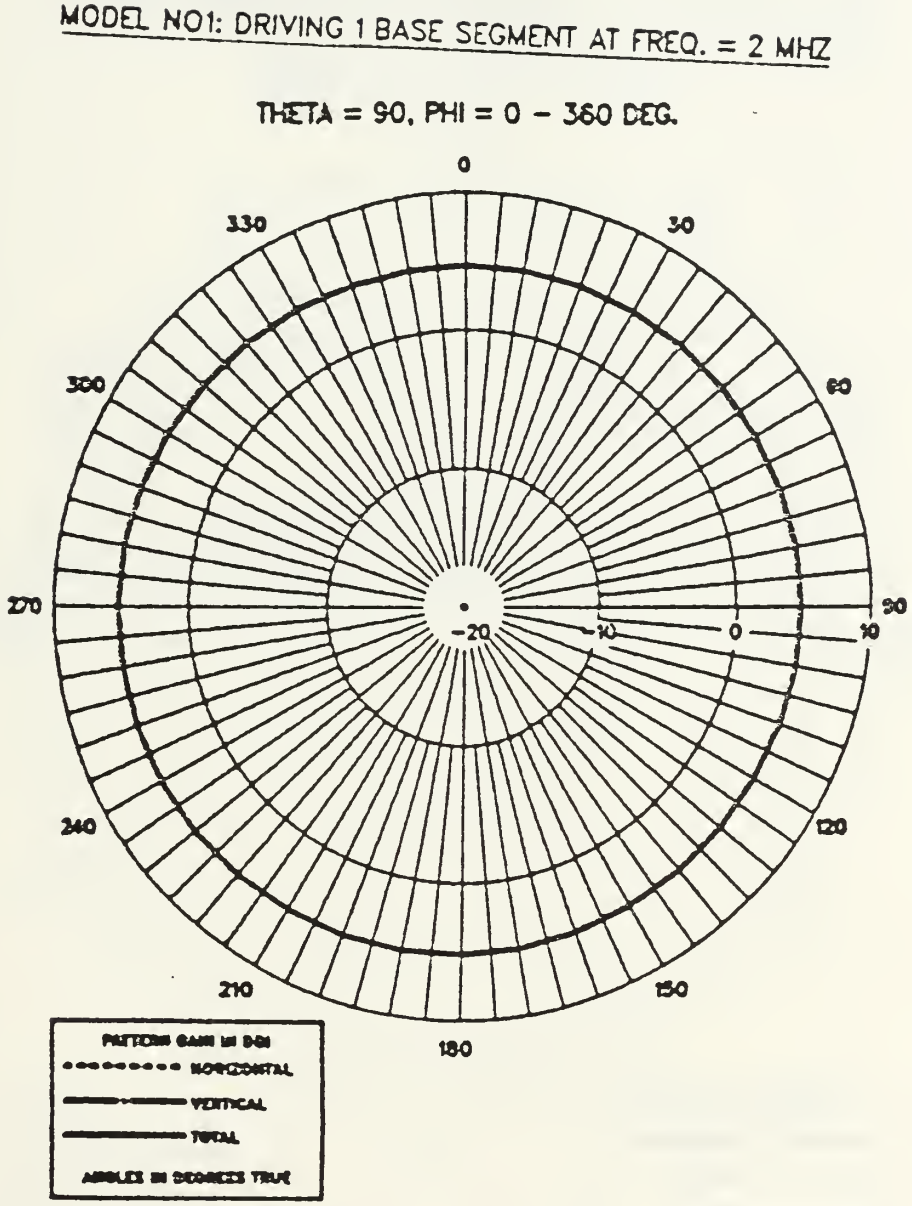

Figure G.10 E-Field Horizontal Radiation Pattern: F = 2 MHz, vs. One Feed Point Position.

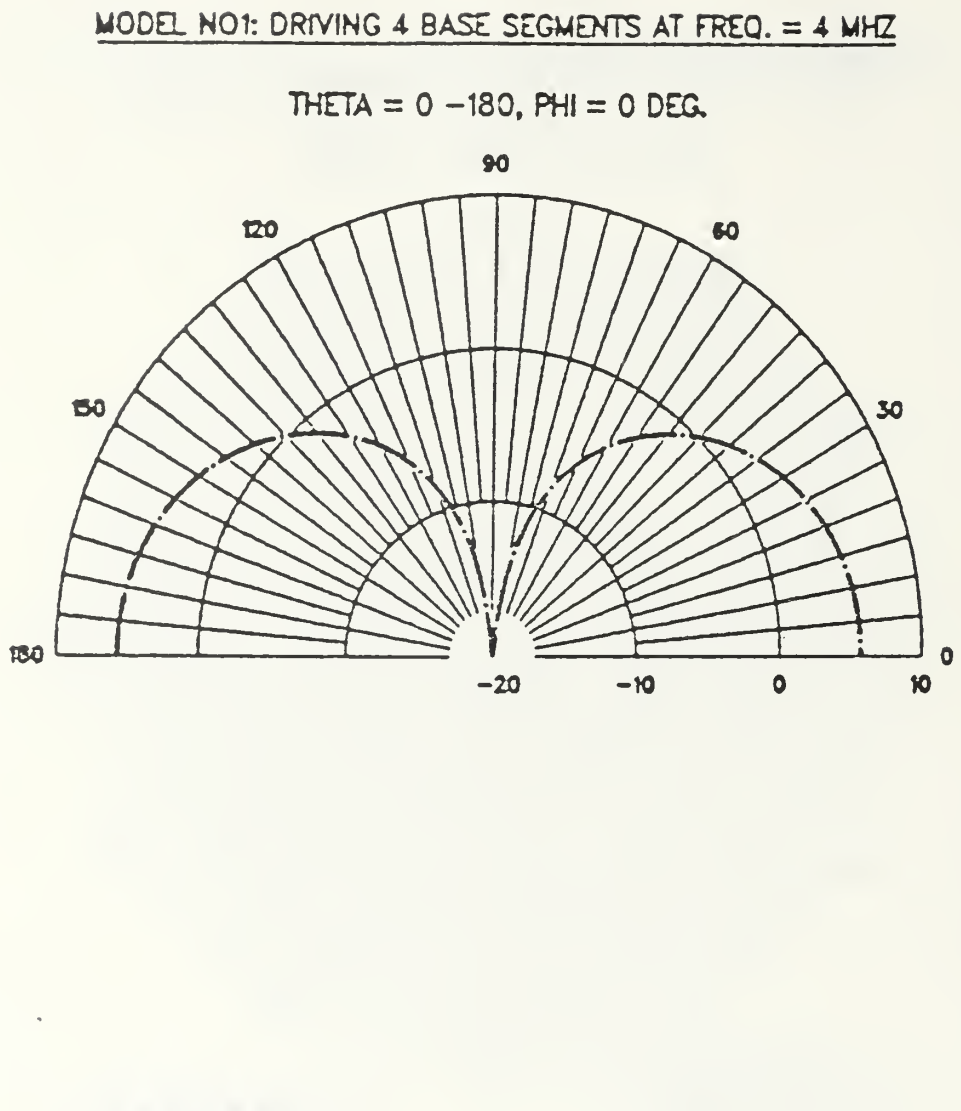

Figure G.11 E-Field Vertical Radiation Pattern: F = Figure 4 MHz, vs. Four Feed Point Positions.

MODEL NO1: DRIVING 4 BASE SEGMENTS AT FREQ. = 4 MHZ

THETA = 90, PHI = 0 – 360 DEG.

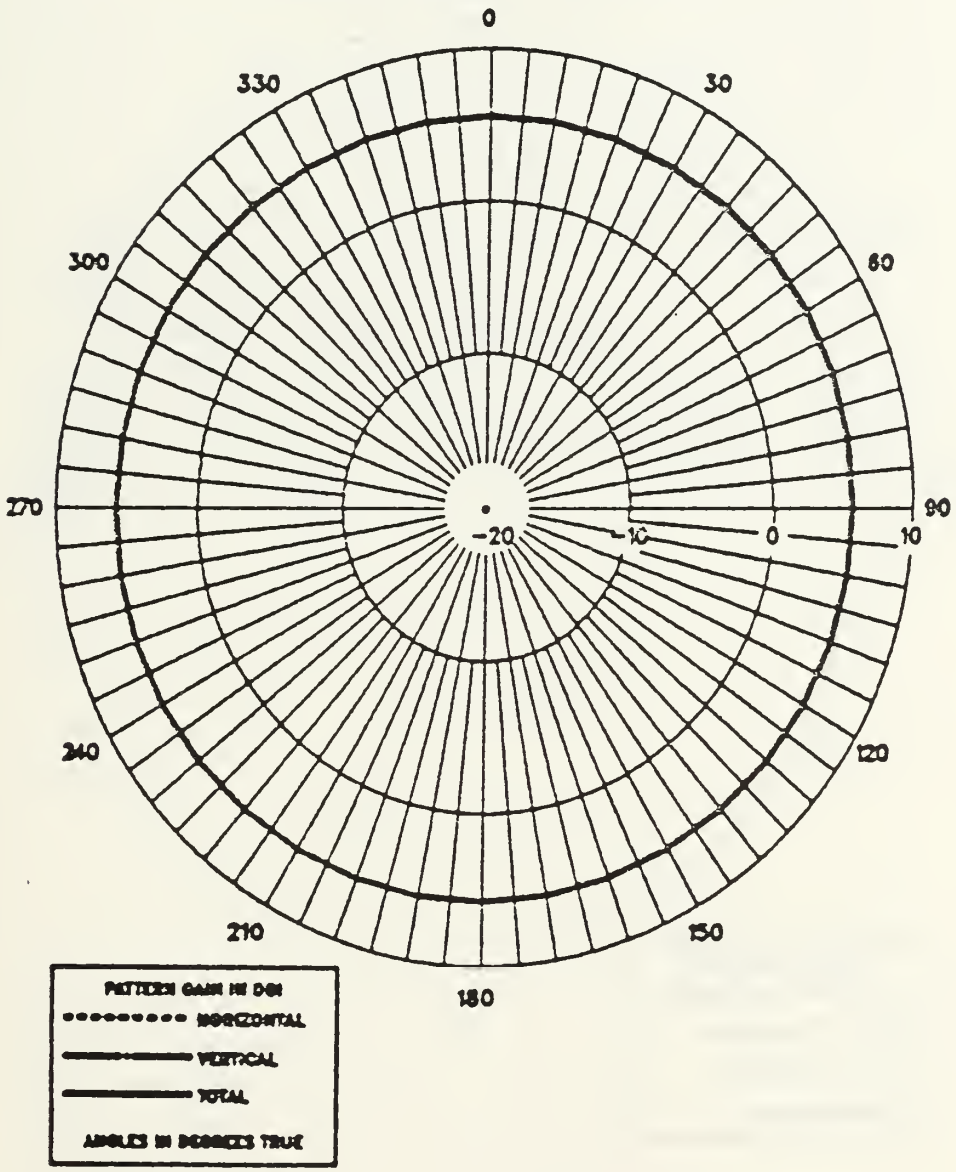

Figure G.12 E-Field Horizontal Radiation Pattern: F = Figure 4 MHz, vs. Four Feed Point Positions.

MODEL NO1: DRIVING 4 BASE SEGMENTS AT FREQ. = 6 MHZ

THETA = 0 −180, PHI = 0 DEG.

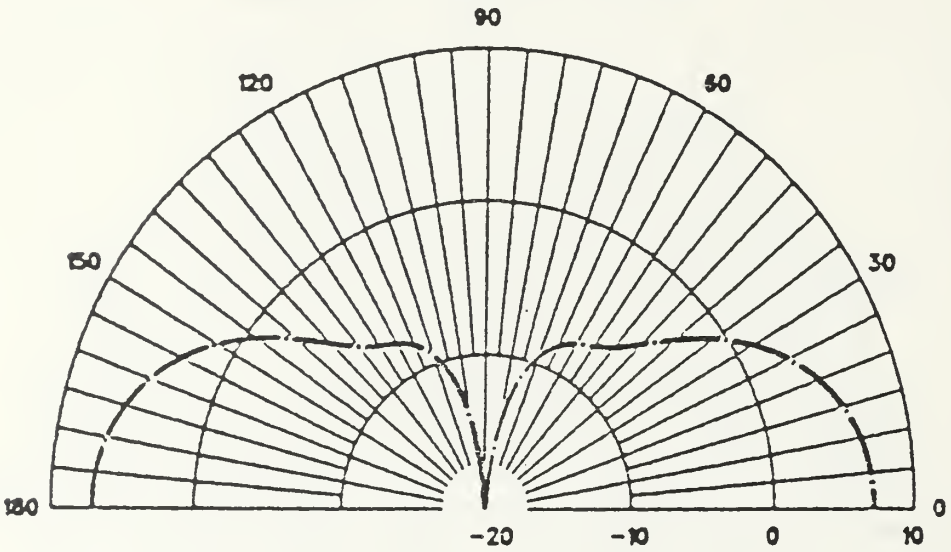

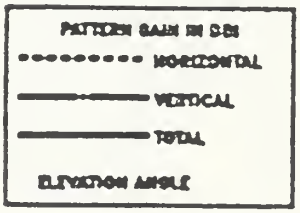

Figure G.13 E-Field Vertical Radiation Pattern: F = 6 MHz, vs. Four Feed Point Positions.

MODEL NO1: DRIVING 4 BASE SEGMENTS AT FREQ. = 6 MHZ

THETA = 90, PHI = 0 – 360 DEG.

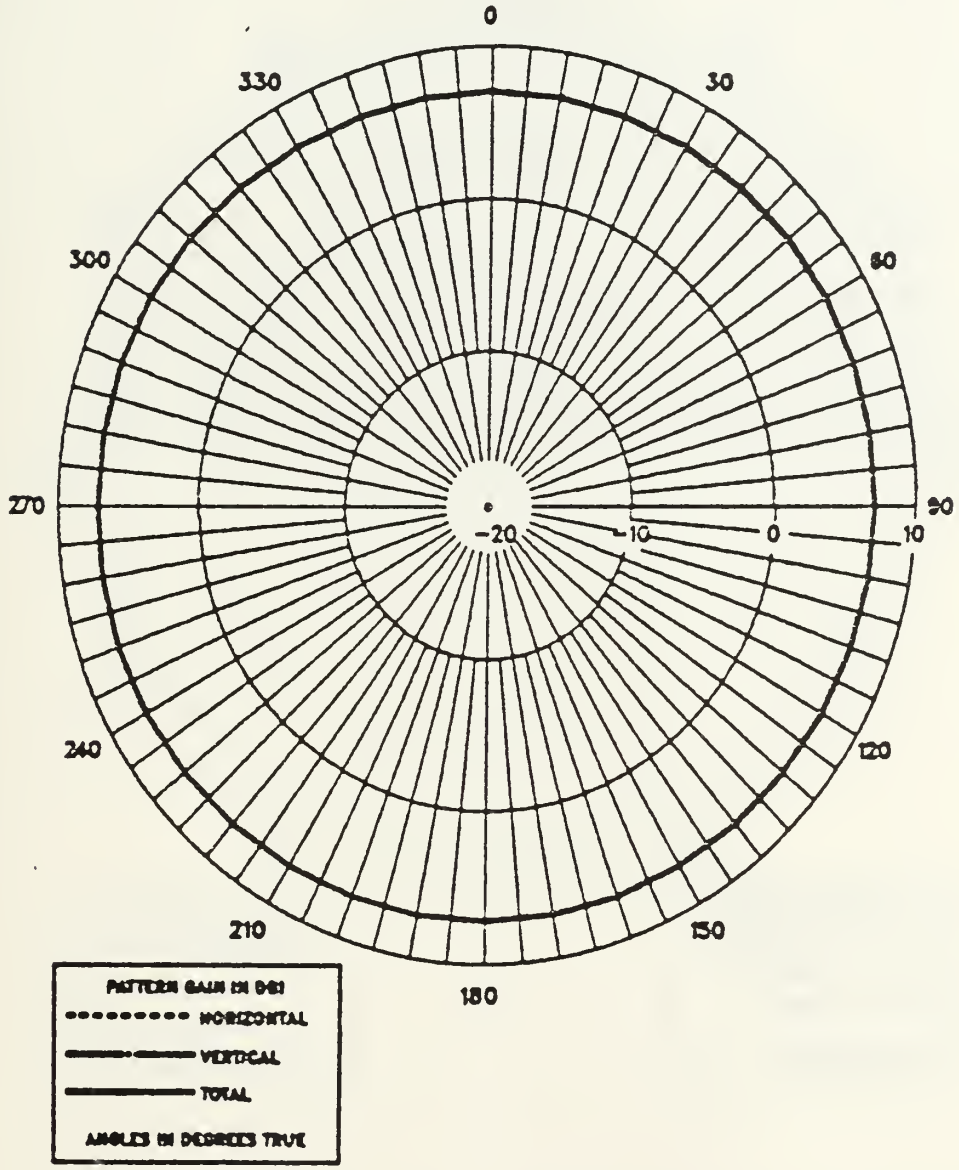

Figure G.14 E-Field Horizontal Radiation Pattern: F = 6 MHz, vs. Four Feed Point Positions.

MODEL NO1: DRIVING 3 BASE SEGMENTS AT FREQ. = 6 MHZ

THETA = 0 −180, PHI = 0 DEG.

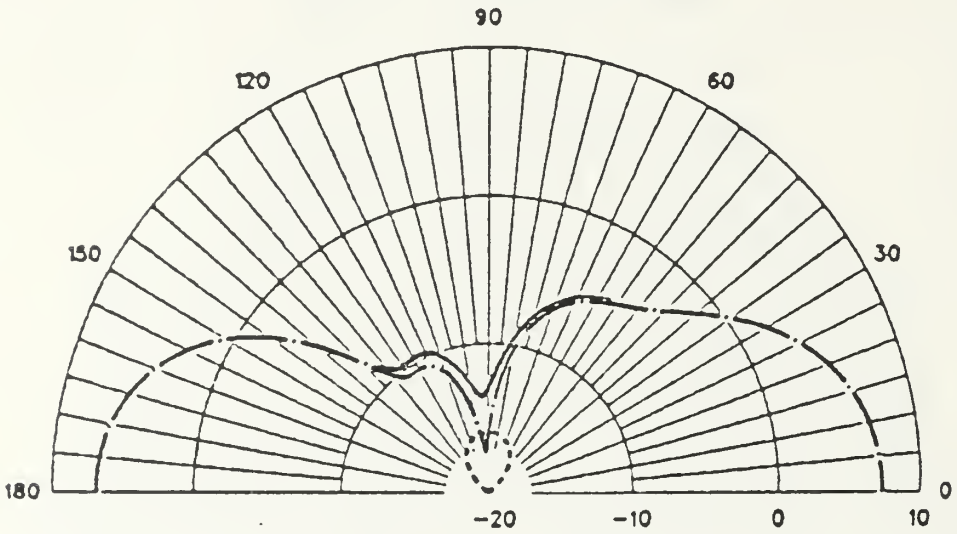

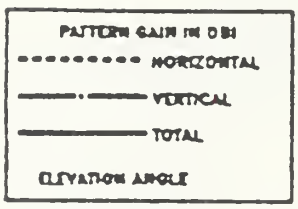

Figure G.15 E-Field Vertical Radiation Pattern: F = 6 MHz, vs. Three Feed Point Positions.

MODEL NO1: DRIVING 3 BASE SEGMENTS AT FREQ. = 6 MHZ

THETA = 90, PHI = 0 – 360 DEG.

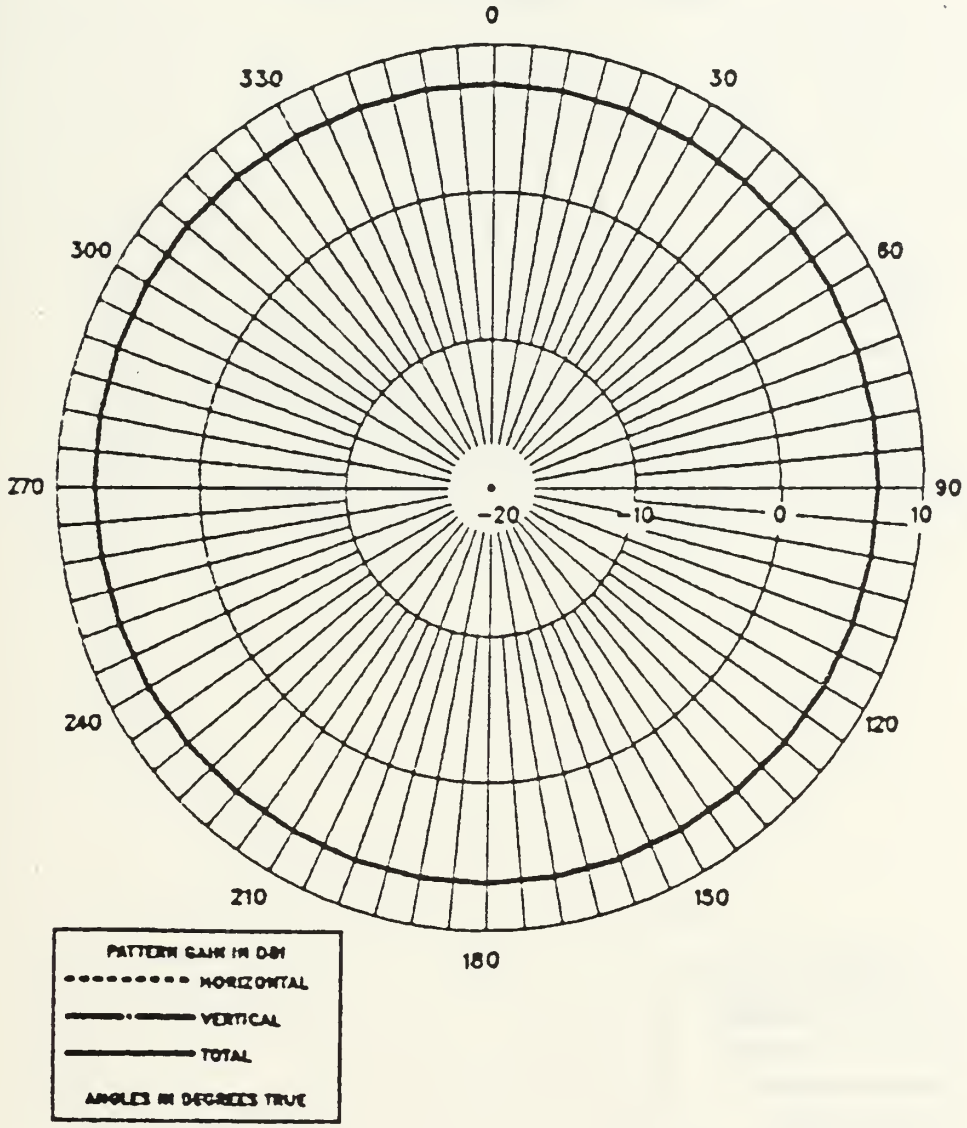

Figure G.16 E-Field Horizontal Radiation Pattern: F = 6 MHz, vs. Three Feed Point Positions.

MODEL NO1: DRIVING 2 ADJACENT BASE SEGMENTS AT FREQ. = 6 MHZ

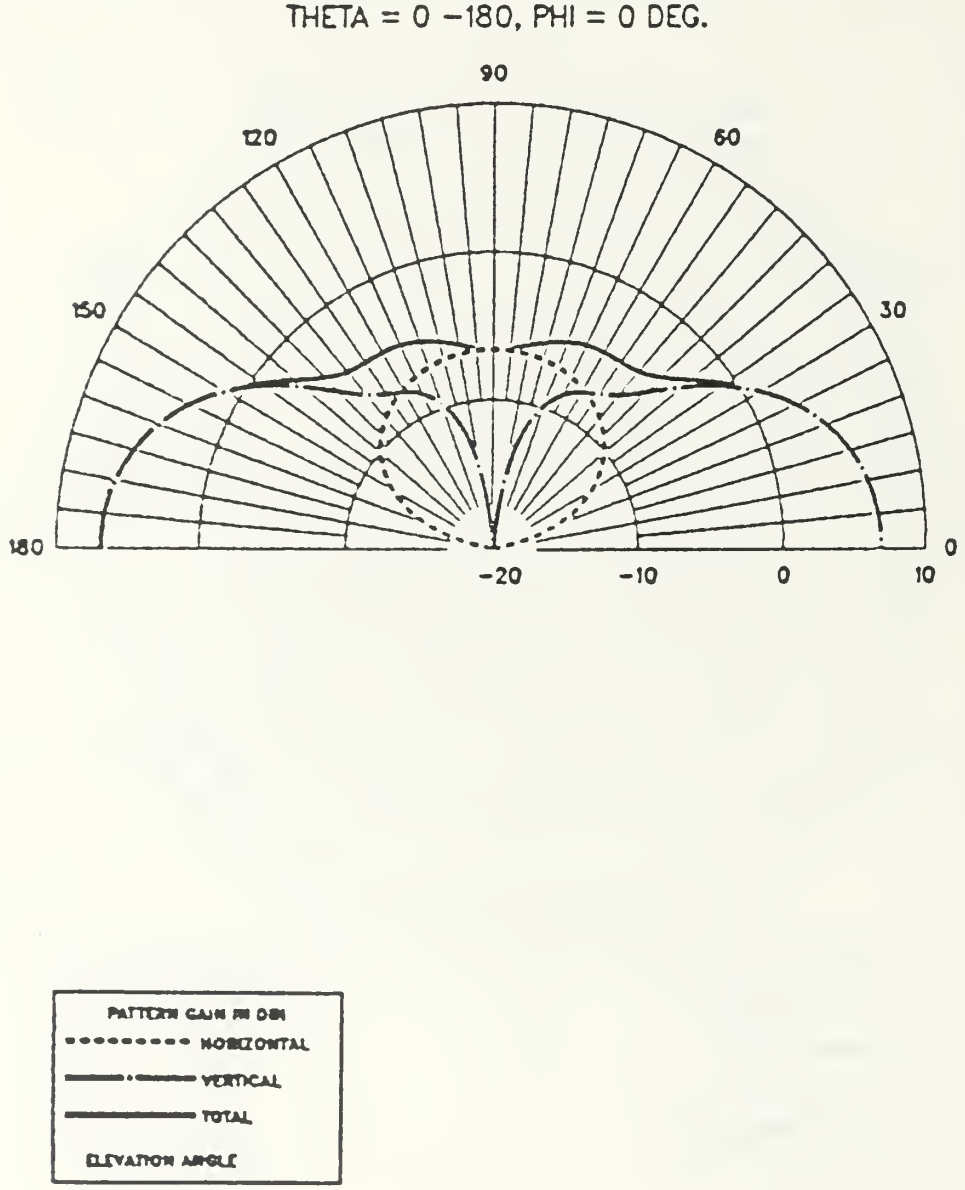

Figure G.17 E-Field Vertical Radiation Pattern: F = 6 MHz, vs. Two Adjacent Feed Point Positions.

MODEL NO1: DRIVING 2 ADJACENT BASE SEGMENTS AT FREQ. = 6 MHZ

THETA = 90, PHI = 0 – 360 DEG.

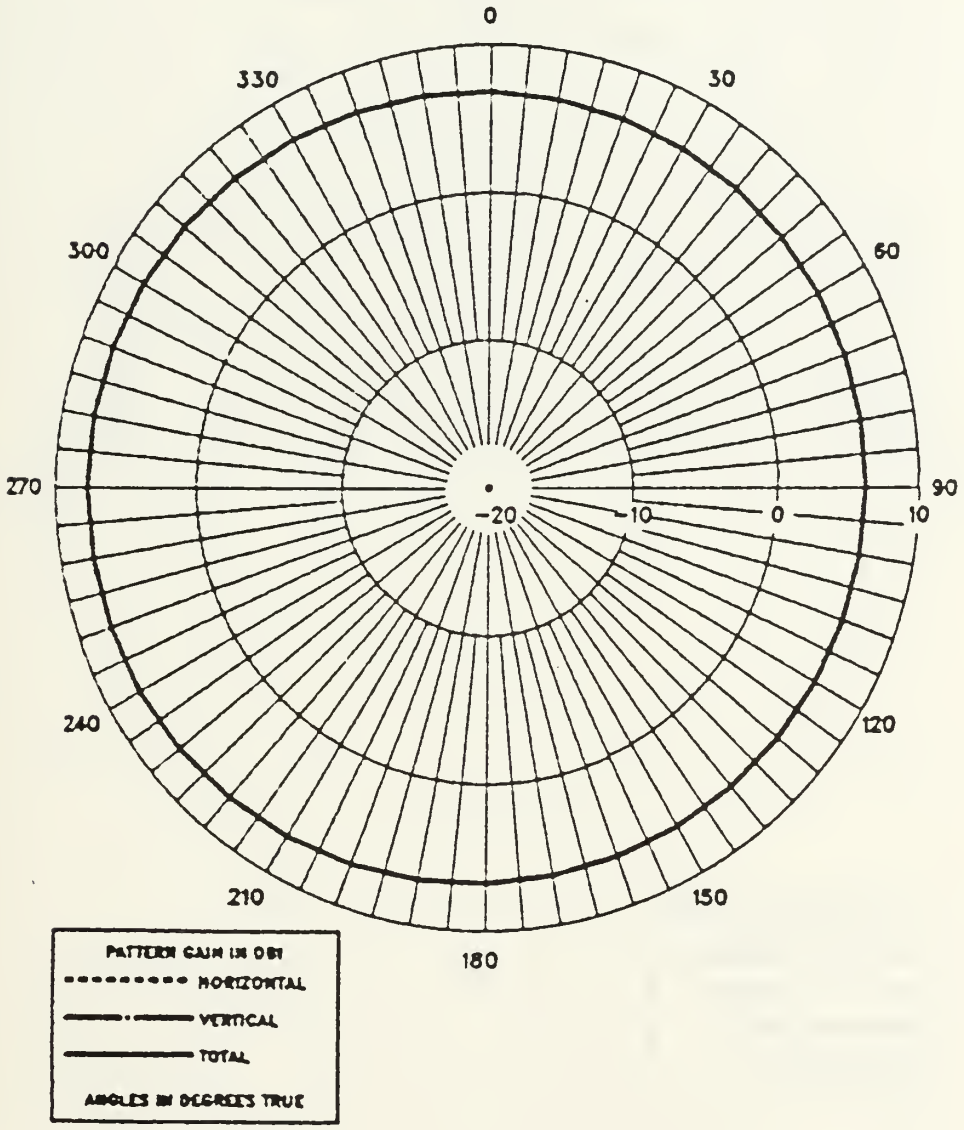

Figure G.18 E-Field Horizontal Radiation Pattern: F = 6 MHz, vs. Two Adjacent Feed Point Positions.

MODEL NO1: DRIVING 2 DIAGONAL BASE SEGMENTS AT FREQ. = 6 MHZ

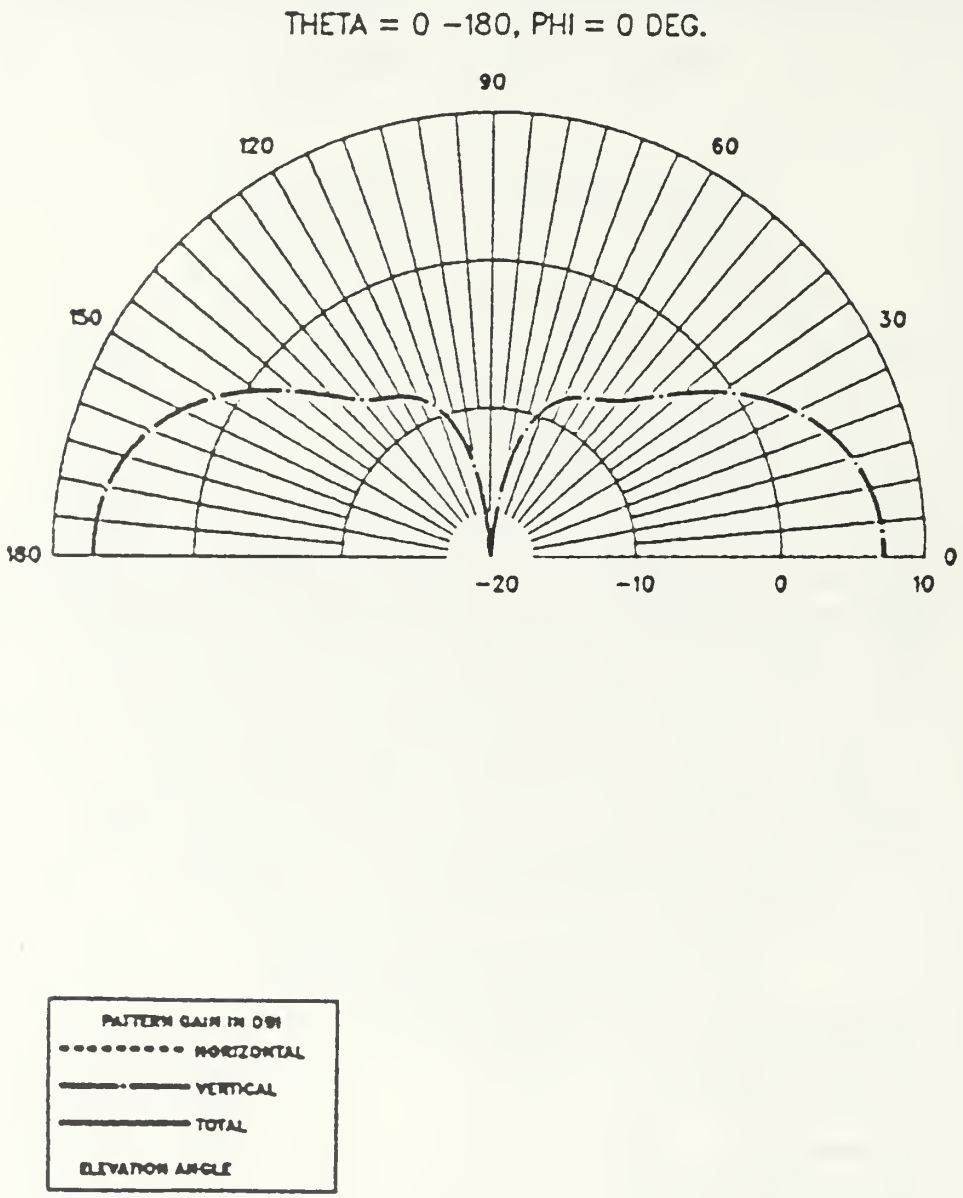

Figure G.19 E-Field Vertical Radiation Pattern: F = 6 MHz, vs. Two Diagonal Feed Point Positions.

MODEL NO1: DRIVING 2 DIAGONAL BASE SEGMENTS AT FREQ = 6 MHZ

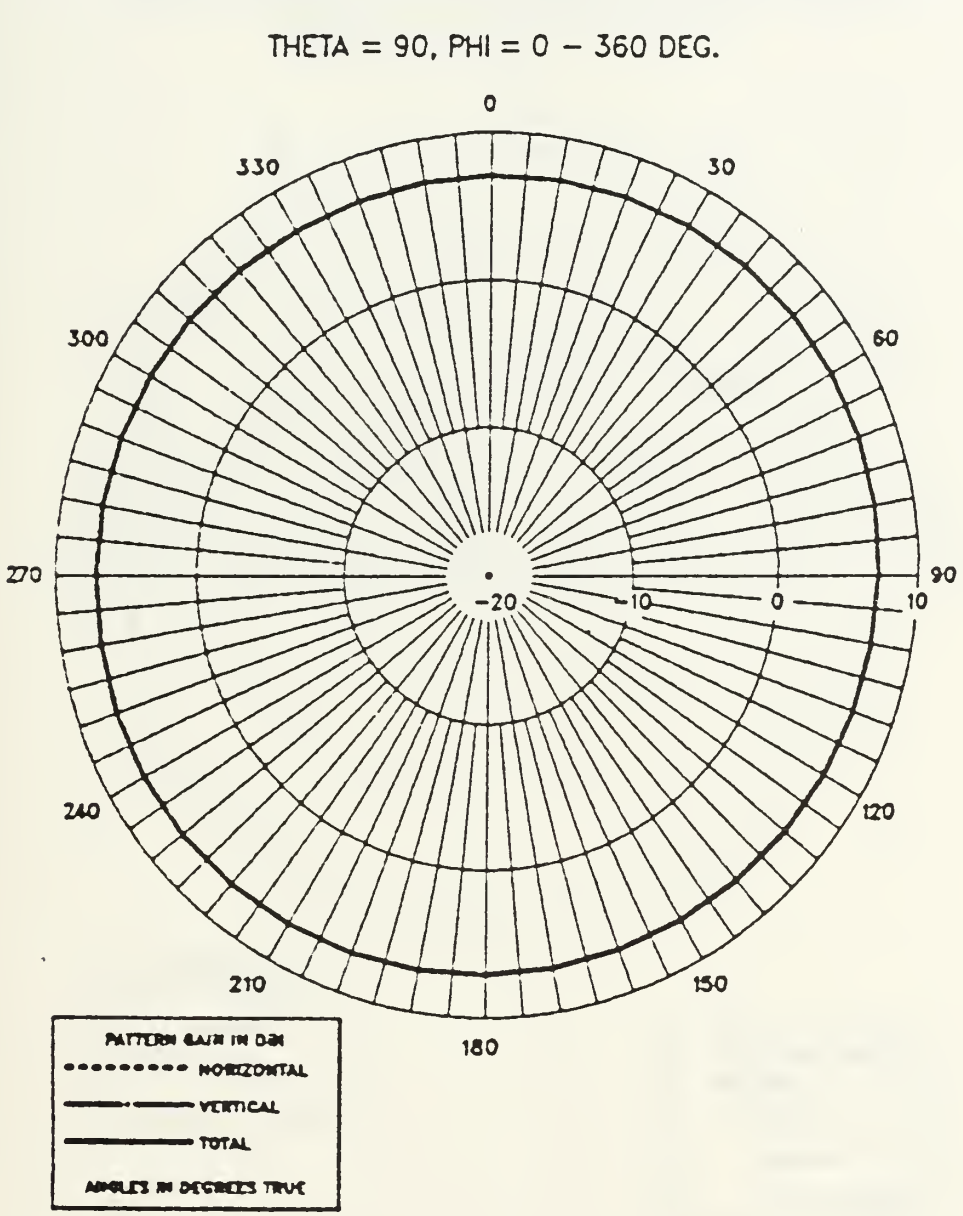

Figure G.20 E-Field Horizontal Radiation Pattern: F = 6 MHz, vs. Two Diagonal Feed Point Positions.

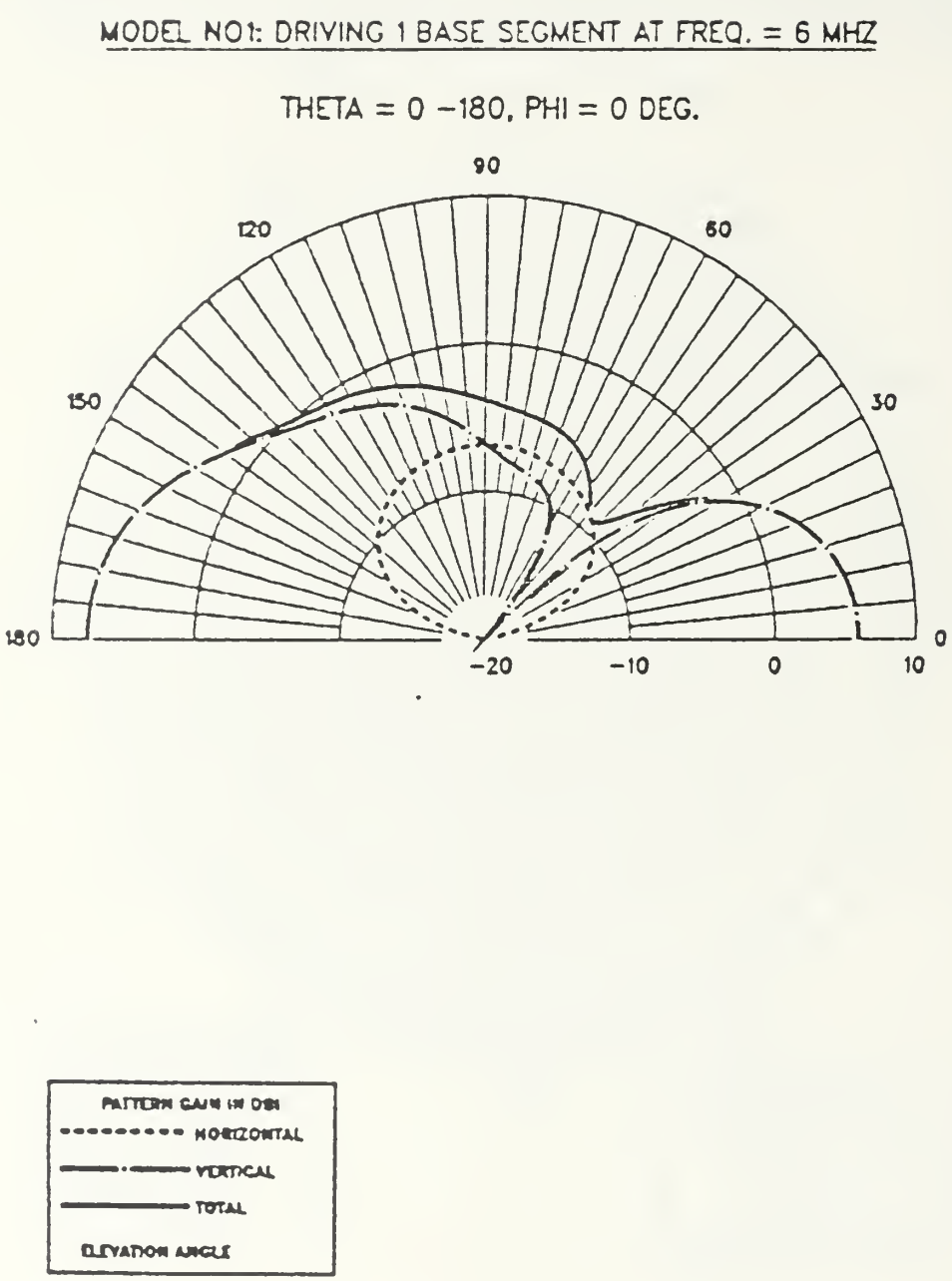

Figure G.21 E-Field Vertical Radiation Pattern: F = 6 MHz, vs. One Feed Point Position.

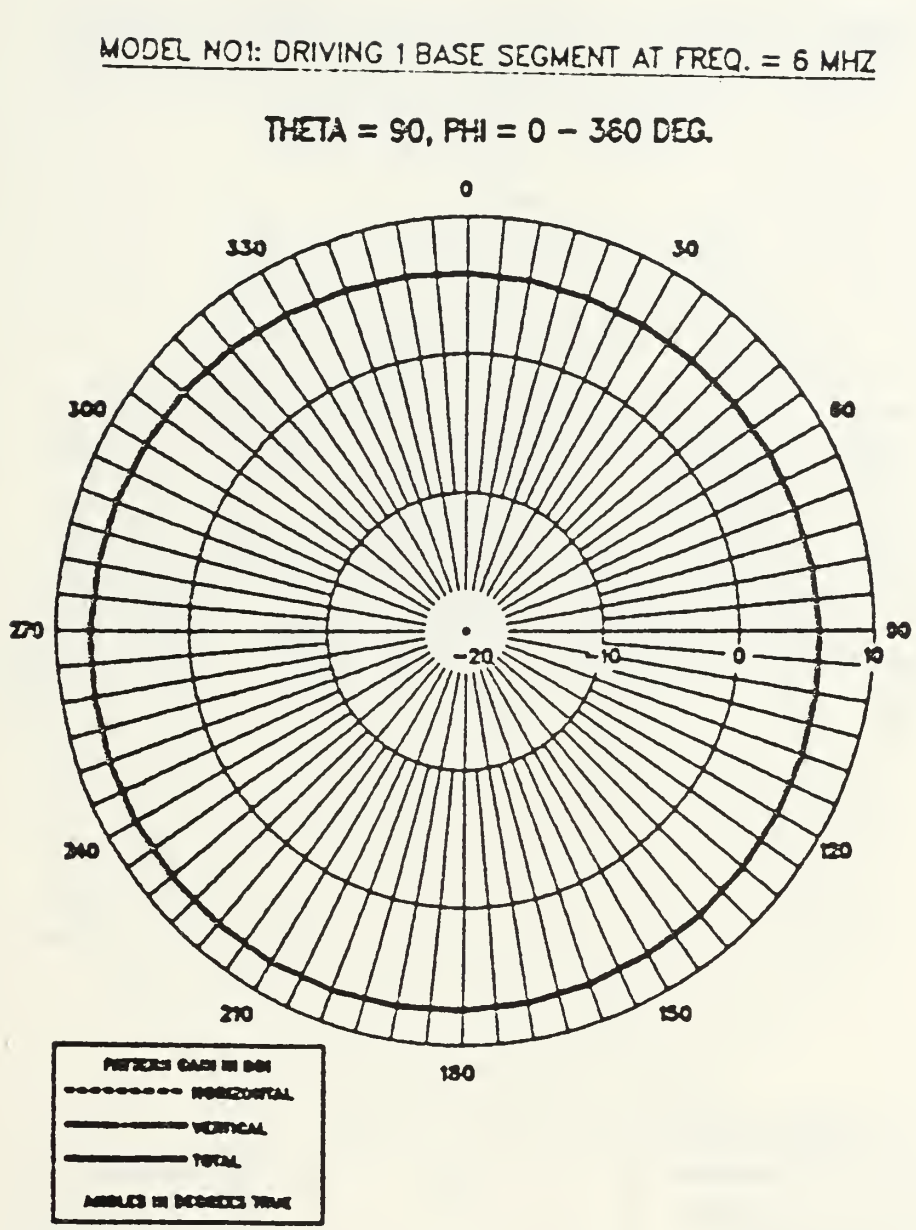

Figure G.22 E-Field Horizontal Radiation Pattern: F = 6 MHz, vs. One Feed Point Position.

MODEL NO1: DRIVING 4 BASE SEGMENTS AT FREQ. = 7.74 MHZ

THETA = 0 −180, PHI = 0 DEG.

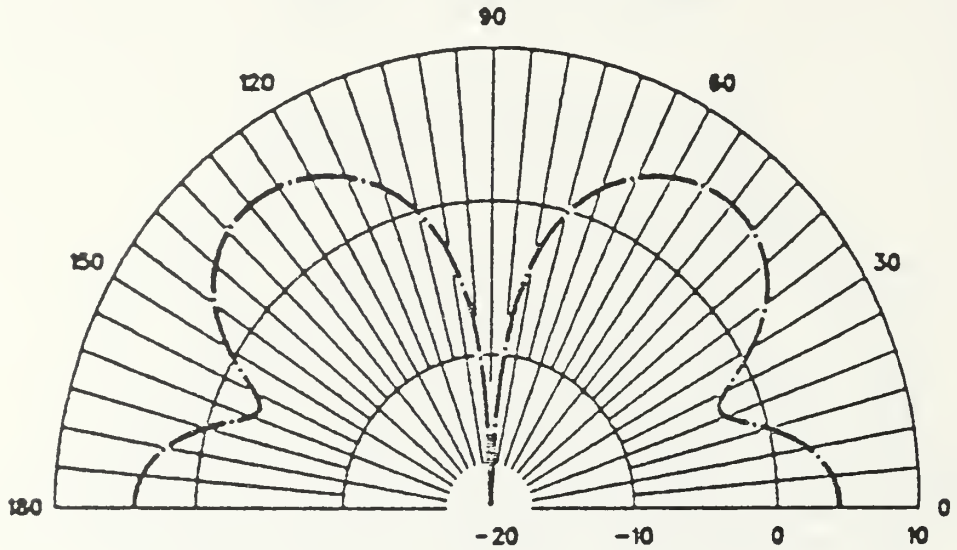

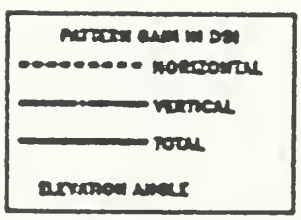

Figure G.23 E-Field Vertical Radiation Pattern: F = 7.7Figure 4 MHz, vs. Four Feed Point Positions.

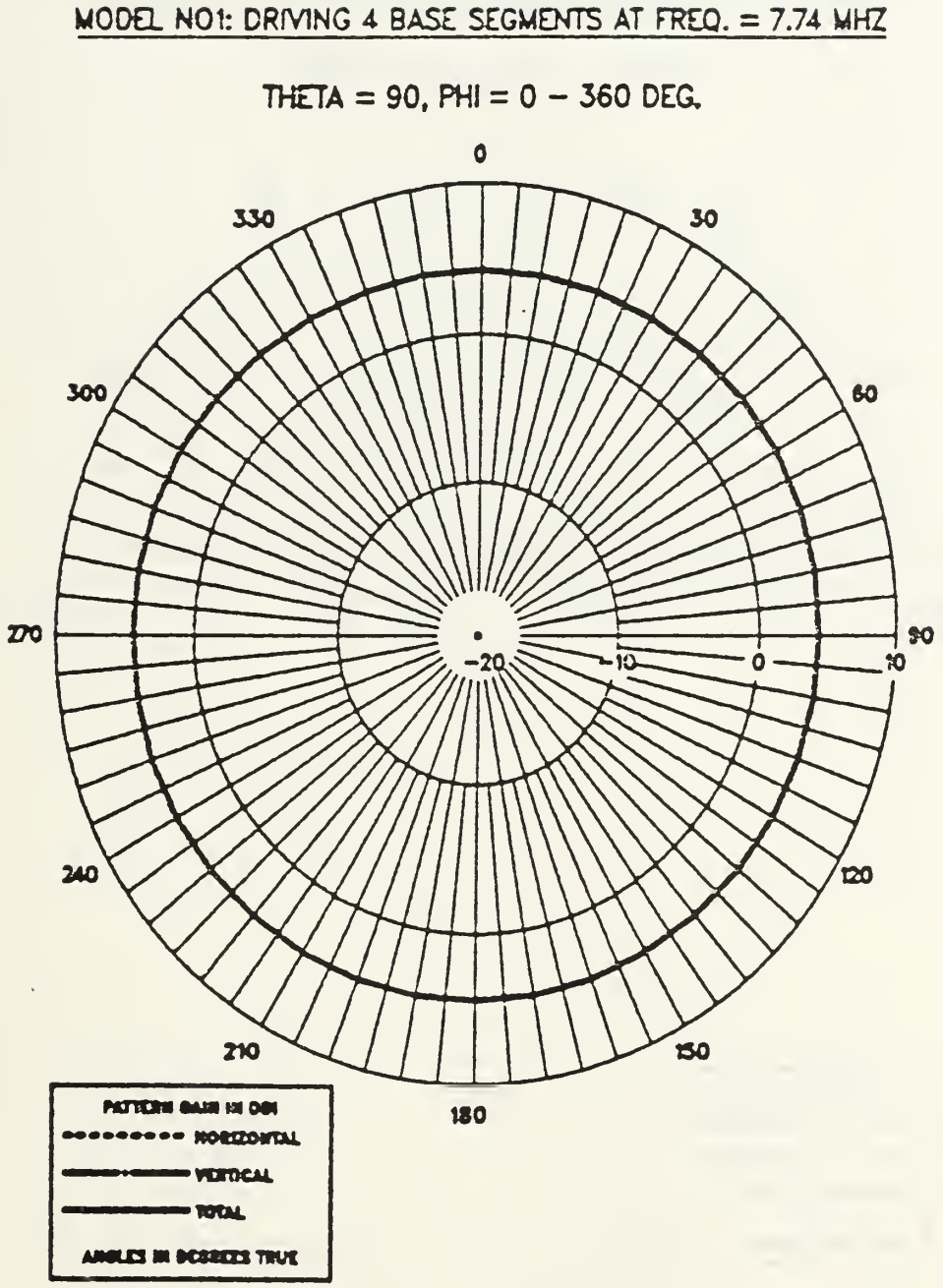

Figure G.24 E-Field Horizontal Radiation Pattern: F = 7.7Figure 4 MHz, vs. Four Feed Point Positions.

MODEL NO1: DRIVING 4 BASE SEGMENTS AT FREQ. = 10 MHZ

THETA = 0 -180, PHI = 0 DEG.

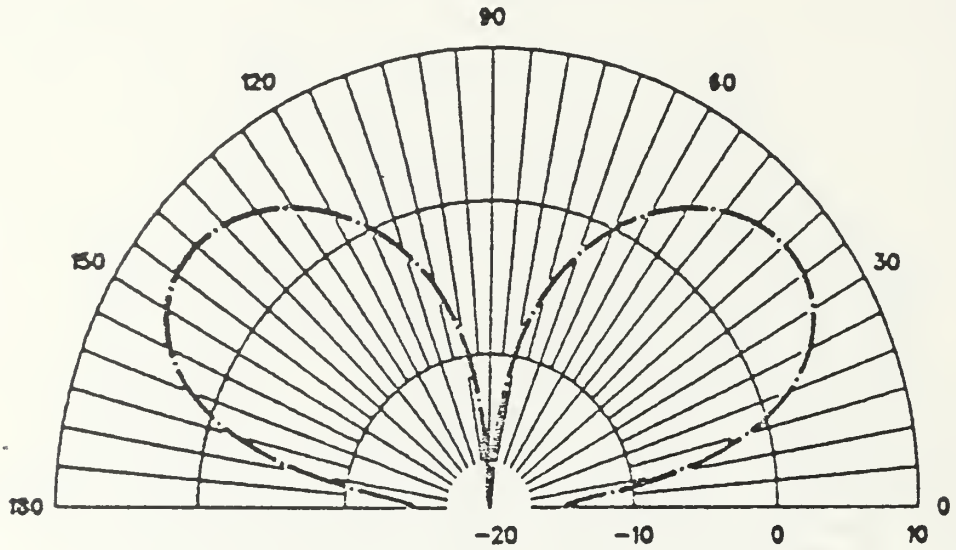

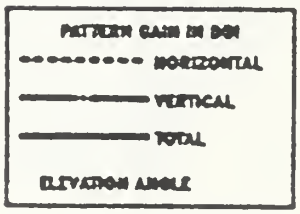

Figure G.25 E-Field Vertical Radiation Pattern: F = 10 MHz, vs. Four Feed Point Positions.

MODEL NO1: DRIVING 4 BASE SEGMENTS AT FREQ. = 10 MHZ

THETA = 90, PHI = 0 – 360 DEG.

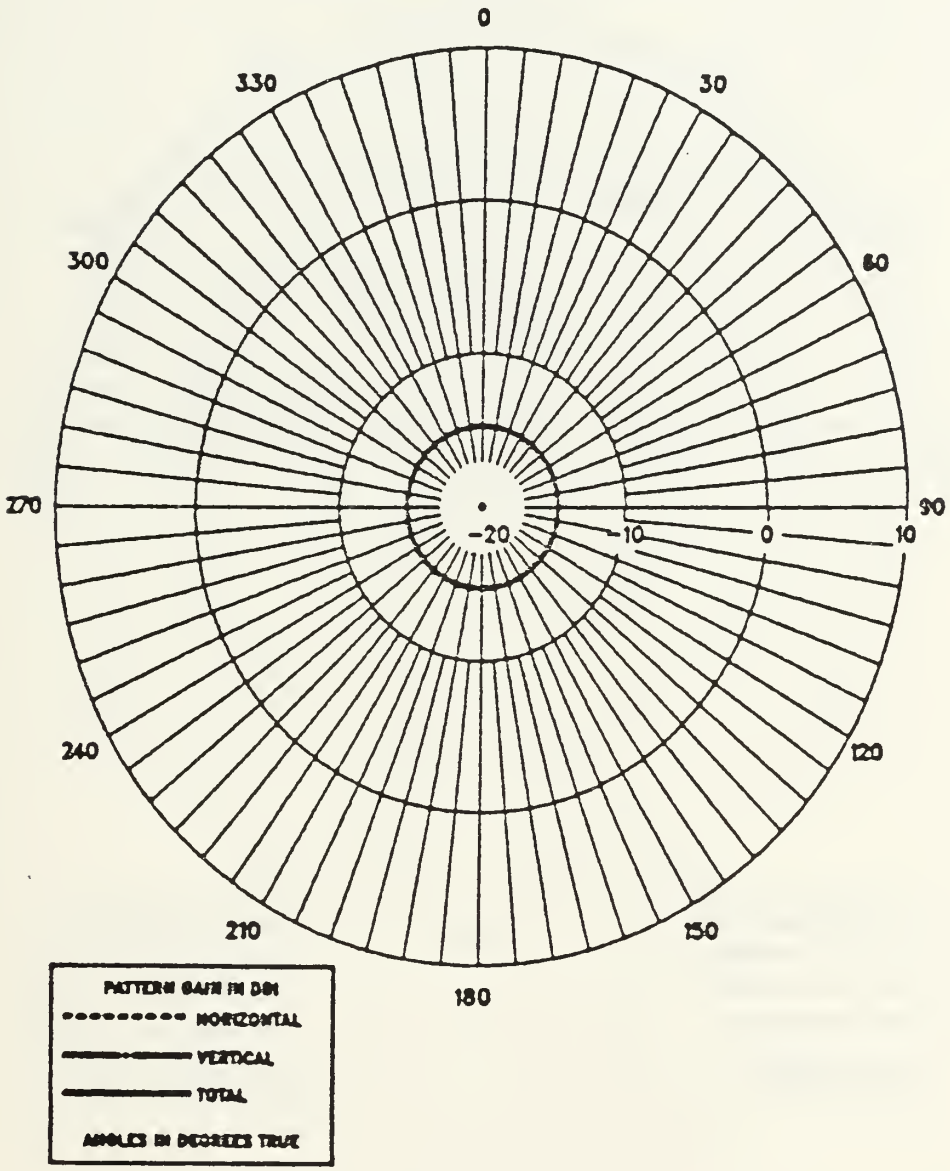

Figure G.26 E-Field Horizontal Radiation Pattern: F = 10 MHz, vs. Four Feed Point Positions.

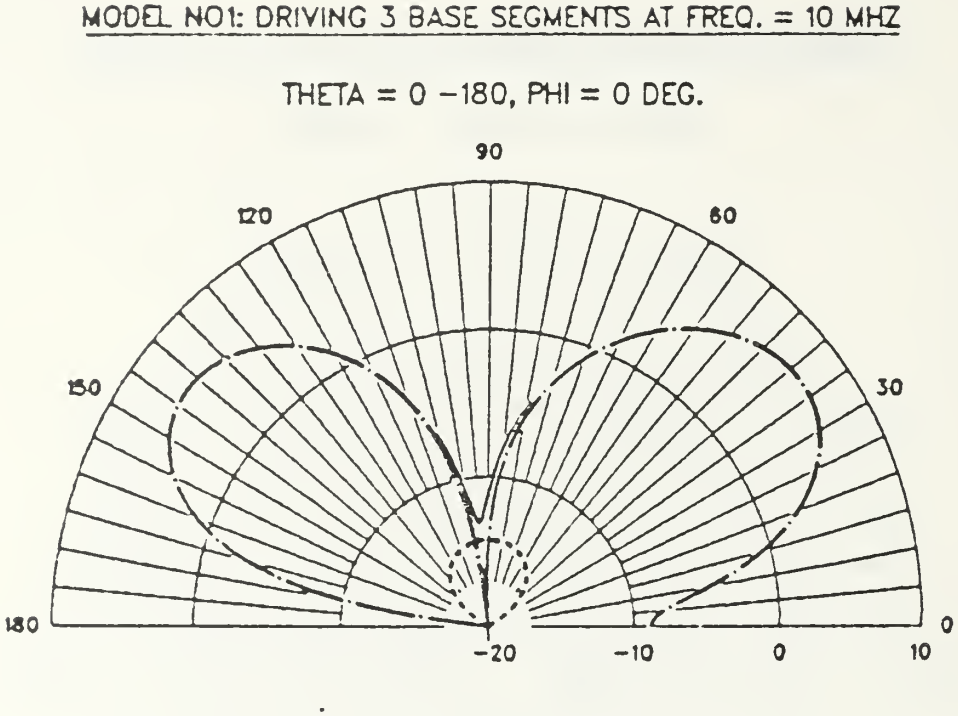

Figure G.27 E-Field Vertical Radiation Pattern: F = 10 MHz, vs. Three Feed Point Positions.

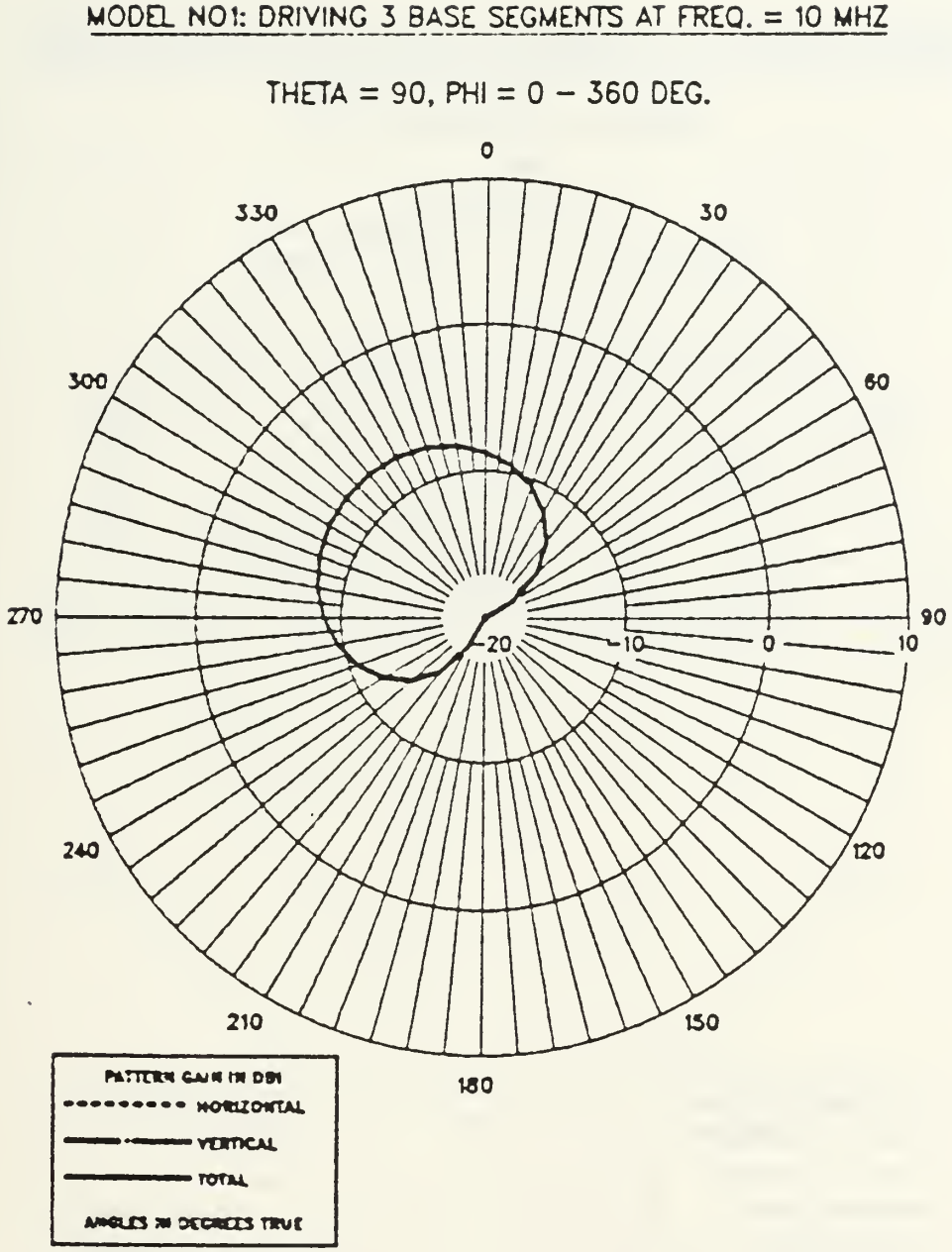

Figure G.28 E-Field Horizontal Radiation Pattern: F = 10 MHz, vs. Three Feed Point Positions.

MODEL NO1: DRIVING 2 ADJACENT BASE SEGMENTS AT FREQ = 10 MHZ

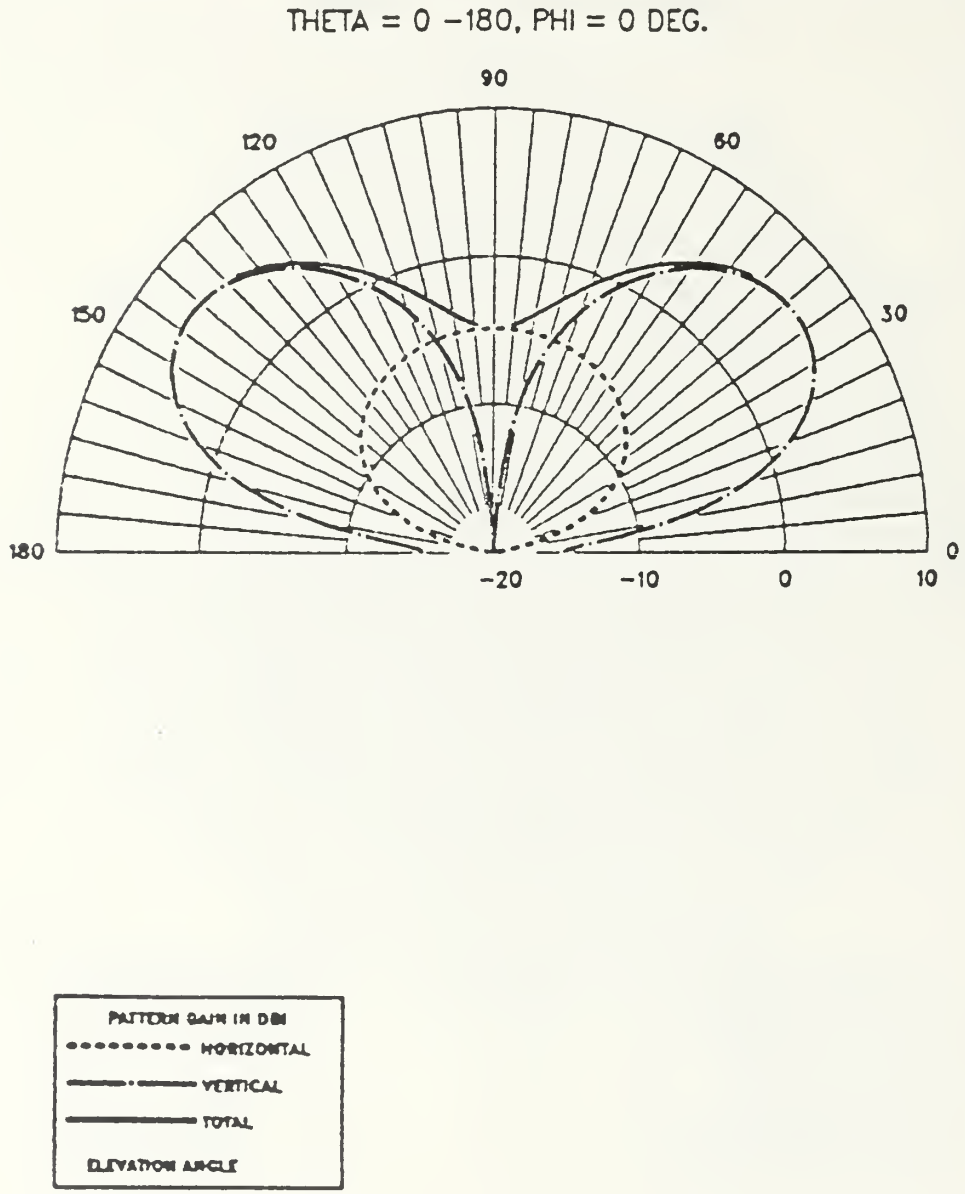

Figure G.29 E-Field Vertical Radiation Pattern: F = 10 MHz, vs. Two Adjacent Feed Point Positions.

MODEL NO1: DRIVING 2 ADJACENT BASE SEGMENTS AT FREQ = 10 MHZ

THETA = 90, PHI = 0 - 360 DEG.

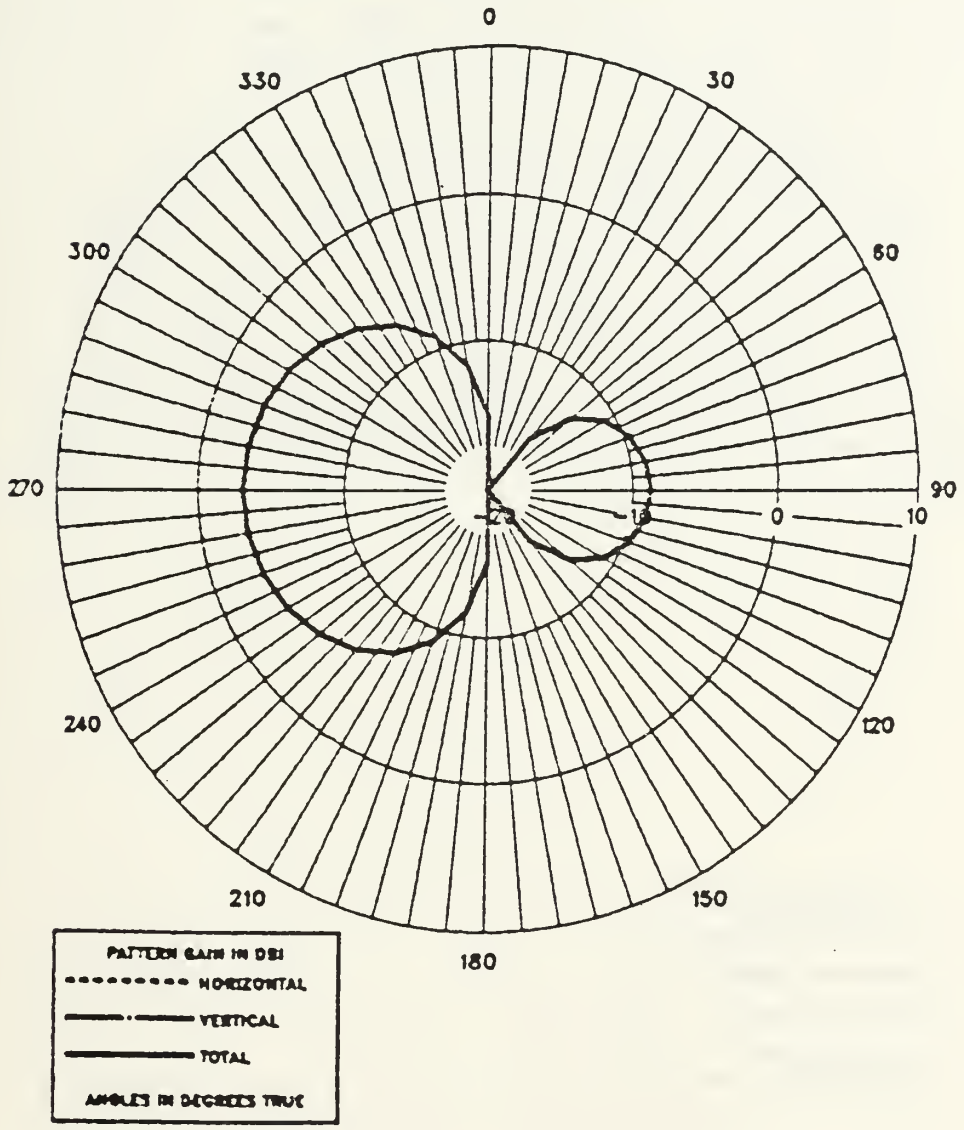

Figure G.30 E-Field Horizontal Radiation Pattern: F = 10 MHz, vs. Two Adjacent Feed Point Positions.

MODEL NO1: DRIVING 2 DIAGONAL BASE SEGMENTS AT FREQ = 10 MHZ

THETA = 0 -180, PHI = 0 DEG.

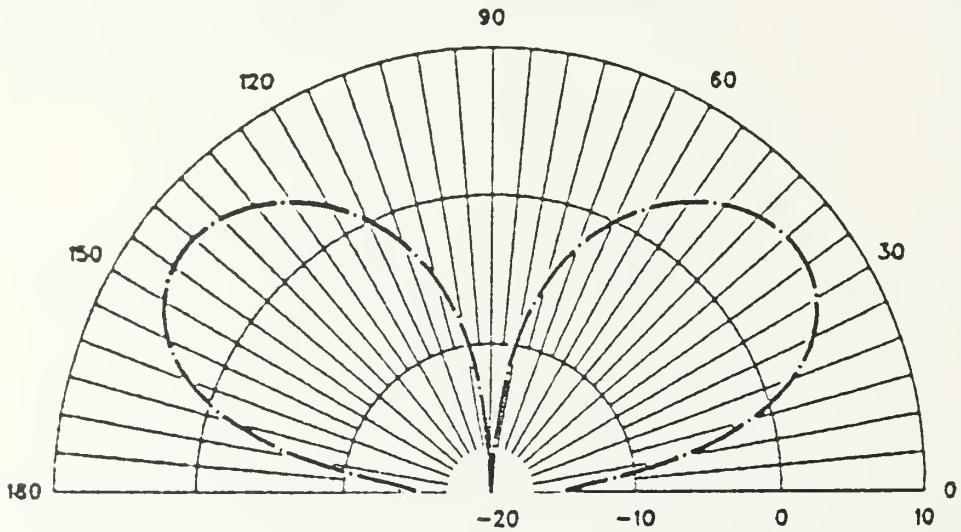

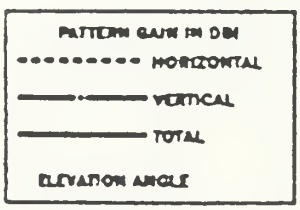

Figure G.31 E-Field Vertical Radiation Pattern: F = 10 MHz, vs. Two Diagonal Feed Point Positions.

MODEL NO1: DRIVING 2 DIAGONAL BASE SEGMENTS AT FREQ = 10 MHZ

THETA = 90, PHI = 0 – 360 DEG.

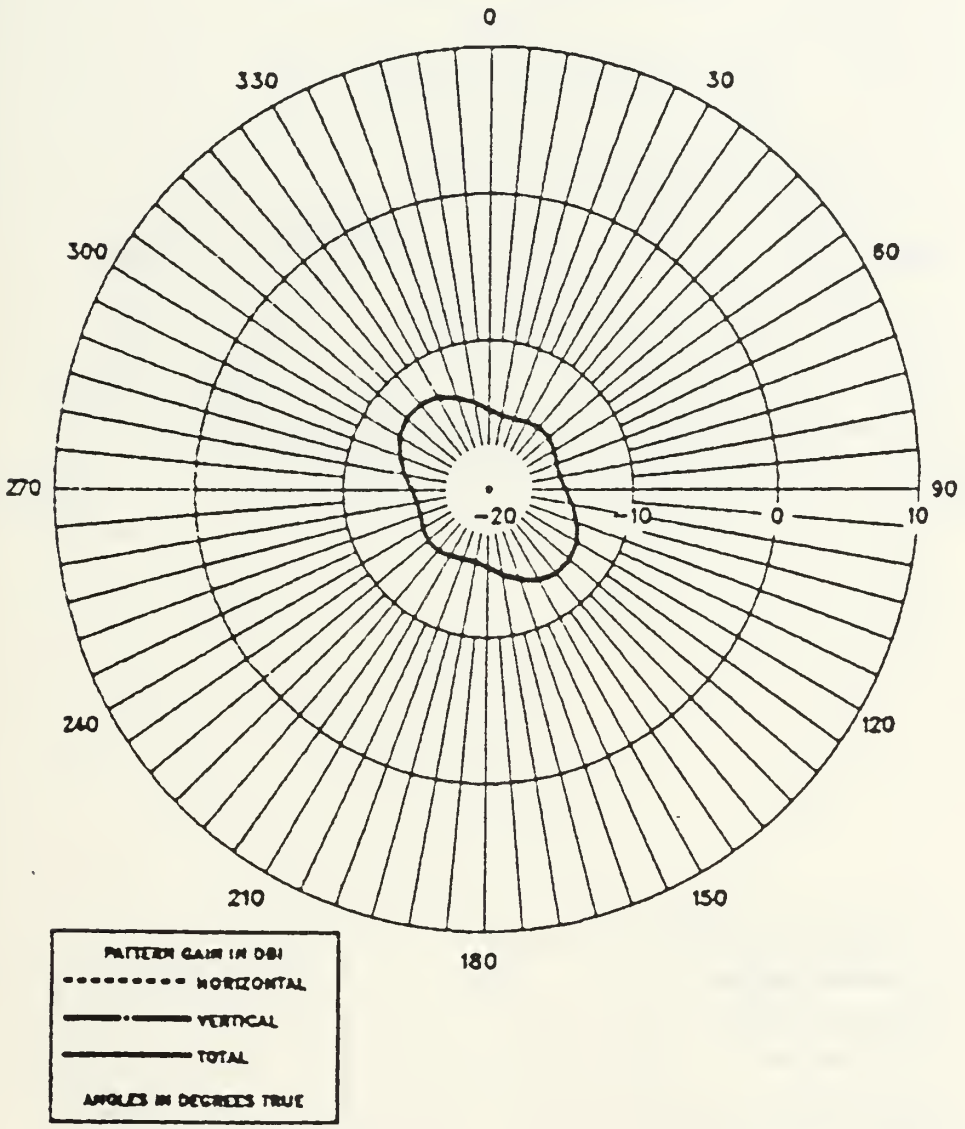

Figure G.32 E-Field Horizontal Radiation Pattern: F = 10 MHz, vs. Two Diagonal Feed Point Positions.

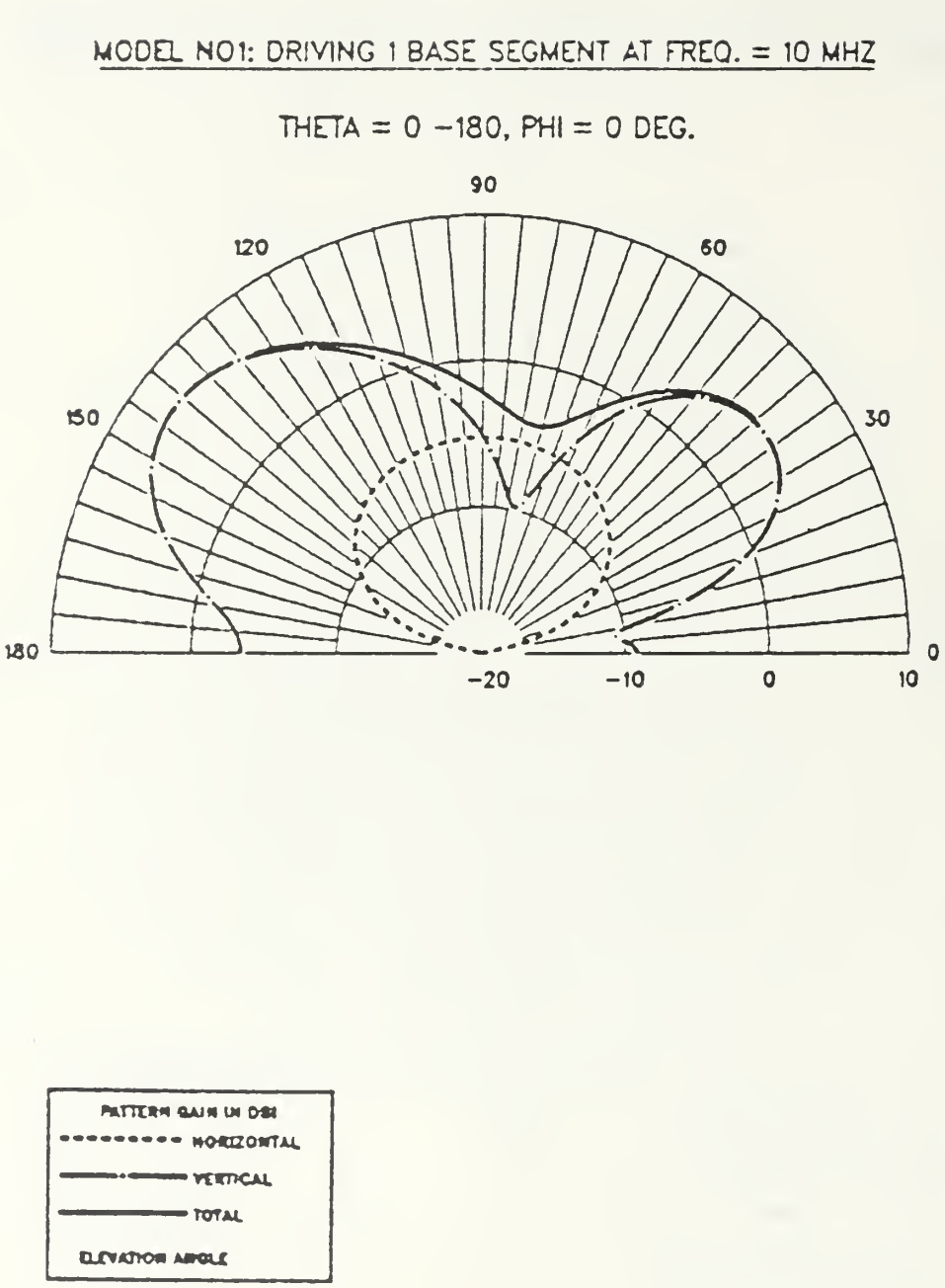

Figure G.33 E-Field Vertical Radiation Pattern: F = 10 MHz, vs. One Feed Point Position.

MODEL NO1: DRIVING 1 BASE SEGMENT AT FREQ. = 10 MHZ

THETA = 90, PHI = 0 – 360 DEG.

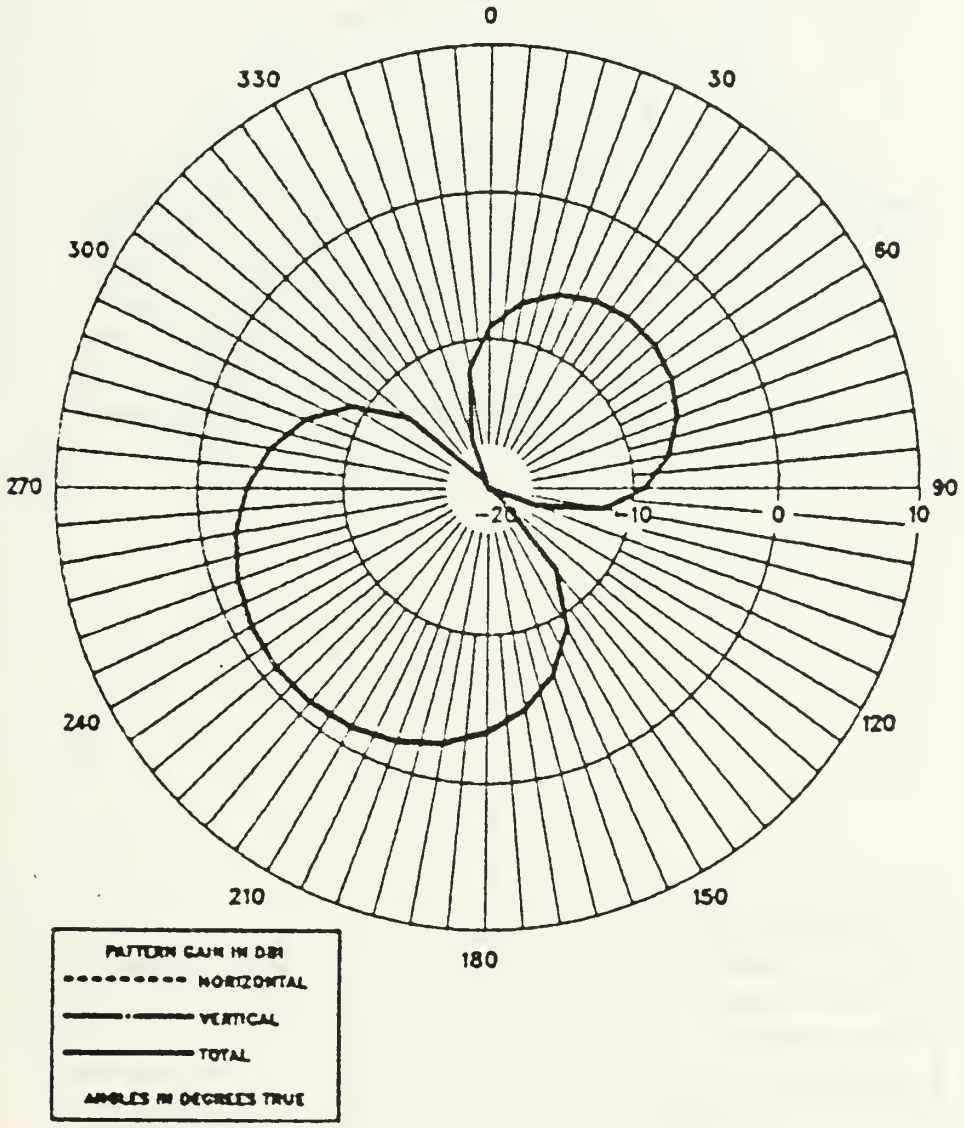

Figure G.34 E-Field Horizontal Radiation Pattern: F = 10 MHz, vs. One Feed Point Position.

MODEL NO 2: DRIVING 12 BASE SEGMENTS AT FREQ. = 11 MHZ

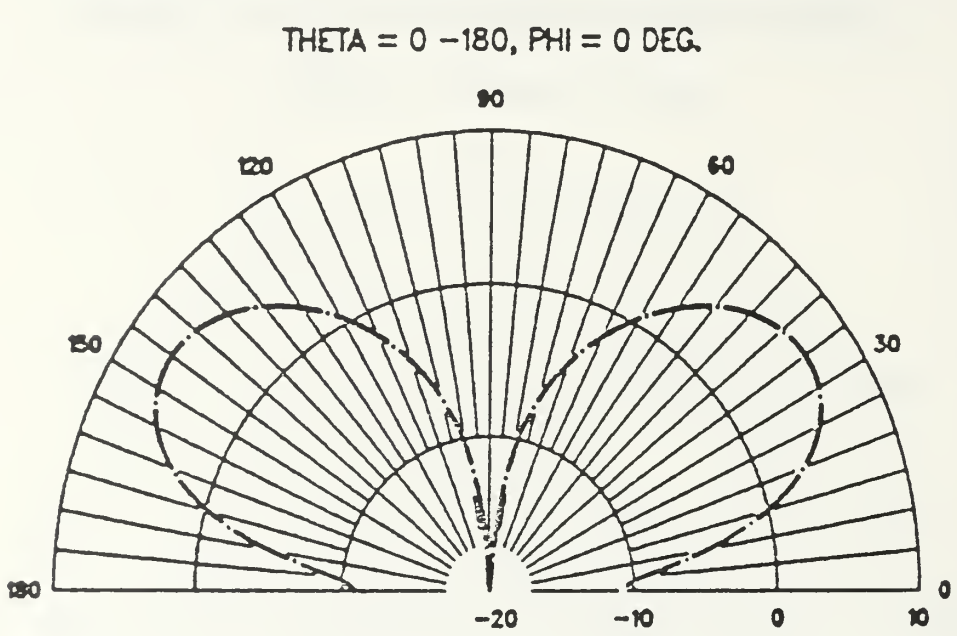

Figure G.35 E-Field Vertical Radiation Pattern: F = 11 MHz, vs. All Base Feed Point Positions.

MODEL NO 2: DRIVING 12 BASE SEGMENTS AT FREQ. = 11 MHZ

THETA = 90, PHI = 0 – 360 DEG.

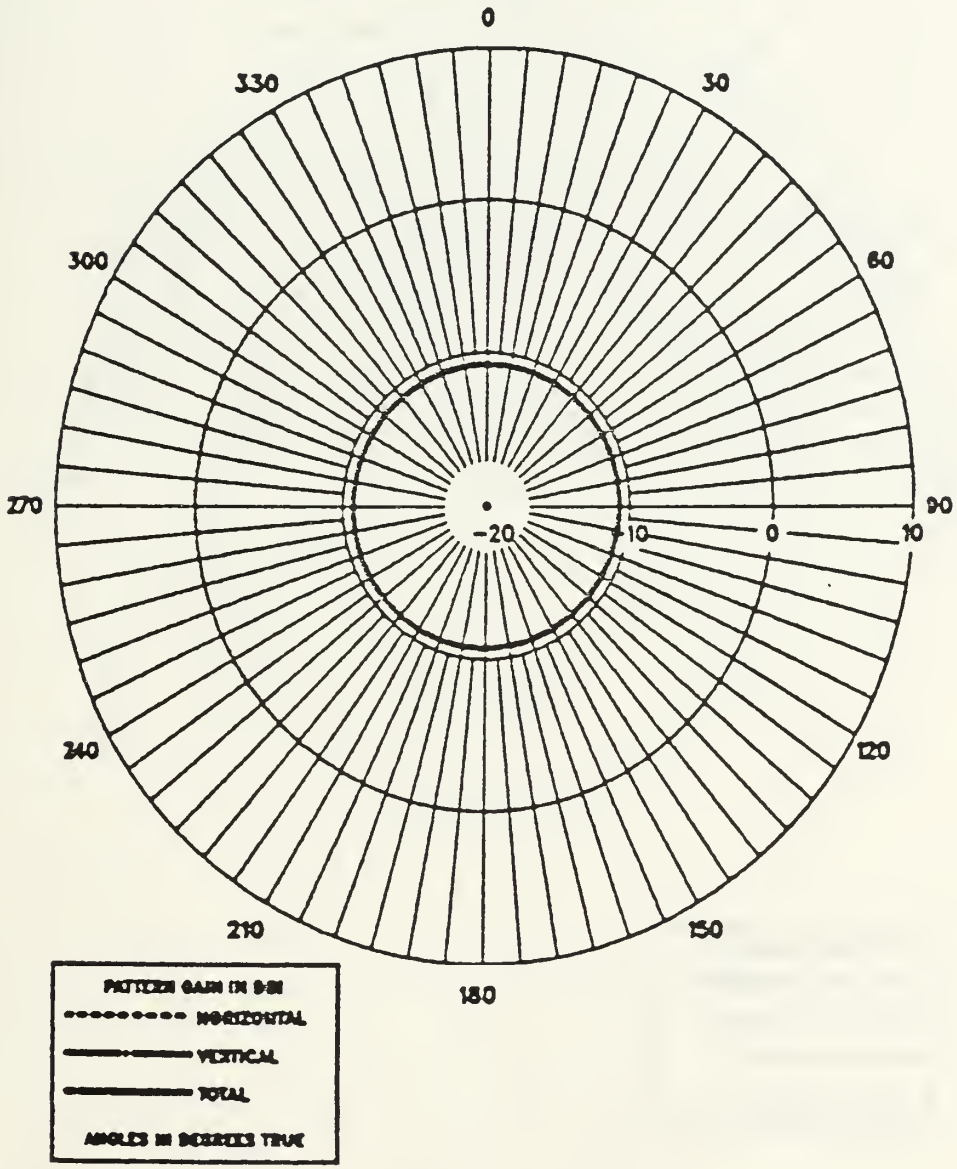

Figure G.36 E-Field Horizontal Radiation Pattern: F = 11 MHz, vs. All Base Feed Point Positions.

MODEL NO 2: DRIVING 12 BASE SEGMENTS AT FREQ. = 12.85 MHZ

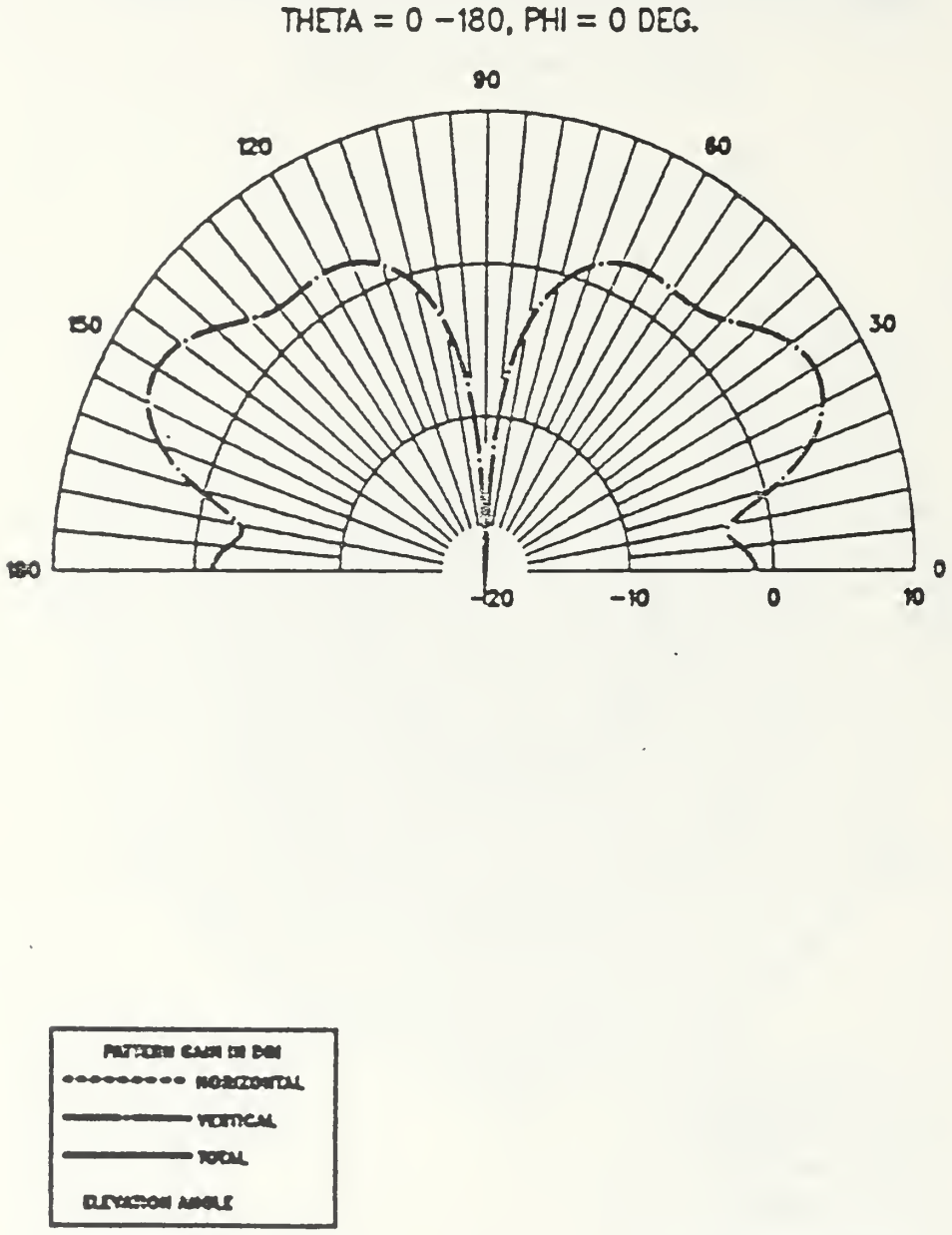

Figure G.37 E-Field Vertical Radiation Pattern: F = 12.85 MHz, vs. All Base Feed Point Positions.

MODEL NO 2: DRIVING 12 BASE SEGMENTS AT FREQ. = 12.85 MHZ

THETA = 90, PHI = 0 – 360 DEG.

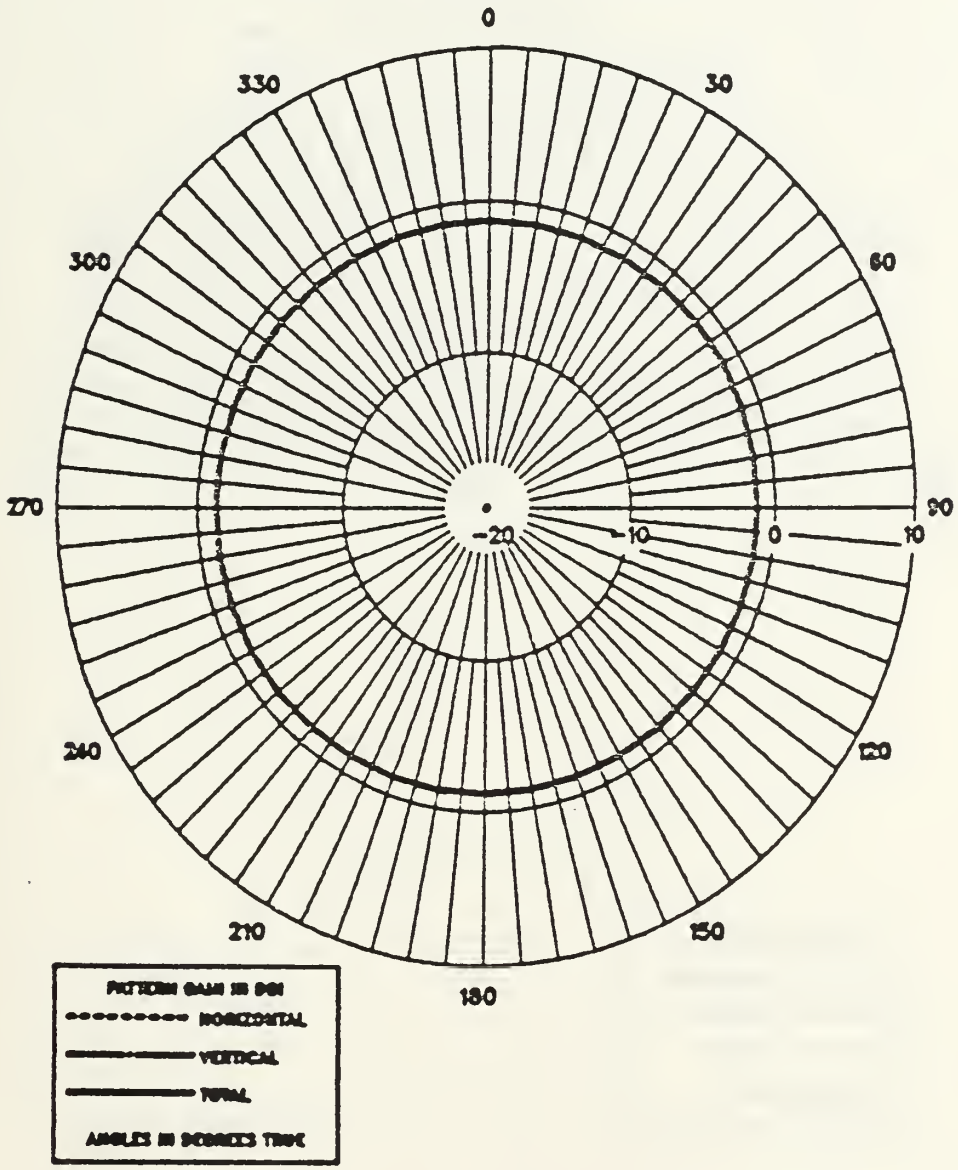

Figure G.38 E-Field Horizontal Radiation Pattern: F = 12.85 MHz, vs. All Base Feed Point Positions.

MODEL NO 2: DRIVING 12 BASE SEGMENTS AT FREQ. = 15 MHZ

THETA = 0 -180, PHI = 0 DEG.

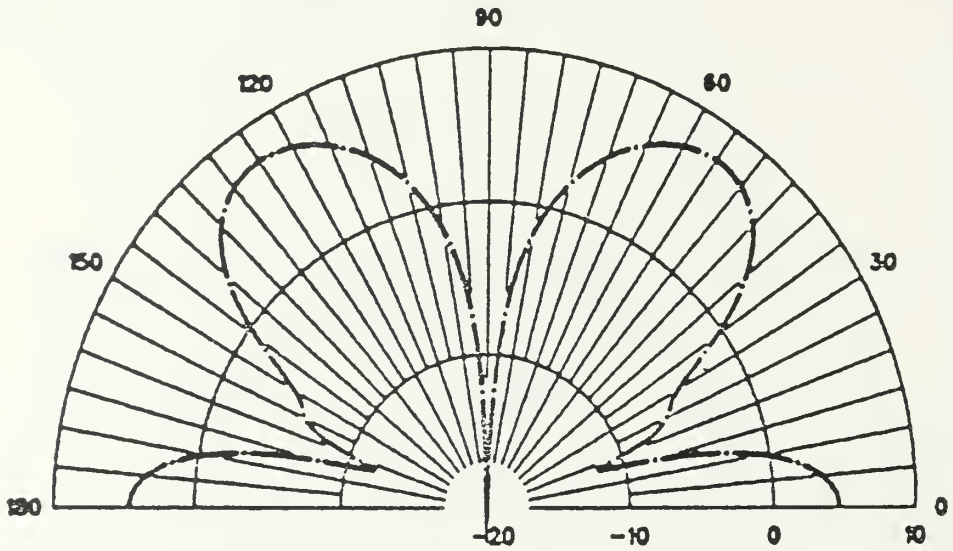

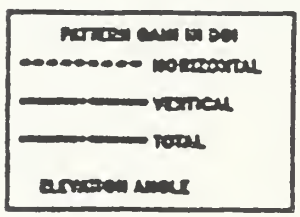

Figure G.39 E-Field Vertical Radiation Pattern: F = 15 MHz, vs. All Base Feed Point Positions.

MODEL NO 2: DRIVING 12 BASE SEGMENTS AT FREQ. = 15 MHZ

THETA = 90, PHI = 0 – 360 DEG.

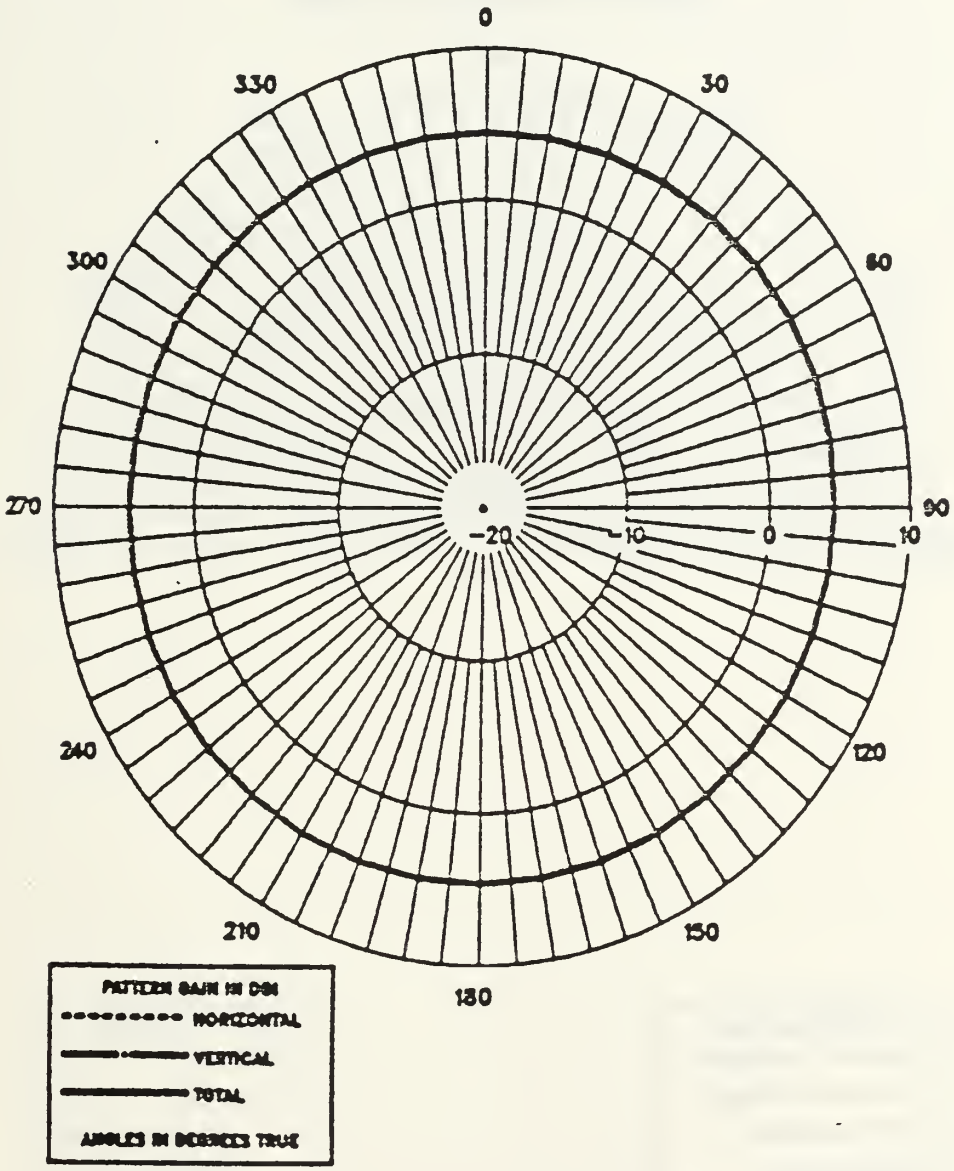

Figure G.40 E-Field Horizontal Radiation Pattern: F = 15 MHz, vs. All Base Feed Point Positions.

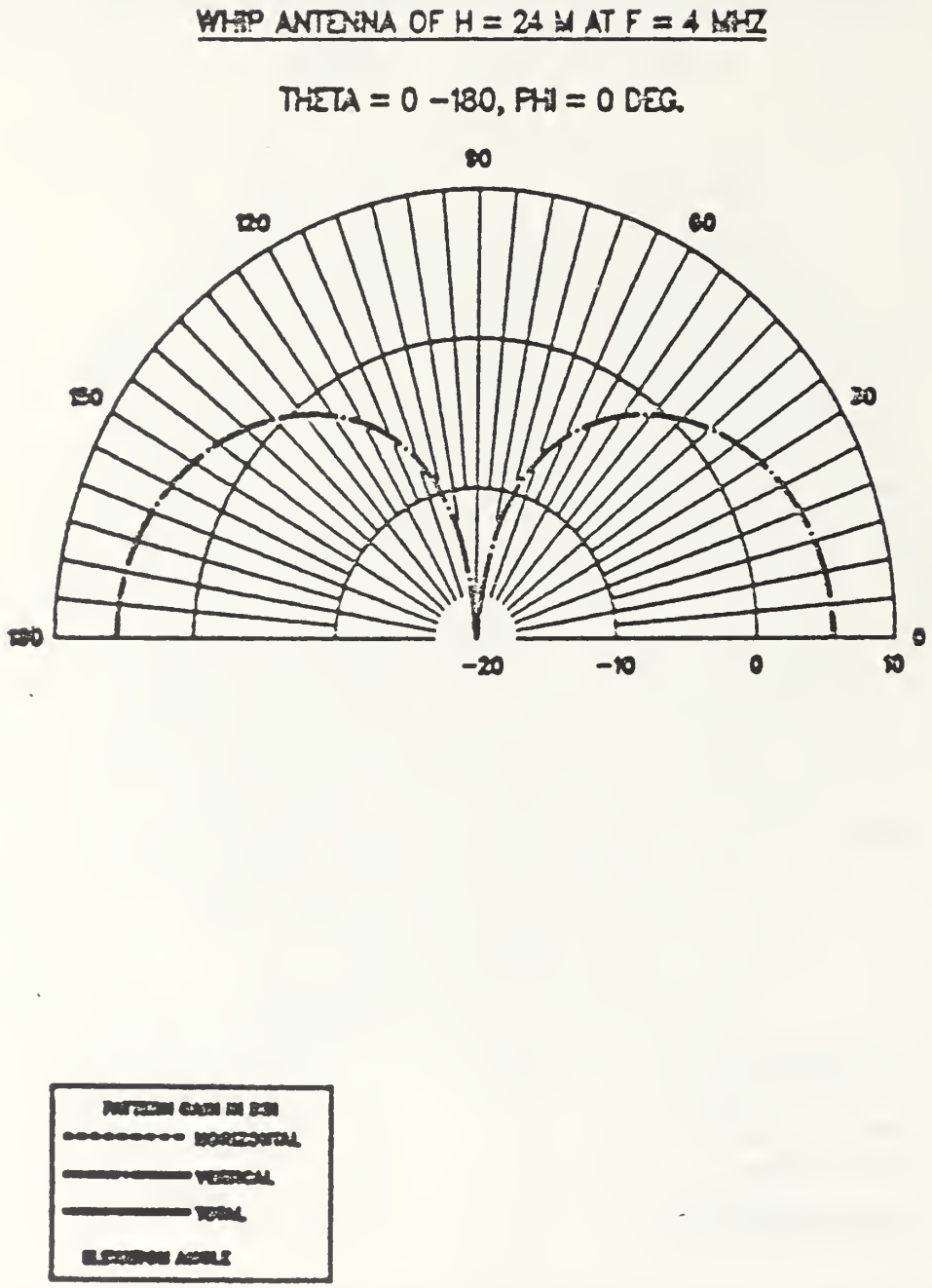

Figure G.41 E-Field Vertical Radiation Pattern of Whip Antenna Whose Height Is Equal to That of the Antenna of Figures G.1-G.40 in Frequency 4 MHz.

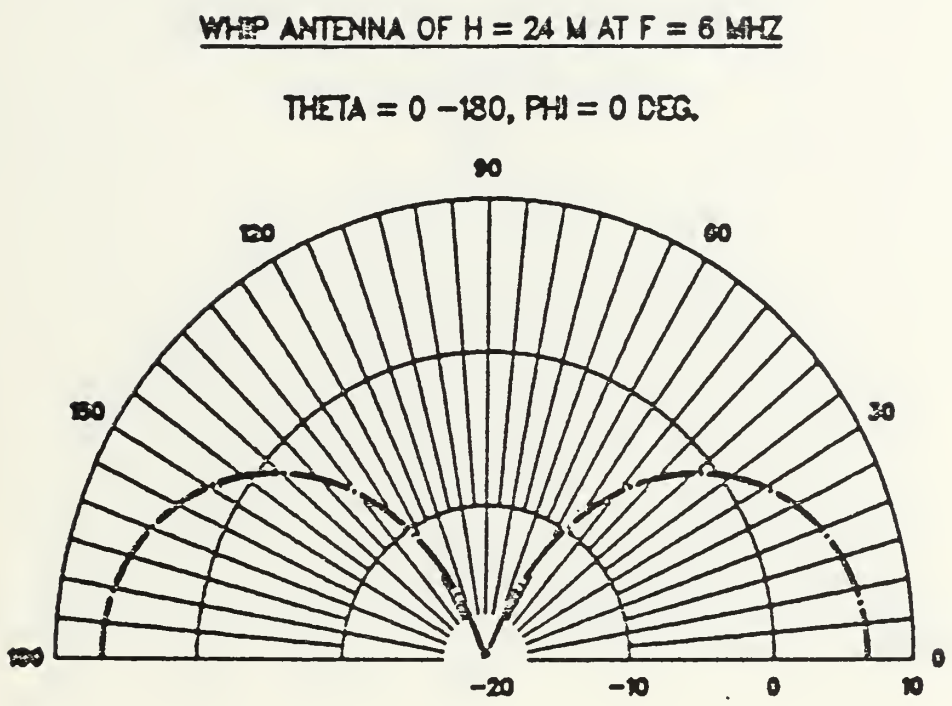

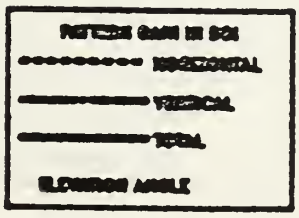

Figure G.42 E-Field Vertical Radiation Pattern of Whip Antenna Whose Height Is Equal to That of the Antenna of Figures G.1-G.40 in Frequency 6 MHz.

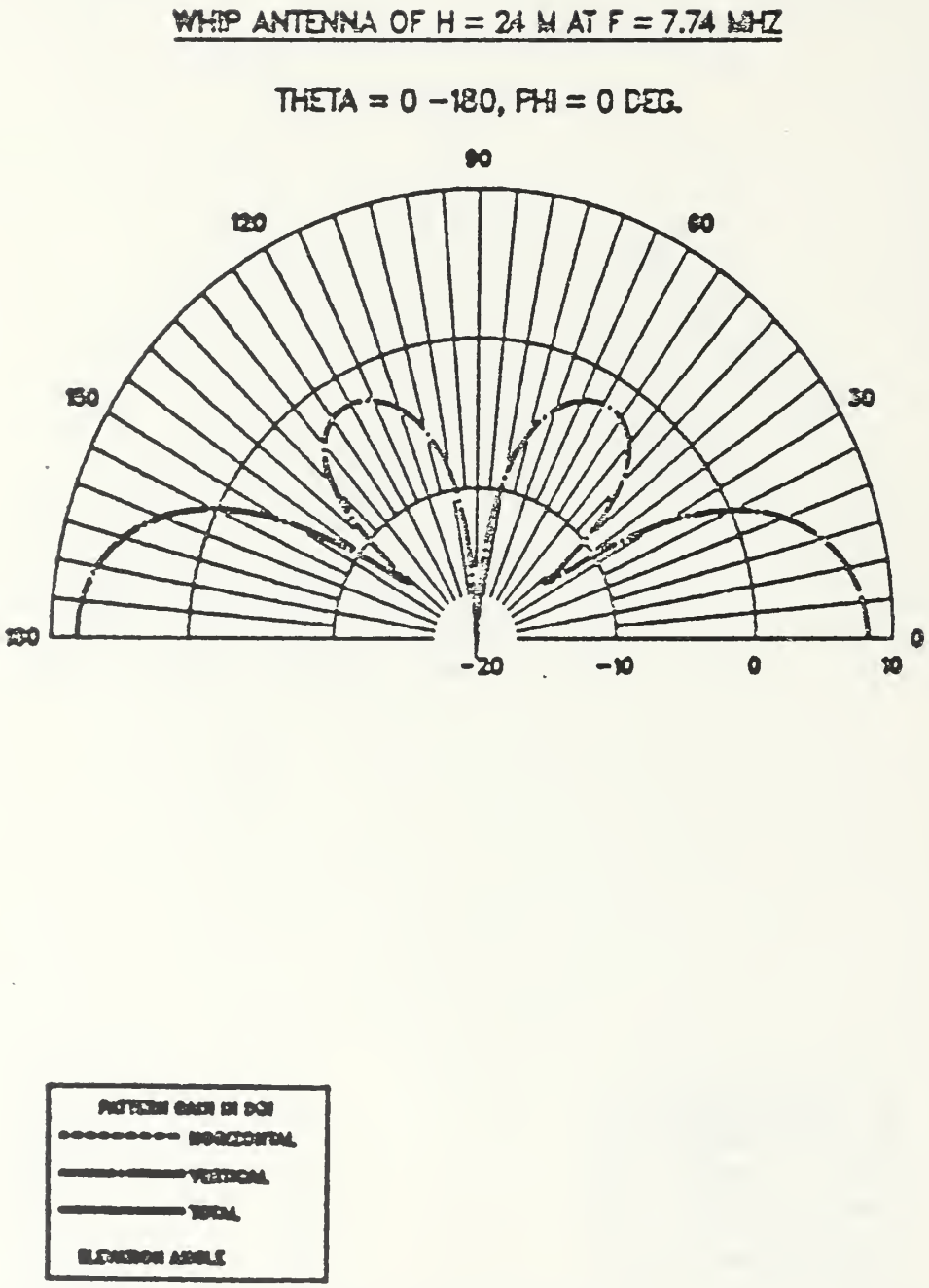

Figure G.43 E-Field Vertical Radiation Pattern of Whip Antenna Whose Height Is Equal to That of the Antenna of Figures G.1-G.40 in Frequency 7.74 MHz.

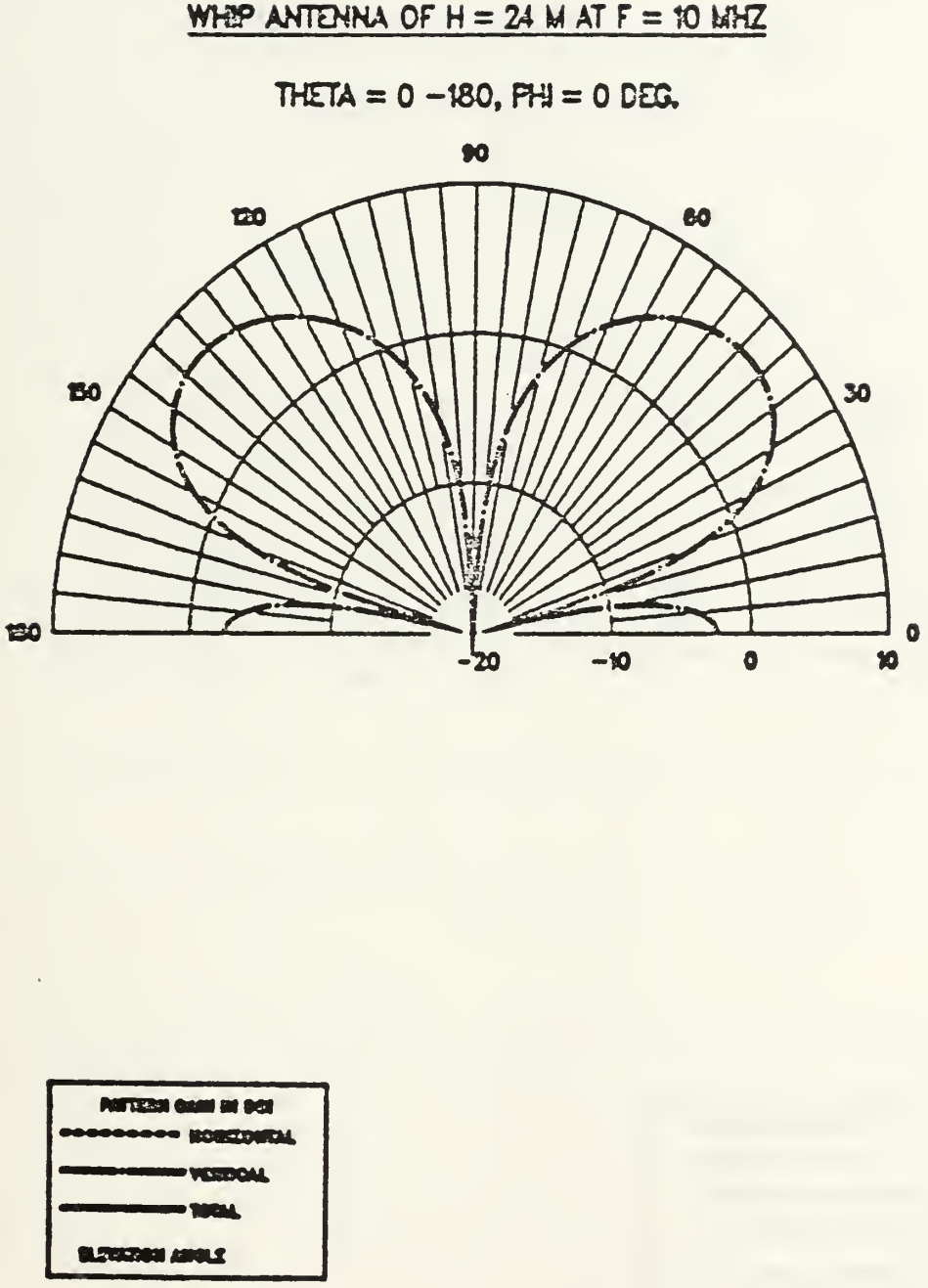

Figure G.44 E-Field Vertical Radiation Pattern of Whip Antenna Whose Height Is Equal to That of the Antenna of Figures G.1-G.40 in Frequency 10 MHz.

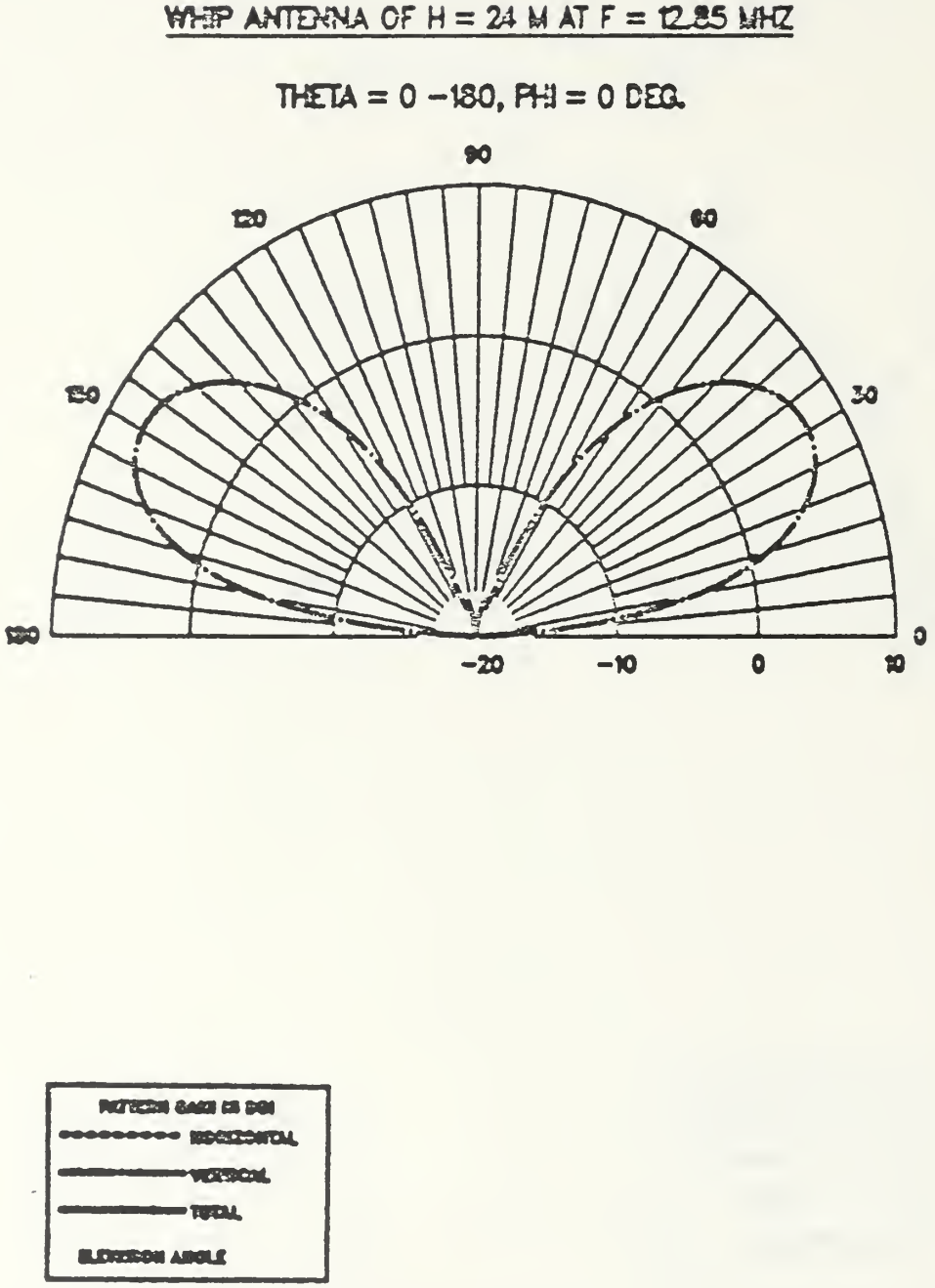

Figure G.45 E-Field Vertical Radiation Pattern of Whip Antenna Whose Height Is Equal to That of the Antenna of Figures G.1-G.40 in Frequency 12.85 MHz.

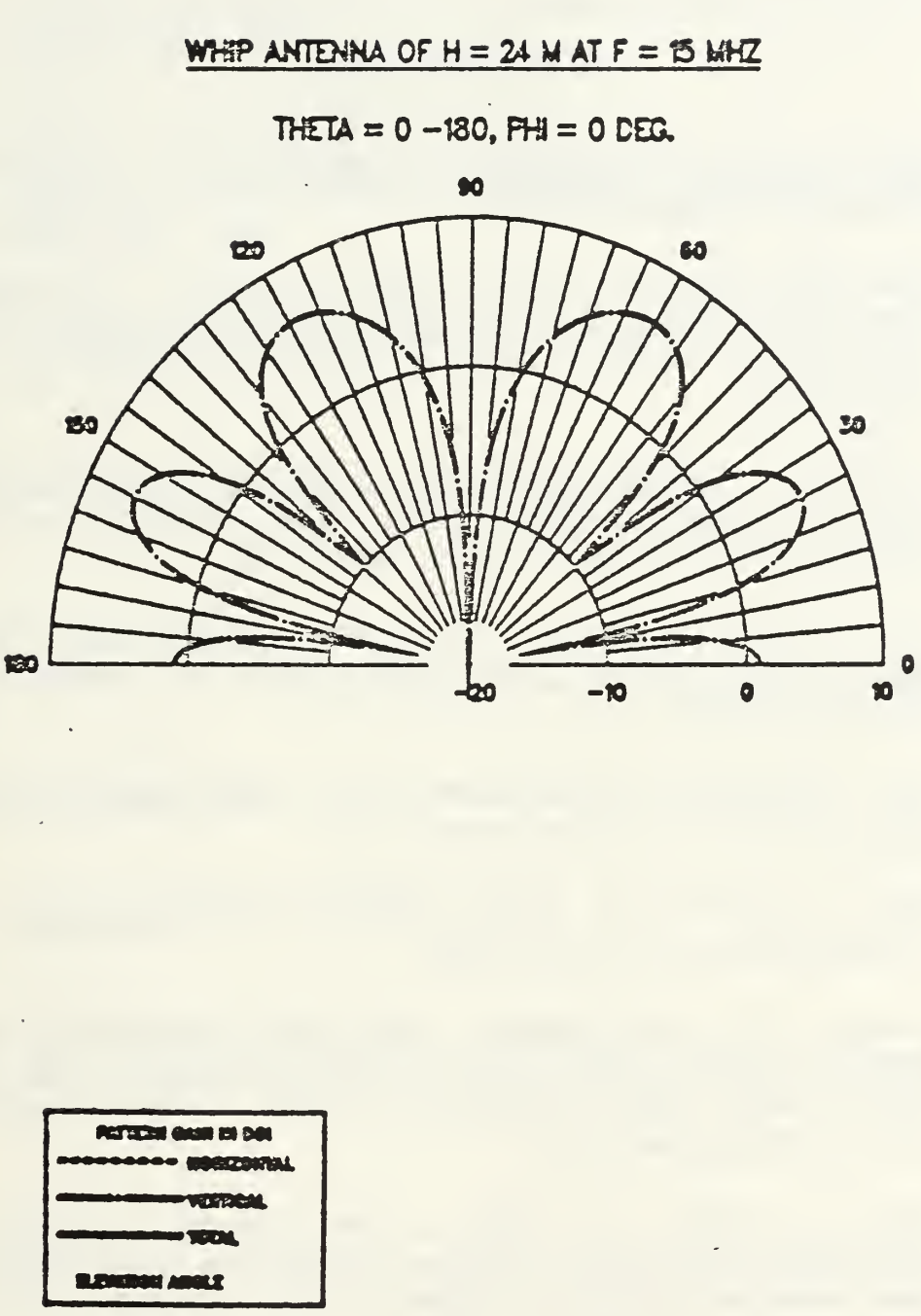

Figure G.46 E-Field Vertical Radiation Pattern of Whip Antenna Whose Height Is Equal to That of the Antenna of Figures G.1-G.40 in Frequency 15 MHz.

LIST OF REFERENCES

1. Peebles, P. Z. Jr., Communication System Principles, Addison-Wesley Publishing Company, p. 3, 1976.

2. Naval Ocean Systems Center Technical Document 116, Volume 2, Numerical Electromagnetic Code (NEC) - Methods of Moments, by G. J. Burke and A. J. Pogio of Lawrence Livermore Laboratory, pp. 3-14, January 1981.

3. Tertocha,C. J., A Feasibility Study of a Shipboard Combat Survivable HF Antenna Design, M.S.E.E. Thesis, Naval Postgraduate School, Monterey, California, pp. 16, 68-72, March 1986.

4. Naval Electronic Systems Command, FFG-45 Thru. FFG-55 Communication Antenna Configuration Data, p. 11, Washington, DC. 20360, July 1984.

5. Naval Postgraduate School Report MVS-01, User's Guide to MVS at NPS, by J. Favorite, p. 29, November 1983.

6. Moore, J., and Pizer, R., Moment Methods in Electromagnetics, John Wiley and Sons, pp. 8-10, June 1983.

7. Thomson, D. D., Electromagnetic Near-Field Computations for a Broadcast Monopole Using Numerical Electromagnetics Code (NEC), M.S.E.E. Thesis, Naval Postgraduate School, Monterey, California, pp. 43-45, September 1983.

8. Burke, G.J., Poggio, A.J., Logan, J.C., and Rockway, J.W., Numerical Electromagnetics Code--A Program for Antenna System Analysis, Paper presented at the EMC Symposium and Exhibition, Rotterdam, Netherlands, pp. 1-2, May 1-3, 1979.

9. Lawrence Livermore Laboratory, Wires and Wire Grid Models for Radiation and Scattering Including Ground Effects, by E. K. Miller, May 30, 1976.

10. Stutzman, W. L., and Thiele, G. A., Antenna Theory and Design, John Wiley and Sons, 1981.

11. Kraus, J. D., Antennas, McGraw-Hill, 1950.

12. Jonhson, R. C., and Jasik, H., Antenna Engineering Handbook, McGraw-Hill, 1984.

INITIAL DISTRIBUTION LIST

		No. Copies
1.	Defense Technical Information Center Cameron Station Alexandria, Virginia 22304-6145	2
2.	Library, Code 0142 Naval Postgraduate School Monterey, California 93943-5000	2
3.	Department Chairman, Code 62 Department of Electrical and Computer Engineering Naval Postgraduate School Monterey, California 93943-5000	1
4.	Professor R. W. Adler, Code 62Ab Department of Electrical and Computer Engineering Naval Postgraduate School Monterey, California 93943-5000	5
5.	Professor S. Jauregui, Code 62Ja Department of Electrical and Computer Engineering Naval Postgraduate School Monterey, California 93943-5000	1
6.	Hellenic Navy General Staff 2nd Branch, Education Department Stratopedon Papagou, Holargos Athens 155.61, GREECE	4
7.	LT George L. Lyberopoulos, H.N Ferron St. 48-50 Athens 104.40, GREECE	3
8.	W.F. Flanigan, Code 825 Naval Ocean Systems Center 271 Catalina Blvd. San Diego, California 92152	1

9. M. Selkellick, Code 1202 — 1
David Taylor Naval Ship Research
Development Center
Betheseda, Maryland 20084-5000

10. D. Washburn, Code 7403 — 1
Naval Ocean Systems Center
271 Catalina Blvd.
San Diego, California 92152

11. Jim Logan, Code 822 — 1
Naval Ocean Systems Center
271 Catalina Blvd.
San Diego, California 92152

12. Rick Thowless, Code 822 — 1
Naval Ocean Systems Center
271 Catalina Blvd.
San Diego, California 92152

13. Jim K. Breakall — 1
Lawrence Livermore National Laboratory
P.O. Box 5504, 1-156
Livermore, California 94550

14. G. Burke — 1
Lawrence Livermore National Laboratory
P.O. Box 5504, 1-156
Livermore, California 94550

15. E. Domning — 1
Lawrence Livermore National Laboratory
P.O. Box 5504, 1-156
Livermore, California 94550

16. Robert Latorre — 1
Lawrence Livermore National Laboratory
P.O. Box 5504, 1-156
Livermore, California 94550

17. Donn Cambell — 1
CECOM-CENCOMS
Fort Monmouth, New Jersey 07703

18. Ron Corry — 1
USAISEA/ASBH-SET-P
Fort Huachuca, Arizona 85613-5300

19. Bill Alvarez — 1
USAISEA/ASBH-SET-P
Fort Huachuca, Arizona 85613-5300

20. Janet McDonald — 1
USAISEA/ASBH-SET-P
Fort Huachuca, Arizona 85613-5300

21. Dr. Tom Tice — 1
Department of Electrical and Computer Engineering
Arizona State University
Tempe, Arizona 85287

22. Dr. Roger C. Rudduck — 1
Ohio State University
Electrophysics Laboratory
1320 Kinnear Rd.
Colombus, Ohio 43212

23. Commander Naval Space and Naval — 1
Warfare Systems Command
Attention: Dick Pride
PDW 110-243
Washington D.C. 20363

24. Naval Sea Systems Command — 1
Attention: P. Law C61X41
Washington D.C. 20362

25. LT James C. Tertocha — 1
6711 Agnes St.
N. Hollywood, California 91606

26. LT John Vorrias — 1
1001 Funston Ave #3
Pacific Grove, California 93950

27. LT Costas Theophanopoulos — 1
355 Casa Verde Way #8
Monterey, California 93940

28. LCDR Mario C. Neiva — 1
Brazilian Naval Commision
4706 Wisconsin Ave., N.W.
Washington D.C. 20016

29. Director Research Administration, Code 012 — 1
Naval Postgraduate School
Monterey, California 93943-5000

NAVAL POSTGRADUATE S
MONTEREY, CALIFORNIA

Th
L9
c.
Thesis
L9503
c.1
Lyberopoulos
Numerical models of
new HF shipboard communi-
cation antenna system for
improved survivability.
5 APR 89
23 APR 90
23 MAY 91
35648
30138
37837

Thesis
L9503
c.1
Lyberopoulos
Numerical models of
new HF shipboard communi-
cation antenna system for
improved survivability.

Numerical models of new HF shipboard com
3 2768 000 71648 4
DUDLEY KNOX LIBRARY